Cerebral and Ocular Fluid Balance as a Function of Space-Related Environmental Factors: Insights into Visual Impairment in Astronauts

Inaugural Dissertation

zur

Erlangung des Doktorgrades
philosophiae doctor (PhD)
der Medizinischen Fakultät
der Universität zu Köln

vorgelegt von

Karina Marshall-Bowman
aus Karlskrona, Schweden

Druckerei Deutsches Zentrum für Luft und Raumfahrt e.V, Köln, Deutschland

2017

Gedruckt mit Genehmigung der Medizinischen Fakultät der Universität zu Köln, 2017

Referenten: Prof. Dr. Claus Cursiefen

Prof. Dr. Mathias Hoehn

Datum der Mündlichen Prüfung: 6. Februar 2017

Table of Contents

1 List of Tables

2 List of Figures

3 Overview of the Appendix

4 Abbreviations

ANOVA	Analysis of Variance
ART	Automatic Real Time
BDC	Baseline Data Collection
BMI	Body Mass Index
CBF	Cerebral Blood Flow
CPP	Cerebral Perfusion Pressure
CSA	Cross-Sectional Area
CSF	Cerebrospinal Fluid
CO_2	Carbon Dioxide
CVP	Central Venous Pressure
DBP	Diastolic Blood Pressure
enVIIP Study	Cerebral and Ocular Fluid Balance as a Function of Hydrostatic Pressure Gradients and Environmental Factors: Insights into the VIIP Syndrome
EDI	Enhanced Depth Imaging
FOV	Field of View
GM	Gray Matter
HDT	Head-Down Tilt
HR	Heart Rate
ICA	Internal Carotid Artery
ICP	Intracranial Pressure
IIH	Idiopathic Intracranial Hypertension
IJV	Internal Jugular Vein
IOP	Intraocular Pressure
ISS	International Space Station
LBNP	Lower Body Negative Pressure
MAP	Mean Arterial Pressure
MOS	Microgravity Ocular Syndrome
MPRAGE	Magnetization-Prepared Rapid Acquisition of Gradient Echo
MRI	Magnetic Resonance Imaging
OCT	Optical Coherence Tomography

ON	Optic Nerve
ONH	Optic Nerve Head
ONSD	Optic Nerve Sheath Diameter
$PaCO_2$	Arterial Partial Pressure of Carbon Dioxide
PaO_2	Arterial Partial Pressure of Oxygen
PC-MRI	Phase Contrast Magnetic Resonance Imaging
PCO_2	Partial Pressure of Carbon Dioxide
RNFL	Retinal Nerve Fiber Layer
SAS	Subarachnoid Space
SBP	Systolic Blood Pressure
SD-OCT	Spectral Domain Optical Coherence Tomography
SEM	Standard Error of the Mean
SETI Study	Studying the Effects of Tilt with Lower Body Negative Pressure on Intraocular Pressure
SpaceCOT Study	Studying the Physiological and Anatomical Cerebral Effects of CO_2 and Tilt
SPAIR	Spectral Attenuated Inversion Recovery
TA	Acquisition Time
TCD	Transcranial Doppler
TE	Echo Time
TI	Inversion Time
TLPD	Translaminar Pressure Difference
TR	Repetition Time
TSE	Turbo Spin Echo
VA	Vertebral Artery
VIIP	Visual Impairment and Intracranial Pressure
WM	White Matter

5 Summary

The visual impairment and intracranial pressure (VIIP) syndrome affects more than half of astronauts during 6-month missions on the International Space Station (ISS) resulting in significant structural and functional ophthalmic changes. Although the exact pathophysiological mechanisms underlying the ocular changes are unknown, headward fluid shifting due to the absence of gravity and subsequent alterations in cerebral hemodynamics and intracranial pressure (ICP) may play a major role. The overarching aim of this thesis was to elucidate the effects of cephalad fluid shifting during head-down tilt (HDT), commonly used as a spaceflight analog model, on cerebral and ocular anatomy and physiology. As a secondary aim, the potential additive effects of increased ambient carbon dioxide (CO_2) during HDT were assessed as well as the ability of lower body negative pressure (LBNP) to counteract headward fluid shifting.

The scope of the PhD thesis work was split into three main studies. In the first study, cerebral as well as ocular fluid and pressure balance was assessed during 5 h HDT exposure in 5 experimental conditions: -6°, -12° and -18° HDT, -12° with 1% CO_2 and -12° HDT with -20 mmHg LBNP. Thereafter, the second study investigated a longer duration exposure to -12° HDT (29 h) with and without increased ambient CO_2. Finally, the third study tested the effects of stronger LBNP (-40 mmHg) for shorter durations of time with an extended range of tilt angles.

The results show that HDT leads to signs of cerebral venous congestion demonstrated by the large increase in internal jugular vein cross-sectional area and decreased cerebral venous outflow. Furthermore, HDT induced increases in intracranial as well as periorbital cerebrospinal fluid (CSF) volume, consistent with decreased CSF absorption due to elevated cerebral venous pressure. Intraocular pressure (IOP) remained greater than ICP during HDT, resulting in a small, positive intraocular-intracranial pressure difference (IOP > ICP) during both acute and overnight HDT, contrary to the hypothesized shift to a greater ICP. In addition, exposure to increased ambient CO_2 on the ISS was hypothesized to be a contributing factor to the ocular changes in astronauts by further increasing intracranial blood volume and therefore pressure. In combination with HDT, exposure to elevated ambient CO_2 increased cerebral blood flow and venous outflow, however, had little additive effect on IOP or ICP during acute or longer-duration exposure.

Alterations in cerebral hemodynamics secondary to headward fluid shifting are central to the hypothesized mechanisms underlying the VIIP syndrome and may induce a cascade of ophthalmic changes over long-duration exposure.

Finding a way to mitigate vision changes in space is vital to ensure long-duration exploration class mission feasibility and success. Therefore, LBNP, a technique that redistributes venous blood volume to the lower limbs, was tested as a mechanical countermeasure to cephalad fluid shifting. Notably, low-level LBNP (-20 mmHg) during -12° HDT was able to successfully attenuate the HDT-induced increase in periorbital as well as intracranial CSF volume. Although -20 mmHg LBNP had no effect on IOP or ICP, exposure to -40 mmHg LBNP was able to attenuate HDT-induced increases in IOP during a range of tilt angles.

Overall, the presented studies represent novel investigations into the cerebral and ocular effects of various degrees of cephalad fluid shifting as well as the unique combination of HDT and increased ambient CO_2 as a more realistic analog of the ISS environment. Impediment of venous return by LBNP was also established as a promising technique to counteract cephalad fluid shifting and redistribute CSF and may be able prevent future development of structural ocular changes associated with the VIIP syndrome. These studies have contributed to the further understanding of potential mechanisms involved in the development of ocular changes in astronauts, notably the central role of cerebral hemodynamics and cerebral venous congestion.

6 Zusammenfassung

Mehr als die Hälfte aller Astronauten sind nach 6-monatigen Missionen auf der Internationalen Raumstation (ISS) vom VIIP-Syndrom (von der engl. Bezeichnung Visual Impairment and Intracranial Pressure, Sehstörungen und Hirndruck) betroffen. Dieses führt zu erheblichen funktionellen und strukturellen Veränderungen des Auges. Die genauen pathophysiologischen Vorgänge, die zu diesen Veränderungen am Auge führen, sind unbekannt. Kopfwärts-gerichtete Verschiebungen von Flüssigkeit infolge der Schwerelosigkeit mit nachfolgenden Veränderungen der zerebralen Hämodynamik und des Hirndrucks (Intracranial Pressure, ICP) könnten jedoch ein wesentlicher Faktor sein. Hauptziel dieser Arbeit war die Klärung der Folgen der Flüssigkeitverschiebungen beim Head-Down-Tilt (HDT, Kopftieflage) auf die Anatomie und Physiologie von Gehirn und Auge. HDT wird üblicherweise als Simulationsmodell für die Raumfahrt herangezogen. Als weiteres Ziel wurden die potenziellen additiven Folgen eines erhöhten Kohlenstoffdioxidgehalts (CO_2) in der Umgebung beim HDT sowie die Möglichkeit bewertet, durch den Einsatz von LBNP-Systemen (von der engl. Bezeichnung Lower Body Negative Pressure, Unterdruck auf die untere Körperhälfte) der Kopfwärtsverlagerung von Flüssigkeit entgegenzuwirken.

Im Rahmen dieser Dissertation wurden drei Hauptstudien durchgeführt. Bei der ersten Studie wurde der Flüssigkeits- und Druckausgleich an Gehirn und Auge in 5 HDT-Versuchsanordnungen evaluiert: HDT (5 h) von −6°, −12° und −18°, HDT von −12° mit 1 % CO_2 und −12° mit LBNP von −20 mmHg. Im Anschluss wurde bei der zweiten Studie eine längere Exposition bei einem HDT von −12° (29 h) mit und ohne erhöhten CO_2-Gehalt in der Umgebung untersucht. Bei der dritten Studie wurden die Folgen eines höheren LBNP (−40 mmHg) über kürzere Zeiträume bei einem größeren Bereich von HDT-Winkeln getestet.

Die Ergebnisse zeigen, dass ein HDT zu Anzeichen von venösen Stauungen im Gehirn führt, wie die starke Vergrößerung der Querschnittsfläche der *v. jugularis interna* und die Verringerung des zerebral-venösen Abflusses zeigen. Der HDT führte zudem zu einem erhöhten intrakraniellen und periorbitalen Volumen der *liquor cerebrospinalis*, was im Einklang mit einer verminderten Liquor-Resorption aufgrund des erhöhten zerebralen Venendrucks steht. Der Augeninnendruck (Intraocular Pressure, IOP) erhöhte sich beim HDT stärker als der ICP, sodass es sowohl bei akuter HDT-Exposition als auch bei Exposition über Nacht zu einer verringerten, aber immer noch positiven Differenz zwischen

Augeninnendruck und Hirndruck (IOP > ICP) kam. Dies widersprach der in den ursprünglichen Hypothesen erwarteten Entwicklung eines höheren ICP.

Außerdem wird ein erhöhter CO_2-Gehalt in der Umgebung in der ISS als Mit-Verursacher für Augenveränderungen bei Astronauten angenommen, da das Blutvolumen und damit auch der Druck im Gehirn dadurch weiter steigen. Zusammen mit dem HDT führte die Exposition bei erhöhtem CO_2-Gehalt in der Umgebung zu einer Steigerung des Blutflusses in den Zerebral-Arterien und -Venen. Die additiven Folgen für IOP und ICP bei akuter Exposition und bei einer Exposition über einen längeren Zeitraum waren jedoch gering. Veränderungen der zerebralen Hämodynamik durch die Kopfwärtsverlagerung von Flüssigkeit sind von zentraler Bedeutung für die angenommenen Vorgänge hinter dem VIIP-Syndrom und können bei Langzeitexposition eine ganze Reihe von Augenveränderungen bedingen.

Es müssen unbedingt Möglichkeiten zur Minderung der Veränderungen der Sehkraft in der Raumfahrt aufgetan werden, um Machbarkeit und Erfolg von Langzeitforschungsmissionen sicherzustellen. Daher wurde LBNP als Verfahren zur Umverteilung des venösen Blutvolumens in die unteren Extremitäten als mechanische Gegenmaßnahme zur Kopfwärtsverlagerung von Flüssigkeit getestet. Insbesondere mit einem niedrigen LBNP (−20 mmHg) bei einem HDT von −12° konnte die durch den HDT verursachte Erhöhung des periorbitalen und intrakraniellen Liquor-Volumens erfolgreich abgeschwächt werden. Während ein LBNP von −20 mmHg keinen Einfluss auf IOP und ICP hatte, konnten mit einem LBNP von −40 mmHg die durch HDT ausgelöste Erhöhung des IOP bei verschiedenen HDT-Winkeln abgeschwächt werden.

Zusammengefasst präsentieren die vorgelegten Studien innovative Untersuchungen zu den Folgen verschiedener Ausmaße der Kopfwärts-gerichteten Verschiebung von Flüssigkeit auf Gehirn und Auge sowie zu der besonderen Kombination aus HDT und erhöhtem CO_2-Gehalt in der Umgebung als realistischere Simulation der ISS-Umgebung. Zudem wurde festgestellt, dass Reduktion des venösen Rückstroms, z.B. durch LNBP, in der Lage zu sein scheint, die kopfwärts-gerichteten Liquorverschiebungen zu unterbinden, sodass strukturellen Augenveränderungen durch das VIIP-Syndrom zukünftig möglicherweise vorgebeugt werden kann. Die Studien haben das Verständnis der möglichen Vorgänge bei der Herausbildung von Augenveränderungen erweitert und damit zur

Untersuchung der zentralen Rolle der zerebralen Hämodynamik und venöser Stauungen im Gehirn beigetragen.

7 Introduction

7.1 Ophthalmic Abnormalities in Astronauts

Exposure to microgravity affects the homeostatic physiology of many human body systems as humans are adapted to a 1-G environment. The effects of short and long-duration exposure to microgravity have been well studied over the past 50 years of human spaceflight including cardiovascular, vestibular and musculoskeletal adaptations (14, 57). For decades, there have also been anecdotal reports of visual impairment during spaceflight, much of which was attributed to the age of the flying population. However, with the deployment of the International Space Station (ISS), continuously inhabited by 4-6 residents since 2000, insights into the effects of long-duration microgravity exposure on the cerebral and ocular systems has greatly increased. With the recent advancement of on-board medical imaging capabilities, it has been determined that the anecdotal changes in vision are accompanied by a number of structural changes. This Visual Impairment and Intracranial Pressure (VIIP) syndrome (3), also known as the Microgravity Ocular Syndrome (MOS; 56), is associated with varying degrees of optic disc edema, globe flattening, choroidal folds, cotton wool spots, optic nerve (ON) sheath distension, increased intracranial pressure (ICP) post-flight and hyperopic refractive error shifts (69, 78, 82, 92).

Since year 2000, the VIIP syndrome has affected more than 65% of American astronauts to varying degrees with unknown long-term implications. A 4-tier classification system has been developed to rank the severity of the affected astronauts, with the majority of astronauts (59%) presenting with class 2 of the VIIP syndrome (Table 1).

Table 1: VIIP syndrome classification for astronauts and the percentage of VIIP-affected astronauts in each classification

	Affected Astronauts	Class definition
Class 1	9%	• ≥ .50 diopter cycloplegic refractive change • And/or cotton wool spot
Class 2	59%	Class 1 findings and: • Choroidal folds • And/or optic nerve sheath distension • And/or globe flattening • And/or scotoma
Class 3	14%	Class 2 findings and: • Papilledema of Grade 0-2 on the Frisen scale (39)
Class 4	18%	Class 2 findings and: • Papilledema grade > 2 on the Frisen scale • Symptoms of new heachache, pulsatile tinnitus and/or transient visual obscurations • CSF opening pressure > 18.4 mmHg (24 cm H_2O)

CSF = cerebrospinal fluid (Source: NASA, 2012)

While the exact etiology of the ocular changes in astronauts is currently unknown, increased ICP has been widely hypothesized to be a contributing factor due to similar signs and symptoms seen in patients on Earth with idiopathic intracranial hypertension (IIH, also known as pseudotumor cerebri), that is, increased ICP with an unknown cause. Thus, research efforts have been turned to understanding the cerebral and ocular effects of real and simulated microgravity to better understand underlying mechanisms in the VIIP syndrome and ultimately, to mitigate these risks through countermeasures.

7.2 Intracranial and Ocular Anatomy and Physiology: General Introduction

7.2.1 The Intracranial Compartment

As the cranium is non-distensible, the intracranial space has a fixed volume made up of ~100-130 ml blood (15% arterial, 40% venous, 45% microcirculation), ~75 ml of cerebrospinal fluid (CSF) and brain tissue (93). According to the classical Monro-Kelli doctrine (88), the sum of the volume of these three intracranial components is constant, therefore, any increase in one will lead to a compensatory decrease in another (mainly CSF or blood volume). This can be seen for both slow (i.e., a mass lesion) and fast processes (i.e.,

arterial pulsatility). However, when the compensatory reserve is low (a shift to the right of the intracranial pressure-volume curve), any increase in intracranial volume will lead to a large rise in ICP (Figure 1; 11, 27). Decreased cranial compliance and increased ICP and flow pulsatility are seen in many pathologies including traumatic brain injury and hydrocephalus (124). Interestingly, changes in cranial compliance occur daily in healthy individuals as well, primarily with changes in posture (5), however, within the clinical norm.

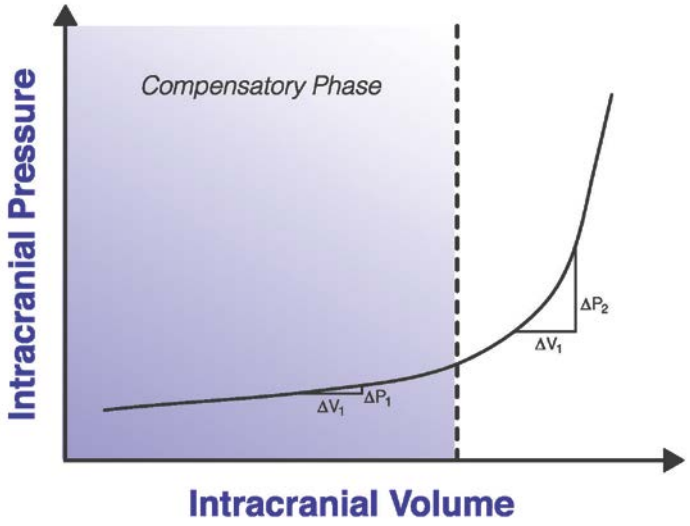

Figure 1: The theoretical intracranial pressure-volume curve demonstrates that when compensatory reserve is present, a certain change in intracranial volume (ΔV_1) results in a small increase in intracranial pressure (ΔP_1). However, once compensatory reserve is exhausted, the same increase in volume (ΔV_1) will result in a much larger increase in pressure (ΔP_2).

ICP is subject to large variations with posture as both the CSF and vascular systems are subject to hydrostatic pressure gradients on Earth. In the upright position, ICP is normally 0 mmHg (or negative) at the level of the external auditory meatus (96, 99), whereas in the supine position, ICP averages about 10 mmHg in healthy adults (34). The classical hypothesis of CSF hydrodynamics is that CSF is produced primarily in the choroid plexuses and ependymal surfaces of the brain ventricles (95) and flows in a unidirectional manner from the brain ventricles into the subarachnoid space (SAS), which lies between the innermost layers of the meninges surrounding the central nervous system (pia matter and arachnoid matter). Recently, CSF circulation has been found to be much more complex than initially thought, involving directed bulk flow, pulsatile movement, and continuous fluid exchange between CSF and the blood brain barrier (23). The CSF-filled SAS continues around the brain, spinal cord and along several nerve tracks, most notably the ON (Figure 2). The

bulk of CSF is then absorbed through the arachnoid villi of the dural venous sinuses into the cerebral venous system, although there is increasing evidence that the lymphatic system plays a role in CSF resorption as well (87, 95). Absorption of CSF into the venous sinuses in the arachnoid villi is dependent upon a pressure gradient ($P_{CSF} - P_{Venous}$). According to the Davson equation (Equation 1-1; 28),

$$ICP = R_{out} \times I_{formation} + P_d \qquad \text{Equation 1-1}$$

where R_{out} = resistance to CSF outflow, $I_{formation}$ = CSF formation rate and P_d = pressure in the dural venous sinuses, an increase in any of these factors will lead to an increase in ICP. Notably, any increase in cerebral venous pressure will have a direct and substantial influence on ICP (132).

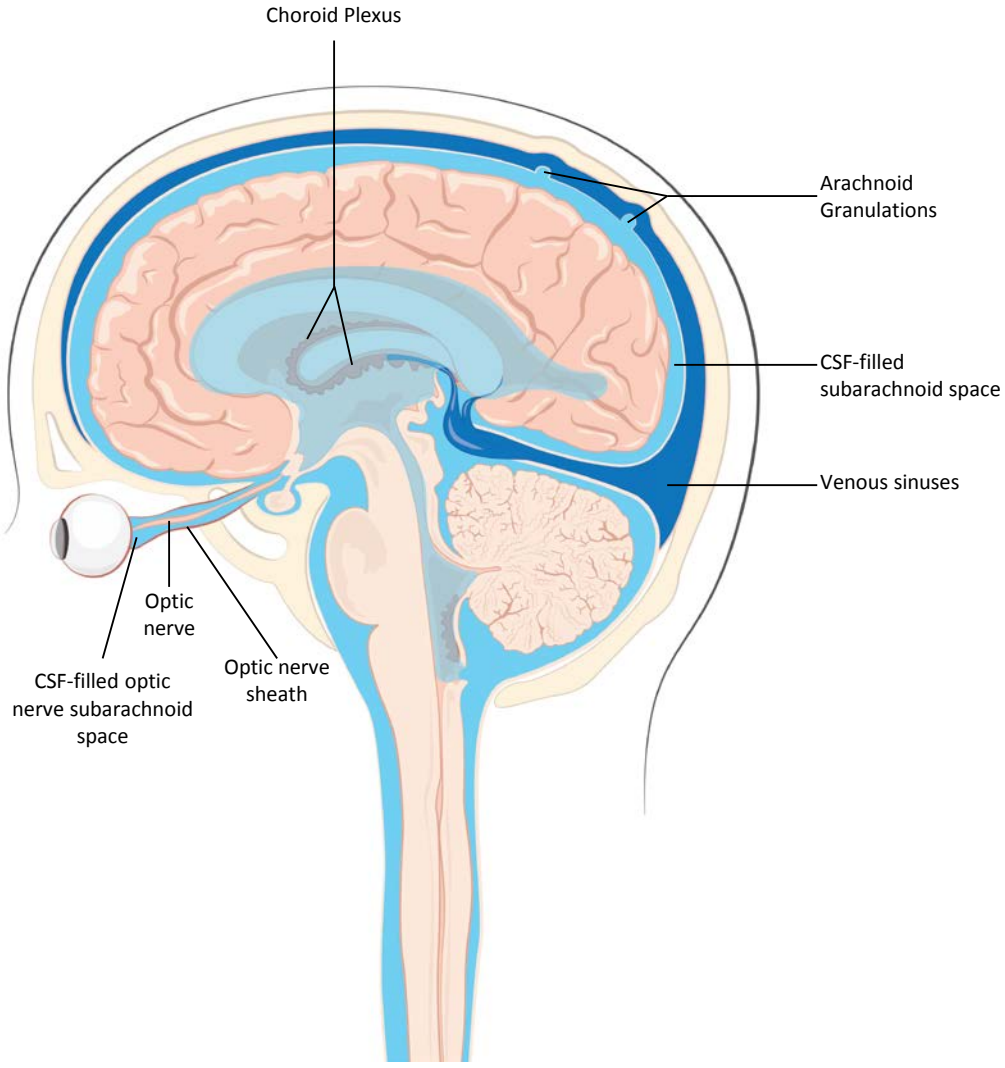

Figure 2: Cerebrospinal fluid (CSF, light blue) circulates around the brain and spinal cord and along nerve tracks including the optic nerve.

7.2.2 Intracranial Blood Circulation

Blood supply to the brain is supported by 4 main arteries: the bilateral internal carotid arteries (ICA) and the bilateral vertebral arteries (VA). The VAs join together to form the basilar artery, which communicates with the ICAs via the posterior communicating arteries at the Circle of Willis. The main arteries then branch out into pial arteries, penetrating arteries and arterioles and eventually capillaries. On the venous side, venuoles and veins merge into several venous sinuses. These are contained between two layers of dura matter, which prevent collapsation when the venous pressure is less than the ICP. From the intracranial venous sinuses, cerebral venous outflow continues predominantly through the internal jugular veins (IJV) and vertebral veins. Interestingly, the main cerebral venous outflow pathway is posture dependent: majority of the venous outflow occurs in the IJVs in the supine position whereas at about +15° head-up tilt, the IJVs collapse, and the vertebral plexus overtake as the main outflow pathway (80). In contrast to the cerebral arterial system, the cerebral venous system can be highly asymmetric with the majority of individuals presenting with right lateral dominance in both the transverse sinus (4) and IJVs (112).

Arterial cerebral blood flow (CBF) is highly regulated to ensure constant and sufficient delivery of oxygen (O_2) to brain tissue. Cerebral autoregulation ensures a normal CBF during large fluctuations in arterial blood pressure between 60 - 140 mmHg. Below or above these limits, CBF decreases or increases exponentially, respectively. According to Ohm's law (Equation 1-2, adapted to fluids), flow (*F*) is proportional to the difference in arterial inflow and venous outflow pressure (ΔP, $P_{arterial}$ - P_{venous}) divided by the vascular resistance to flow (*R*):

$$F = \frac{\Delta P}{R} = \frac{(P_{arterial} - P_{venous})}{R} \qquad \text{Equation 1-2}$$

In addition, according to Poiseuielle's law (Equation 1-3), resistance to flow (*R*) is also related to blood viscosity (*n*), length of the vessel (*L*), and inversely related the radius of the vessel (*r*) to the fourth power:

$$R = \frac{8 \times n \times L}{\pi r^4} \qquad \text{Equation 1-3}$$

Thus, the radius of a vessel is the primary determinant of arterial vascular resistance and thus, blood flow. In addition, the cerebral vasculature is highly sensitive to changes in arterial partial pressure of carbon dioxide ($PaCO_2$) and to a lesser extent, arterial partial pressure of oxygen (PaO_2; 108). The notable effects of increased $PaCO_2$ on cerebral vascular tone are driven by changes in extracellular pH; CO_2 combines with water in the body to form carbonic acid and subsequent dissociation to form H^+ ions. Although several mechanisms involved in the effect of pH on vascular tone have been proposed including sheer stress-mediated release of nitric oxide and prostaglandins as well as K^+ channel activation, the common final step is a decrease in intracellular Ca^{2+} concentration leading to smooth muscle relaxation (1, 25, 29, 49). Thus, the resulting increase in CBF helps to mitigate rising $PaCO_2$ by 'flushing' the excess CO_2 from the brain tissue. The physiological response to increased $PaCO_2$ is termed cerebrovascular CO_2 reactivity (1), and helps maintain central pH by inducing a ventilatory response through the respiratory center in the medulla.

7.2.3 The Eye and Optic Nerve

The anterior portion of the eye is filled with aqueous humor, produced by the ciliary body at a rate of about 3 µL/min. The central eye is composed of the lens and vitreous humor, a gelatinous material that does not flow, although slow diffusion can occur. The eye is surrounded by a rigid outer shell (the sclera), and thus any change in intraocular volume will result in a large change in intraocular pressure (IOP). In healthy adults, IOP averages 15 mmHg and is predominantly determined by the resistance to outflow of aqueous humor through the trabecular meshwork (42), where it then drains into aqueous veins and episcleral veins. Posterior to the vitreous body is the retina, composed of layers of neuronal cells to detect and light and transmit signals. Retinal nerve fibers converge to exit the eye at the optic nerve head (ONH) and then form the ON. The lamina cribrosa is a lattice-like structure that forms a border between the intraocular and extraocular space, namely the retrobulbar CSF space surrounding the ON. Therefore, a pressure gradient exists across the lamina cribrosa, also referred to as the translaminar pressure difference (TLPD; IOP - ICP). In healthy adults, IOP is greater than ICP, resulting in a positive TLPD. However, any alteration in either ICP or IOP can alter this pressure difference and have significant effects on the ONH. Swelling of the ONH (papilledema), a hallmark sign in IIH patients, occurs with

sustained increased ICP due to compression of the ON and retinal nerve fibers and subsequent stasis of axoplasmic transport (120). However, other mechanisms may be involved including hypoxia due to compression of the pial septal blood supply to the ON or metabolic toxicity in the ON SAS CSF (63). On the contrary, a large TLPD can result in ONH cupping. This is a hallmark sign in Glaucoma patients with increased IOP, although ICP has also been found to be lower in patients with primary open-angle and normal-tension Glaucoma compared to age matched controls (18).

The choroid, the vascular layer of the eye, lies between the retina and the sclera. The choroid is a dynamic structure and its thickness depends on several factors including intravascular volume of choroidal vessels, IOP and blood pressure (103). Several branches of the ophthalmic artery supply blood to the eye including the central retinal artery, and venous outflow occurs primarily via the vortex veins, episcleral veins and the ophthalmic veins.

The ON is surrounded by the CSF-filled SAS, continuous with the SAS of the central nervous system. However, the ON SAS represents a unique point in the CSF circulation as lies outside of the rigid cranium surrounded by fatty tissue and expands with even small increases in CSF pressure. Notably, there is no hydrodynamic theory that can explain how CSF enters the ON SAS and then turns around and exits along the same route to reenter the CSF circulation and be reabsorbed in the venous sinuses (62). Therefore, it is likely that the bulk of CSF in the ON SAS is absorbed into the lymphatic system in the retrobulbar space (62, 65).

7.3 Cerebral and Ocular Fluid Balance as a Function of Space-Related Environmental Factors: Mechanistic Hypothesis

The pathophysiological mechanisms underlying the structural and functional ophthalmic changes in astronauts are currently unknown. However, patients with IIH, who normally present with an ICP > 20 mmHg, show very similar ophthalmic findings as in the VIIP syndrome including papilledema, globe flattening, distension of the ON sheath and visual loss (125). This has led to the overall hypothesis that increased ICP is the primary underlying mechanism causing a cascade of effects on cerebral and ocular anatomy and physiology in space due to disruptions in cerebral hemodynamics. Mechanistically, this could occur via several pathways secondary to the unique environmental conditions on the

ISS including headward fluid shifting due to the loss of gravitational forces with further exacerbation due to the addition of elevated ambient CO_2 (Figure 3).

7.3.1 Microgravity

In the upright position on Earth, the Gx gravitational vector retains a large volume of fluid, primarily interstitial fluid and venous blood, in the lower limbs. With the abolishment of all gravitational gradients in microgravity, a headward fluid shift occurs (45, 93). I hypothesize that this leads to cerebral venous congestion with decreased cerebral venous outflow, predominantly in the IJVs, and increased cerebral venous pressure. As noted in Davson's equation (Equation 1-1), ICP is dependent on the cerebral venous pressure, and an increase in cerebral venous pressure secondary to microgravity exposure will lead to a decrease in CSF absorption across the dural venous sinuses and result in an increase in ICP. Furthermore, by effect of bridging veins, which act as starling resistors affected by ICP (17), a vicious positive feedback loop may occur in which increased ICP will result in a decrease in cerebral venous return and increase intracranial blood volume, thus further exacerbating the elevation in ICP (123). However, due to the lack of classical symptomology associated with severe intracranial hypertension including chronic headache, pulse synchronous tinnitus or diplopia (22), the increase in ICP in microgravity may be below the clinical threshold, yet constantly elevated above the 24 h average ICP normally experienced on Earth. Overall, a small yet sustained increase in ICP secondary to microgravity exposure and alterations in cerebral hemodynamics could induce several cascading effects, notably affecting the ocular structures (Figure 3).

As the SAS continues along the ON, increased pressure in the SAS would compress the optic nerve fibers and blood vessels, resulting in stasis of axoplasmic flow and ultimately papilledema and the formation of cotton wool spots (105). Further, as ICP is directly transmitted to the lamina cribrosa at the back of the eye, an increase in ICP would thus result in a decrease in the TLPD. Elevated pressure in the ON SAS would also exert an anterior force on the sclera, resulting in globe flattening and choroidal folds over extended exposure, ultimately leading to axial shortening and a hyperopic shift (Figure 3).

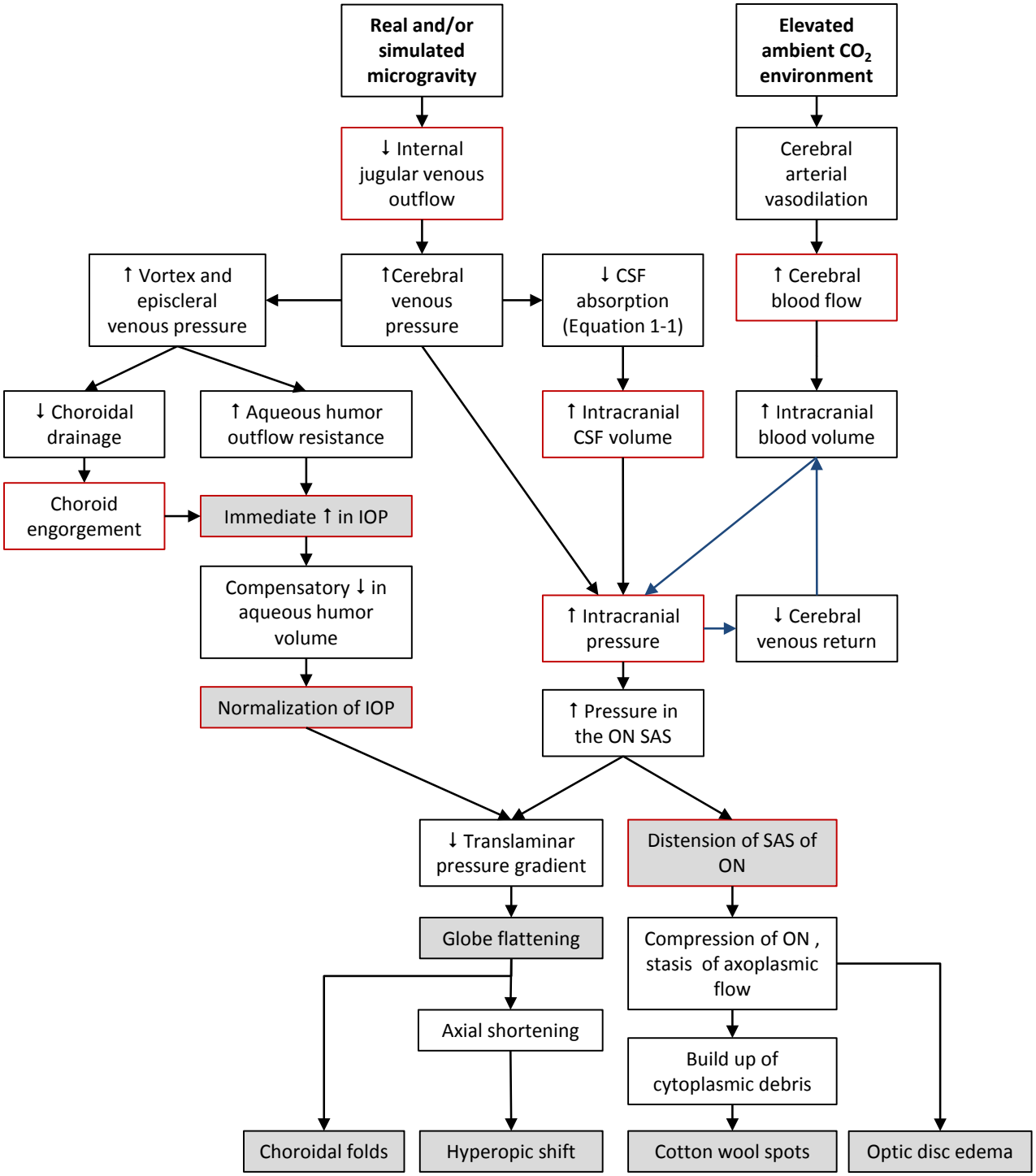

Figure 3: Hypothesized mechanisms underlying ocular changes in microgravity; gray-filled boxes represent parameters/variables measured in astronauts (32, 69, 71, 78), red boxes represent measurements taken in the thesis experiments and blue arrows denote a positive feedback loop; SAS = subarachnoid space, ON = optic nerve, CSF = cerebrospinal fluid, IOP = intraocular pressure

In addition, decreased cerebral venous outflow and increased cerebral venous pressure could also lead to increased pressure in the episcleral and vortex veins, resulting in decreased choroidal drainage and engorgement of the choroid. Coupled with increased aqueous humor outflow resistance due to the increased cerebral venous pressure, IOP would increase immediately. However, overtime IOP may return to baseline values through a compensatory decrease in aqueous humor volume. Thus, a normalized IOP coupled with small yet sustained increase in ICP due to disruptions in cerebral hemodynamics would lead to a decreased TLPD, increased pressure on the posterior eye globe and may ultimately lead to a cascade of ophthalmic effects in microgravity (Figure 3). Further, exposure to increased ambient CO_2 on the ISS is hypothesized to exacerbate the microgravity-induced increase in ICP and the resulting effects.

7.3.2 Increased Ambient Carbon Dioxide

CO_2 is known to affect many physiological systems, notably cerebrovascular physiology. As a potent vasodilator, exposure to elevated ambient CO_2 leads to increased CBF, which in turn increases intracranial blood volume (37, 44, 52) and therefore ICP. On Earth, ambient CO_2 levels average 0.04% (PCO_2 of 0.3 mmHg at standard atmospheric pressure). As the ISS is a closed environment and it is impractical to control CO_2 concentrations to terrestrial levels, the average ambient CO_2 on the ISS averages 0.1 – 0.8% (2.3 – 5.3 mmHg). However, there are large fluctuations over hours and days (71). In addition, there is no natural convection in microgravity and pockets of high CO_2 levels may form around astronaut's mouths in areas of low ventilation (i.e., behind a scientific rack and in sleeping quarters). A computational fluid dynamics analysis revealed that without adequate ventilation, CO_2 levels could rise to 1.2% (9 mmHg) around a sleeping astronaut's mouth within 10 min (110). Although exposure to 0.5-1% CO_2 on Earth has not been found to cause significant health risks (81, 109), existing microgravity-induced alterations in cerebral hemodynamics and impaired cerebral venous drainage may heighten the effects of low level hypercapnia. Specifically, CO_2-induced increases in CBF may increase cerebral blood volume, exacerbating the existing microgravity-induced elevation in ICP (Figure 3), potentially having more profound effects on astronauts with a lower cranial compliance.

7.4 Ground-Based Spaceflight Analog and Countermeasure Models

7.4.1 Head-Down Tilt Bed Rest

For decades, researches have utilized head-down tilt (HDT) bed rest as an analog model to simulate the effects of microgravity through head-to-foot gravitational unloading and inducing a cephalad fluid shift (126). Kakurin et al. (1976) conducted a 5 day bedrest at 0°, -4°, -8°, and -12° HDT and concluded that -12° HDT best reproduced physiological responses to microgravity (58). However, -6° HDT was ultimately chosen for future long-duration HDT studies as a compromise for comfort, acceptability and magnitude of physiological response (59). Thereafter, -6° HDT has been predominately used as a standard to simulate the physiological effects of microgravity on Earth and has been shown to reproduce many of the same effects of spaceflight (36, 119). However, ocular findings similar to those seen in the VIIP syndrome have not been detected during short or long-duration HDT bed rest exposure (117), challenging the notion that -6° HDT creates a sufficient cephalad fluid shift to mimic that of microgravity. Furthermore, subjects in HDT bed rest studies have frequently used pillows to prop up their head, and therefore a strict, full body -6° HDT position is not maintained, but rather the head is at or even above heart level.

7.4.2 Lower Body Negative Pressure

Lower Body Negative Pressure (LBNP), a technique that sequesters fluid volume (principally venous blood) to the lower limbs, has been used for decades to research orthostatic tolerance, simulated blood loss and G-loading (43). LBNP devices are normally composed of a chamber that encompasses the legs and is sealed at the iliac crest. The chamber is then connected to a vacuum pump to reduce the pressure inside the chamber. The physiologic response to LBNP depends on both the magnitude of pressure applied and the duration. Low-level LBNP (-10 to -20 mmHg) approximates a reduction of centrally available blood volume of ~400-550 ml, whereas high-level LBNP (-20 to -40 mmHg) pulls ~550-1000 ml of blood into the lower extremities (26). In addition, central venous pressure (CVP) decreases about 1-2 mmHg per 10 mmHg LBNP (94). Notably, the stronger the LBNP level, the greater the cardiovascular stress and the likelihood of resulting orthostatic

intolerance. Therefore, for long-duration use of LBNP, a low level must be implemented for subject comfort and feasibility.

7.5 Research Aims

As the etiology and long-term implications of the VIIP syndrome are currently unknown, the main aim of this thesis was to elucidate the effects of space-related environmental factors on intracranial and ocular anatomy and physiology, mainly cephalad fluid shifting and increased ambient CO_2. As a secondary aim, LBNP was evaluated as a potential countermeasure to cephalad fluid shifting. Thus, the implemented studies investigated the effects of various degrees of cephalad fluid shifting, increased ambient CO_2 and LBNP on 1) cerebral hemodynamics, 2) ICP, 3) IOP and 4) cardiovascular and respiratory parameters as well as further effects on 5) choroid and retinal nerve fiber layer thickness, 6) intracranial volumes and 7) ON sheath diameter in order to decipher mechanistic pathways underlying the structural and functional ophthalmic changes in microgravity. The scope of the PhD thesis work was split into three main studies. The first study, entitled the enVIIP study (Section 8.1), involved a comprehensive investigation of the effects of headward fluid shifting on cerebral and ocular fluid and pressure balance. In Part I of the enVIIP study, various degrees of HDT were investigated, challenging the standard utilization of -6° HDT as an analog of microgravity. In Part II, as a more realistic analog to the ISS environment, an intermediate HDT angle (-12°) was combined with increased ambient CO_2 to address the hypothesis of elevated CO_2 exposure exacerbating headward fluid shifts and ICP. In Part III, continuous low-level LBNP (-20 mmHg) during HDT was tested as a means of reducing cerebral venous congestion as a countermeasure to headward fluid shifting. The next study (the SpaceCOT Study - Section 8.2) built upon the results of the enVIIP study and investigated a longer duration exposure to -12° HDT (29 h) with and without increased ambient CO_2 as a potential new model for ground-based analog studies. Finally, the SETI study (Section 8.3) was designed to elucidate the effects of exposure to a stronger level of LBNP (-40 mmHg) for shorter durations of time with an extended range of tilt angles. The main findings and their significance are discussed in Section 9, with conclusions and future perspectives presented in Section 10.

8 Experiments

All studies were conducted in the envihab facility at the Institute of Aerospace Medicine, German Aerospace Center (DLR) in Cologne, Germany. Subjects were recruited from an internal database of subjects as well as through social medial and university website platforms. Written and informed consent was obtained from all subjects prior inclusion in experiments. All studies were conducted in accordance with the ethical principles in the Declaration of Helsinki and were approved by the local ethics commission, Ärztekammer Nordrhein [Appendix Documents A1, A2 and A3 for the enVIIP study, SpaceCOT study and SETI study, respectively].

8.1 The enVIIP Study: Cerebral and Ocular Fluid Balance as a Function of Hydrostatic Pressure Gradients and Environmental Factors

8.1.1 Study Design

The enVIIP study was a randomized, cross-over design, 3-part study consisting of a total of 5 experimental HDT conditions (Figure 4). In Part I, three HDT angles were investigated: -6°, -12° and -18° HDT. In Part II, an intermediate HDT angle (-12°) was combined with an increased ambient CO_2 (1%) as a more realistic model of the ISS environment. In Part III, low level LBNP (-20 mmHg) was implemented during -12° HDT as a potential countermeasure to headward fluid shifting. Baseline data was collected before each HDT condition in the supine (0°) position, followed immediately by 5 h in the HDT position. Each intervention experiment was performed on a separate day, with at least one week between experimental conditions to minimize carry-over effects.

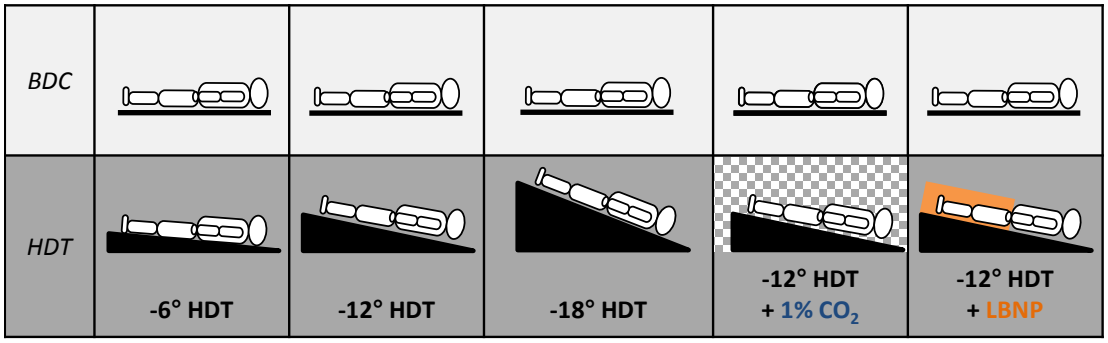

Figure 4: The enVIIP study consisted of 5 experimental conditions. Each condition included 3 h of baseline data collection (BDC) in the supine position followed by 5 h of head-down tilt (HDT). There was a separate visit for each of the five conditions, with at least one week break between experimental conditions.

In the 24 h preceding each experiment, subjects were instructed to consume 40 ml of water per kg body weight and to refrain from caffeinated beverages. All fluid and nutritional intake was standardized for the study as well. On the experimental days, subjects arrived fasted and were provided a standardized breakfast in addition to 250 ml of water and 200 ml of juice. After 3 h of baseline data collection in the supine position, subjects received 250 ml of water and a standardized snack before proceeding directly into HDT. After 2.5 h HDT, subjects received a high caloric shake (200 ml). Urination breaks were set at pre-determined time points and kept consistent across experimental conditions.

8.1.2 Subjects

Nine healthy, male subjects (mean ± SD, age: 25 ± 2 yrs; height: 183 ± 6 cm; weight: 81 ± 11 kg) were enrolled in the randomized cross-over design study. All subjects underwent a basic medical examination prior to inclusion in the study including a medical history and current health status interview, physical examination, urine and blood samples, spirometry test, electrocardiogram and eye examination. Subject inclusion criteria included male subjects between the ages of 18 – 65 and body mass index (BMI) between 26 – 30 kg/m^2. Subject exclusion criteria included current prescription medication usage, smoking, IOP > 20 mmHg, more than +5 or -6 diopters, history of abnormal IOP or diseases of the ON, history of increased ICP or any neurological or cardiovascular disease.

8.1.3 Materials and Methods

An example time table from the enVIIP study showing various measurement time points is displayed in the Appendix (Table A 1).

Intraocular and Intracranial Pressure Measurements

IOP was measured with an Icare pro tonometer (Icare, Helsinki, Finland) at supine baseline and after 3.5 h HDT. At each measurement time point, IOP was measured 3 times in each eye in a randomized order. The median value was then used for statistical analysis. ICP was measured with a non-invasive ICP meter (Vittamed, Kaunas, Lithuania). Using transcranial Doppler (TCD) ultrasound, blood flow pulsations in two segments of the ophthalmic artery, one extracranial and one intracranial, are measured simultaneously. An external pressure cuff on the orbital tissue is then inflated to 6 pressure steps (4, 8, 12, 16, 20 and 24 mmHg), and at the optimal external pressure, the balance point between the two arteries is found (100). ICP was measured at supine baseline and again after 3.5 h HDT, with 1-2 measurements taken at each time point.

Spectral Domain Optical Coherence Tomography

Spectral Domain Optical Coherence Tomography (SD-OCT) is currently the gold standard technique for quantifying tissue layers in the eye, emitting multiple wavelengths of light and measuring the reflected light to produce detailed cross-sectional images of the retina and choroid. An SD-OCT (Spectralis, Heidelberg Engineering, Heidelberg, Germany) with automatic real time (ART) TruTrack technology was implemented in the study. The TruTrack image alignment software allows for real time eye movement tracking and aligns scans with the original baseline image to ensure subsequent scans are taken in the exact same position.

For visualization of the choroid, a line scan with enhanced depth imaging (EDI, scan parameters: IR&OCT 30° ART EDI [HS] ART(100) Q:37) was taken through the fovea and ONH (Figure 5A). Custom-built software was then used to enhance the choroid for better visualization (Figure 5C) and to delineate the boundaries of the retina and choroid in a semi-automated process (Figure 5D, software courtesy of Dr. Nimesh Patel). The point of the fovea was determined by the thinnest section of the retina, and the thickness of the choroid

underneath was measured (average taken of 250 µm of choroid under the fovea). One subject was excluded from analysis due to a very thick choroid and unclear delineation of the posterior choroid border.

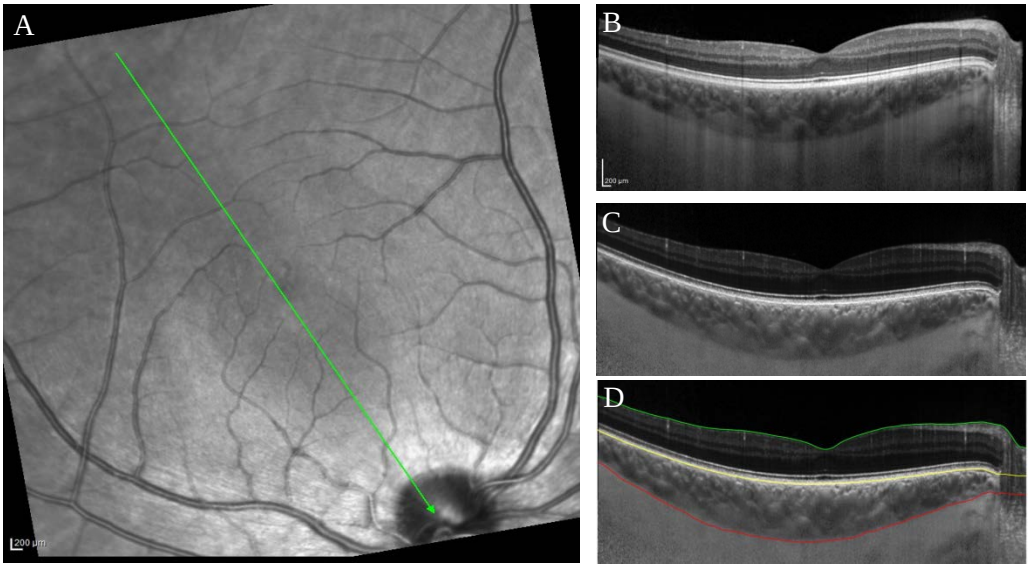

Figure 5: A) The SD-OCT line scan was taken through the fovea and optic nerve head across the posterior eye globe resulting in (B) an image of the retinal nerve fiber layers, choroid and sclera. C) For image processing and analysis, the choroid was enhanced and D) semiautomatic delineations were made of the inner limiting membrane (green line), the hyper-reflective retinal pigment epithelium (yellow line) and the inner surface of the sclera (red line).

In addition, a circle scan (scan parameters: IR&OCT 30° ART [HS] ART(100) Q:34) around the ONH was taken to measure the peri-ONH retinal nerve fiber layer (RNFL) thickness (Figure 6). The RNFL boundaries were automatically delineated with the Heyex software (Heidelberg Eye Explorer Version 3.1, Heidelberg Engineering, Heidelberg, Germany) and the global RNFL thickness was calculated. All SD-OCT scans were taken in the right eye on a custom-built platform allowing for measurements to be made in the upright (head tilted), supine and HDT positions (Appendix Figure A 1). Scans were taken at baseline in both the upright and supine positions and again after 1.5 h and 3 h HDT.

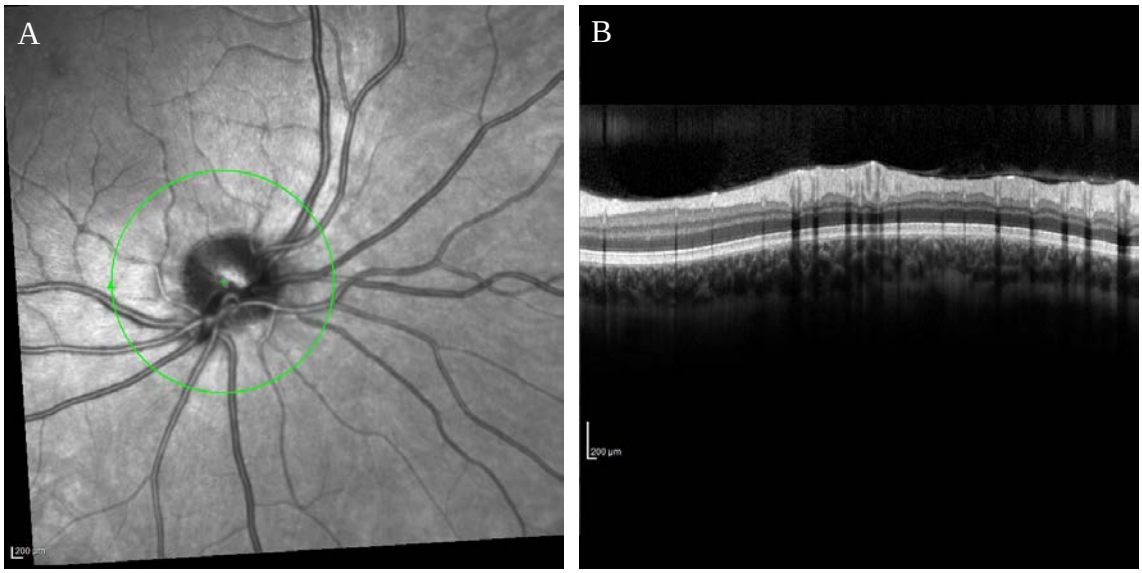

Figure 6: A circle SD-OCT scan was positioned around the optic nerve head (A), imaging the underlying layers (B).

Magnetic Resonance Imaging

MRI data was acquired with a Siemens Biograph mMR 3-T scanner (Siemens, Erlangen, Germany) with a 16 channel head coil. The total duration of the MR scan was about 1 hour. Baseline scans were taken in the supine position before each experimental condition, and intervention scans were taken between the 4-5th h of HDT. During HDT, all five experimental conditions were maintained within the MRI scanner. Custom-built wedges in the -6°, -12° and -18° positions were implemented within the scanner. For the 1% ambient CO_2 condition, a MR-compatible mask and tank system was designed for use inside the scanner as well. Lastly, a MR-compatible LBNP system was designed in the -12° HDT position (Appendix Figure A 2).

3D Volumetric MRI: After localization scans, a 3D volumetric T1-weighted MPRAGE (magnetization-prepared rapid acquisition of gradient echo) scan was acquired for a volumetric assessment of the CSF, gray matter (GM) and white matter (WM). The following scan parameters were implemented: acquisition time (TA) 9:20 min, repetition time (TR) 2500 ms, echo time (TE) 4.82 ms, inversion time (TI) 1100 ms for fat suppression, flip angle 7°, bandwidth 140 Hz/Px. The field-of-view (FOV) covered 256 mm with an isotropic resolution of 1 mm. The images were analyzed using voxel-based morphometry with the VBM8 toolbox from the SPM8 software package (http://www.fil.ion.ucl.ac.uk/spm). After field bias correction and registration to a common space, the tissue was segmented into

GM, WM and CSF and volumes were calculated. Large vessels such as the internal carotid arteries were excluded from segmentation.

Orbital Scans: In addition, T2-weighted transverse scans of the eye globe and ON were also obtained for the right and left eye (Figure 7A). A turbo spin echo (TSE) sequence with spectral attenuated inversion recovery (SPAIR) fat suppression was used with the following parameters: TA 3:02 min, TR 3000 ms, TE 103 ms, flip angle 180°, bandwidth 395 Hz/Px. The FOV covered 96*96 mm with a 129*128 matrix, which resulted in a resolution of 0.75 mm. The matrix was interpolated in 258 * 256 with a 0.375 mm resolution. A 100% phase oversampling was utilized to avoid fold-in artefacts. Parallel imaging with an acceleration factor of 2 was enabled (GRAPPA algorithm). The slab consisted of 30 slices with a slice thickness is 1.56 mm and 2 averages were obtained. A custom-built Matlab software (Release 2012b, The MathWorks Inc., Natick, Massachusetts, USA) was used to measure the diameter of the ON sheath 3, 4 and 5 mm behind the eye globe (Figure 7B).

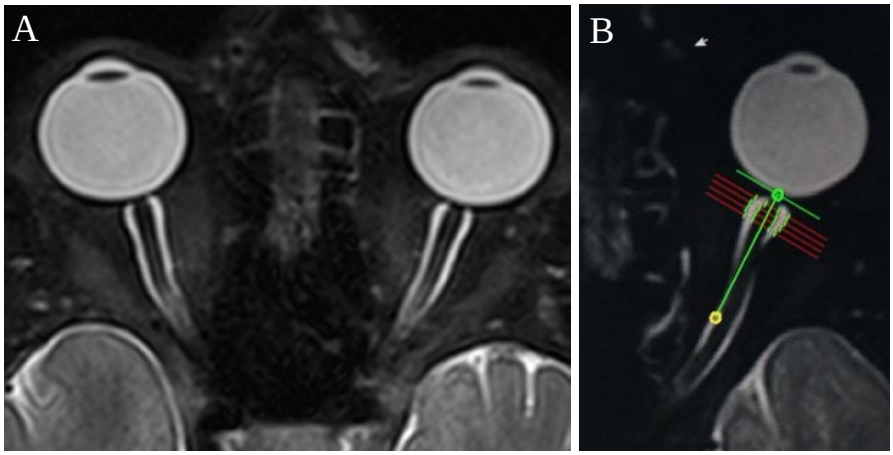

Figure 7: A) Transverse T2-weighted MR images of the eye globe and optic nerve were obtained during all conditions. B) Using custom-built software, the optic nerve sheath diameter was measured 3, 4 and 5 mm behind the posterior globe.

Phase-Contrast MRI: A flow sensitive MRI technique, phase-contrast MRI (PC-MRI), was implemented to measure cross-sectional area (CSA) and blood flow velocity in the major arteries and veins of the neck, allowing for flow to be calculated. When a strong magnetic field is applied, proton spins align parallel and anti-parallel to the axis of the external field. With the addition of radio frequency energy (90° pulse), a small surplus of spins excite orthogonally and are set in phase. In PC-MRI, the effect of 'phase shift' (the change in the moving protons' axis of spin) and its proportionality to the protons' velocity is

utilized (74). Thus, stationary tissue contrasts from flowing fluid where the signal is linearly proportional to the velocity of the spins (faster spins produce a larger phase shift) (111). In addition, direction can be determined. In gray-scaled images, for example, stationary tissue is typically coded in gray, spins moving in one direction are coded in white and spins moving in the opposite direction in black. Thus, the vascular anatomy (magnitude image, Figure 8A) and the velocity and direction of flow (phase image, Figure 8B) can be quantitatively displayed. The 3D MPRAGE scan was used for planning of the perpendicular PC-MRI plane above the bifurcation of the carotid artery. The bilateral internal carotid arteries (ICA), vertebral arteries (VA) and IJVs were measured between the second and third cervical vertebrae.

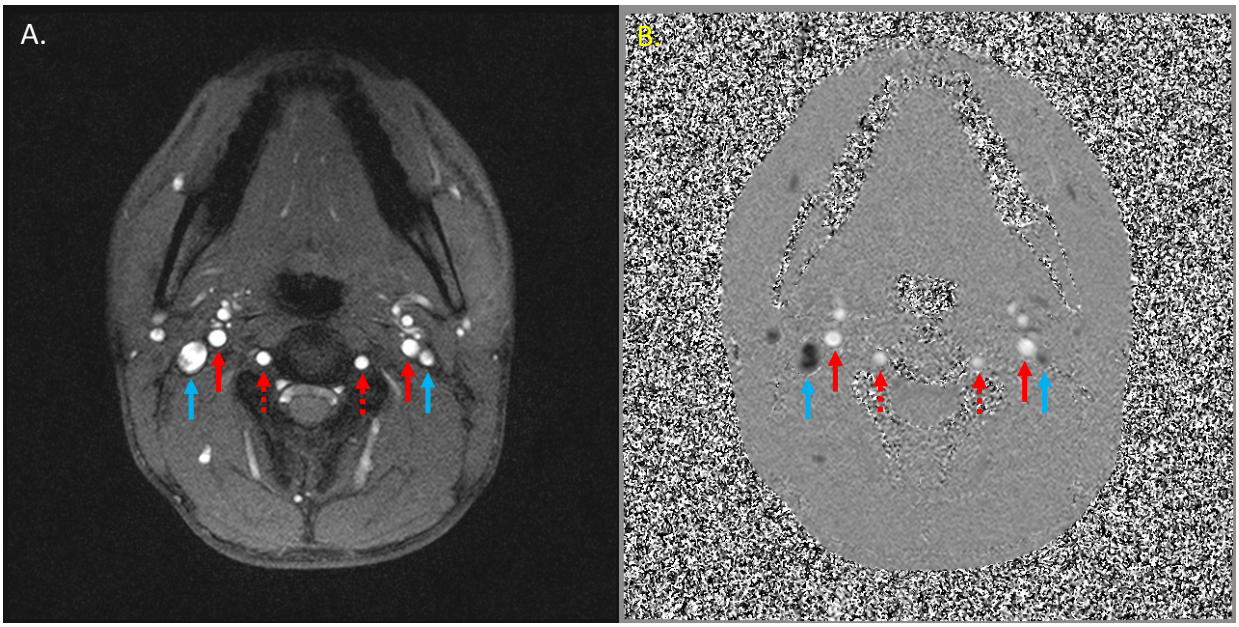

Figure 8: An anatomical (magnitude) image (A) and velocity (phase) image (B) from phase contrast-MRI scans taken between the second and third cervical vertebrae showing the bilateral internal jugular veins (blue arrows), internal carotid arteries (solid red arrows) and vertebral arteries (dashed red arrows)

PC-MRI scans were obtained with the following parameters: total TA (heart-rate dependent): 7-11 min, TR 21.4 ms, TE 6.71 ms, slice thickness 5 mm, 15° flip angle, 200 × 200 mm field of view, 320 × 320 acquisition matrix, 0.625 × 0.625 mm in-plane resolution with 32 calculated phases and two averages. Parallel imaging with a GRAPPA algorithm acceleration factor 2 was used with 24 reference lines. The velocity encoding value was 70 cm/s and retrospective peripheral pulse gating was used. Image analysis and post

processing was conducted with Segment v1.8 software (http://medviso.com/products/segment). A region of interest was drawn manually to delineate the lumen of the artery/vein, and an automated, contour-active model was then used to track the boundaries during the cardiac cycle (46). Blood flow was also calculated by multiplying the CSA (cm^2) by the blood flow velocity (cm/s) of the vessel. Total CBF was calculated as the sum of the mean blood flow through the bilateral ICAs and VAs and the total jugular venous outflow was calculated as the sum of the mean blood flow through the bilateral IJVs.

Cardiovascular and Respiratory Measurements

Several cardiovascular parameters were measured at baseline and after 1, 2, 3 and 4 h HDT during the various HDT conditions. Beat-by-beat mean arterial pressure (MAP), systolic blood pressure (SBP) and diastolic blood pressure (DBP) were measured continuously for 10 min with a Finometer (Finapres Medical Systems, Amsterdam, The Netherlands). In addition, subjects were donned with a 3-lead electrocardiogram to measure beat-by-beat heart rate (HR) (Biopac Systems, Goleta, California, USA). Respiratory parameters including end tidal CO_2 and minute ventilation were measured at supine baseline and after 3 h HDT with the Innocor system (Innovision, Odense, Denmark). Subjects breathed into the Innocor mouthpiece continuously for 10 min at each each measurement time point, with the last 5 min used for statistical analysis.

Statistical Analysis

Analysis of variance (ANOVA) and linear mixed effect models were created with time (baseline vs. HDT) and condition (-6°, -12°, -18°, -12° + 1% CO_2 and -12° + -20 mmHg LBNP) as main effects, allowing for a time-condition interaction, and subject ID as a random effect. For measurements taken bilaterally (IOP, PC-MRI, ONSD), side was included as an additional term to determine the effect of lateralization. The level for statistical significance was set to $\alpha = 0.05$ and β was set to 0.2. When main effects were found to be statistically significant, Bonferroni post-hoc analyses were implemented for further comparison. All data are presented as mean and standard deviation (SD) in the tables and shown as mean and standard error of the mean (SEM) in the figures to demonstrate uncertainty. Statistical

analyses were carried out with R (version 3.1.2, 64-bit, www.r-project.org) in the R-studio environment (version 0.98.1049).

8.1.4 Results

Intraocular Pressure[*]

IOP was found to have significant main effects of time ($F(1,158) = 132.2$, $p < 0.001$) and condition ($F(4,158) = 10.97$, $p < 0.001$) with a significant time-condition interaction ($F(4,158) = 7.4$, $p < 0.001$). In addition, a trend towards significance was found for eye lateralization as a main effect ($F(1,158) = 3.6$, $p = 0.06$). Post-hoc analysis revealed that after 3.5 h HDT, IOP increased from supine baseline (average of 15.3 ± 0.1 mmHg) to 17.9 ± 0.4 mmHg during -12° HDT ($p < 0.001$) and 18.7 ± 0.4 mmHg during -18° HDT ($p < 0.001$, Figure 9). However, IOP was unchanged from supine baseline during -6° HDT (16.3 ± 0.3 mmHg, $p = 0.6$). When comparing the HDT conditions, IOP increased step-wise from -6° to -12° HDT ($p < 0.001$) and further from -12° to -18° HDT ($p = 0.02$). The addition of a 1% CO_2 air mixture during -12° HDT resulted in a small decrease in IOP compared to -12° HDT plus ambient air ($p < 0.001$), although IOP was still increased compared to baseline in both conditions (Figure 9). IOP remained increased from 0° baseline with the addition of -20 mmHg LBNP during -12° HDT, with no further change from -12° HDT alone ($p = 0.2$).

[*] Intraocular pressure results from the enVIIP study have been published (84)

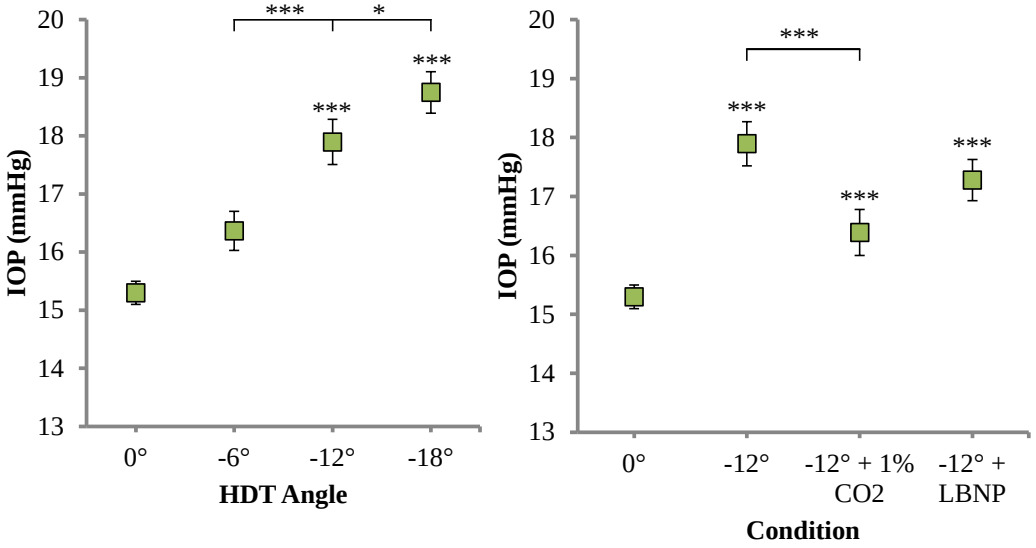

Figure 9: Intraocular pressure (IOP) at 0° baseline and during various head-down tilt (HDT) conditions, * $p < 0.05$, *** $p < 0.001$

Intracranial Pressure[†]

Significant main effects of time ($F(1,146) = 29.7$, $p < 0.001$) and condition ($F(4,146) = 7.6$, $p < 0.001$) were found for ICP, with a significant time-condition interaction ($F(4,146) = 6.9$, $p < 0.001$). Mean ICP during supine baseline was found to be 9.6 ± 0.3 mmHg. Post-hoc analysis revealed that ICP increased to 14.4 ± 1 mmHg after 3.5 h exposure to -18° HDT ($p < 0.001$), however, was not found to increase significantly during -6° or -12° HDT ($p = 0.9$ and $p = 0.4$, respectively; Figure 10). The addition of a 1% CO_2 environment during -12° HDT had no further effects on ICP compared to -12° HDT alone ($p = 0.7$). Further, -20 mmHg LBNP during -12° HDT had no further effects on ICP compared to -12° HDT without LBNP ($p = 0.6$).

[†] Intracranial pressure results from the enVIIP study have been published (84)

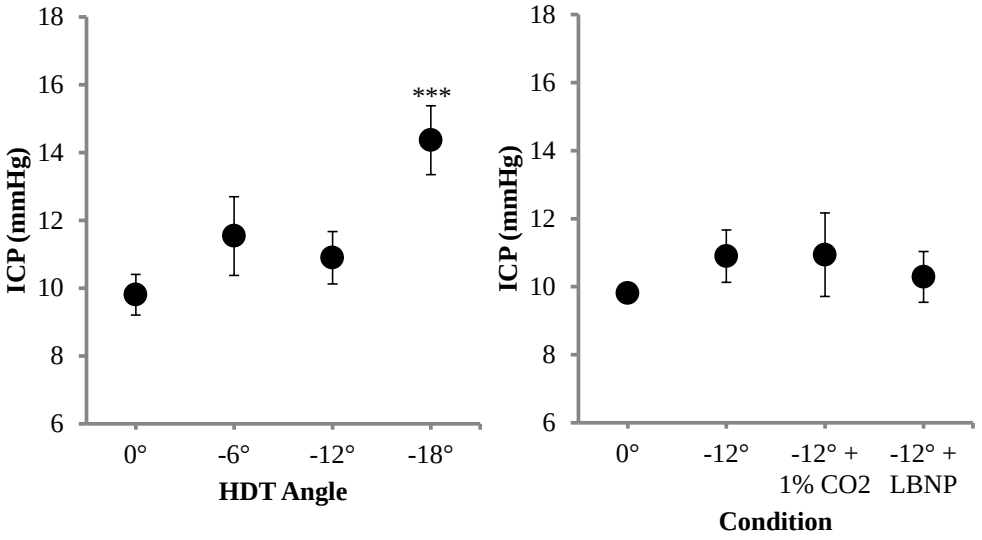

Figure 10: Intracranial pressure (ICP) at supine baseline and during various head-down tilt (HDT) conditions, *** $p < 0.01$

Optical Coherence Tomography: Choroidal and Retinal Nerve Fiber Layer Thickness

Mean sub-foveal choroidal thickness and global RNFL thickness measured in the upright and supine baseline positions and again after 1.5 and 3 h HDT are shown in Table 2. No significant main effects of time or condition were found for sub-foveal choroidal thickness ($F(3,151) = 1.4$, $p = 0.26$, and $F(4,151) = 0.85$, $p = 0.5$, respectively). Global periorbital RNFL thickness had a significant main effect of condition ($F(4,150) = 4.5$, $p = 0.02$) but not time ($F(3,150) = 1.6$, $p = 0.18$). No significant time-condition interactions were found.

Table 2: Mean sub-foveal choroidal thickness and global retinal nerve fiber layer (RNFL) thickness during upright and supine baseline measures and after 1.5 h and 3 h head-down tilt (HDT) during various conditions

Condition	Time Point			
	Baseline (upright)	**Baseline (supine)**	**1.5 h HDT**	**3 h HDT**
	Sub-foveal Choroidal Thickness (µm)			
-6° HDT	389 ± 70	403 ± 88	398 ± 83	400 ± 82
-12° HDT	388 ± 73	391 ± 76	398 ± 73	391 ± 82
-18° HDT	396 ± 83	392 ± 78	401 ± 77	403 ± 85
-12° HDT+ 1% CO_2	397 ± 86	399 ± 76	395 ± 87	401 ± 80
-12° + -20 mmHg LBNP	394 ± 91	399 ± 85	393 ± 76	391 ± 84
	Global RNFL Thickness (µm)			
-6° HDT	98 ± 7	98 ± 7	98 ± 7	98 ± 7
-12° HDT	97 ± 6	98 ± 6	98 ± 7	98 ± 6
-18° HDT	97 ± 7	98 ± 6	98 ± 7	99 ± 6
-12° HDT+ 1% CO_2	98 ± 7	99 ± 6	98 ± 6	98 ± 6
-12° + -20 mmHg LBNP	98 ± 7	98 ± 7	98 ± 7	99 ± 7

Data presented as mean ± SD, LBNP = Lower Body Negative Pressure

Phase Contrast Magnetic Resonance Imaging: Cross-Sectional Area, Blood Flow Velocity and Blood Volume Flow[‡]

PC-MR images were analyzed for 4/5 HDT conditions. The -12° HDT plus LBNP condition had to be excluded from analyses due to significant motion artifacts in 7/9 subjects.

Cross-Sectional Area and Blood Flow Velocity: On the arterial side, ICA CSA was found to have a main effect of time ($F(1,124) = 12.3$, $p < 0.001$) increasing slightly during -18° HDT compared to baseline (0.27 ± 0.03 cm^2 vs. 0.21 ± 0.01 cm^2, $p < 0.01$, Figure 11). In addition, a main effect of time ($F(1,124) = 69.5$, $p < 0.001$) and condition ($F(3,124) = 3.4$, $p = 0.02$) was found for ICA blood flow velocity. A decrease in ICA blood flow velocity was found during all

[‡] Phase contrast-MRI results from the enVIIP study have been published (83)

HDT angles from 22.4 ± 0.5 cm/s at baseline to 18.3 ± 1.4 cm/s at -6° (p = 0.01), 15.1 ± 1.2 cm/s at -12° (*p* < 0.001), 20 ± 1.6 cm/s at -12° with 1% CO_2 (p = 0.04), and 16 ± 1.2 cm/s at -18° HDT (p < 0.001, Figure 12). No change in total VA CSA or blood flow velocity was found.

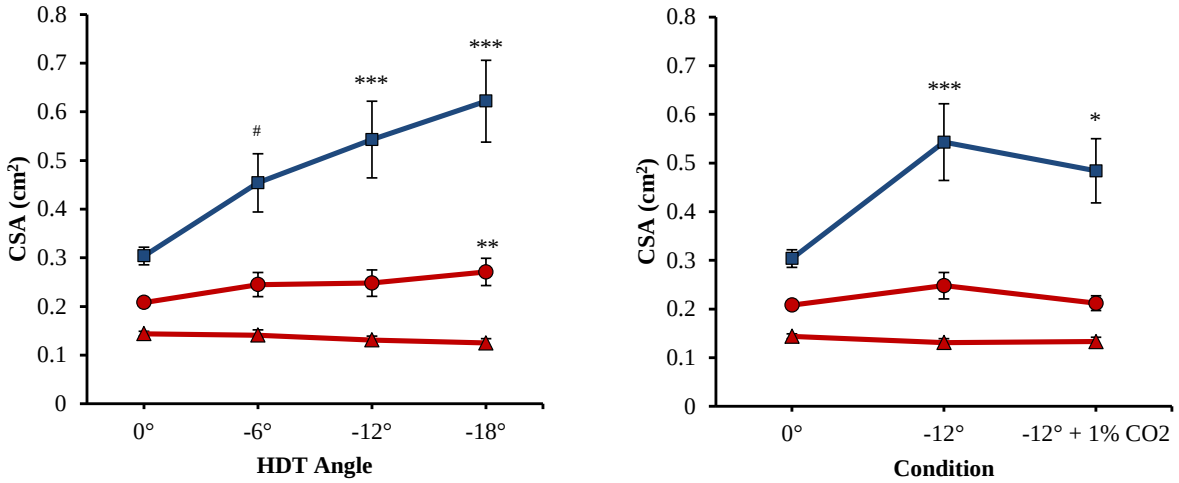

Figure 11: Cross-sectional area (CSA) of the internal jugular veins (blue), internal carotid arteries (red circles) and vertebral arteries (red triangles) during various head-down tilt (HDT) conditions, # p < 0.1, * p < 0.05, ** p < 0.01, *** p < 0.001

On the venous side, IJV CSA was found to have a significant main effect of time ($F(1,116) = 44.9$, $p < 0.001$), increasing from an average baseline of 0.304 ± 0.02 cm^2 at baseline to 0.54 ± 0.08 cm^2 during -12° (p < 0.001) and 0.62 ± 0.08 cm^2 during -18° HDT (p < 0.001; Figure 11). IJV CSA also increased from baseline to 0.48 ± 0.07 cm^2 during -12° HDT with 1% CO_2 (p = 0.04). With the HDT-induced increase in IJV CSA also came a significant main effect of time for IJV blood flow velocity ($F(1,116) = 25.9$, $p < 0.001$): IJV blood flow velocity decreased from an average of 14.9 ± 0.9 cm/s at baseline to 8.1 ± 1.3 cm/s during -12° (p < 0.001) and to 8.9 ± 1.8 cm/s during -18° HDT (p = 0.002, Figure 12).

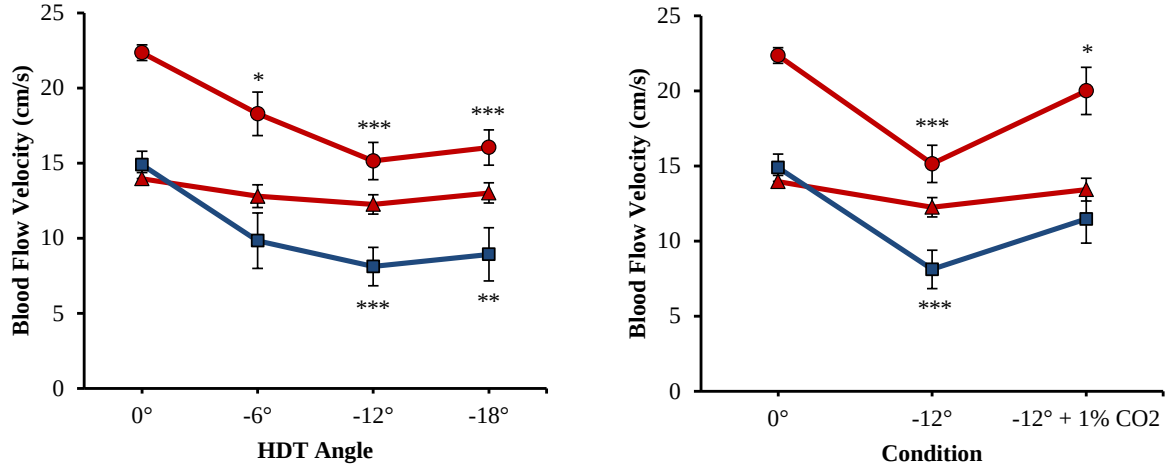

Figure 12: Blood flow velocity of the internal jugular veins (blue), internal carotid arteries (red circles) and vertebral arteries (red triangles) during various head-down tilt (HDT) conditions, * $p < 0.05$, ** $p < 0.01$, *** $p < 0.001$

Blood volume flow: Blood flow was automatically calculated by multiplying the velocity by the CSA for each vessel. Total arterial inflow is defined as the sum of the mean flow of the bilateral ICAs and VAs and the total jugular venous outflow is defined as the sum of the mean flow of the bilateral IJVs. Total arterial inflow was found to have a significant main effect of time ($F(1,53) = 51.7$, $p < 0.001$) and a trend towards significance for condition ($F(3,53) = 2.4$, $p = 0.07$). Total arterial inflow decreased from baseline during -6°, -12°, and -18° HDT ($p < 0.05$, $p < 0.001$ and $p = 0.002$, respectively, Figure 13). Interestingly, the maximum decrease was seen at -12° HDT compared to the average baseline (606 ± 40 ml/min vs. 782 ± 16 ml/min, respectively).

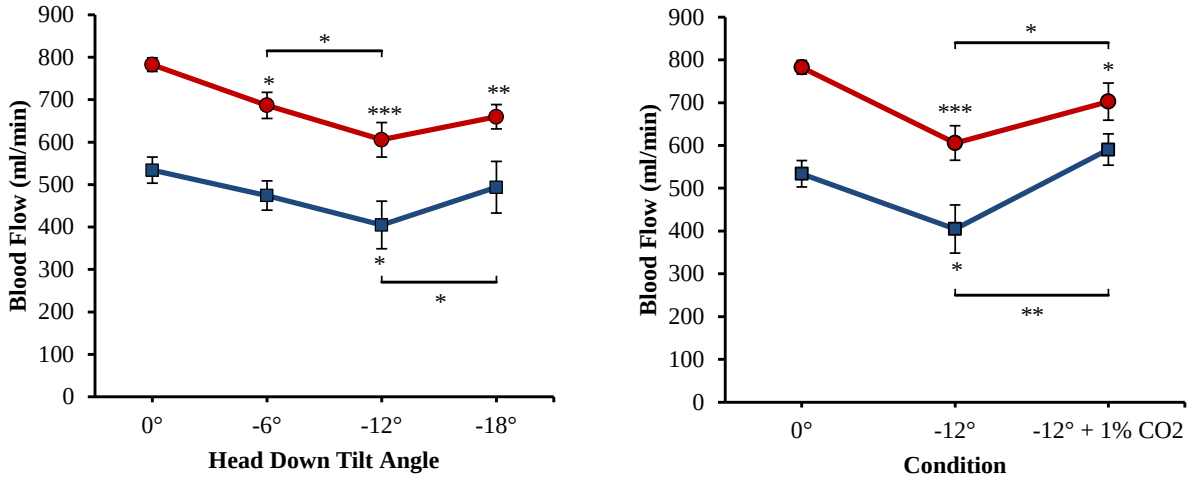

Figure 13: Total arterial inflow (red) and total internal jugular venous outflow (blue) during various head-down tilt conditions, * $p < 0.05$, ** $p < 0.01$, *** $p < 0.001$

Furthermore, the addition of 1% CO_2 during -12° HDT increased total arterial inflow compared to -12° HDT alone ($p = 0.02$), however, remained below baseline values ($p = 0.02$). The relative contribution of the ICAs versus VAs to total arterial inflow was consistent across all conditions with an average of 69% and 31%, respectively. Total internal jugular venous outflow was found to have a significant time-condition interaction ($F(3,47) = 2.9$, $p = 0.046$), with a decrease from baseline during -12° HDT ($p = 0.039$). In addition, an increase in total venous outflow was seen when going from -12° to -18° HDT ($p = 0.01$). Furthermore, in a similar manner to the total arterial inflow, total jugular venous outflow increased during -12° HDT with 1% CO_2 compared to -12° HDT alone ($p < 0.01$). Notably, there was a strong effect of lateralization, with 6/8 subjects having higher mean blood volume flow through the right IJV compared to the left.

Volumetric Magnetic Resonance Imaging: Cerebrospinal Fluid, Gray Matter and White Matter Volumes

Volumes for CSF, GM and WM were calculated and analyzed separately. For CSF volume, a main effect of time ($F(1,71) = 21.5$, $p < 0.001$) and a trend towards significance for condition ($F(4,71) = 2.2$, $p = 0.073$) were found. There was a small increase from 259 ± 10 ml at baseline to 264.4 ± 11 ml during -12° HDT ($p = 0.01$), however no significant change from baseline during any other HDT condition (Table 3). Notably, compared to -12° HDT, there was a trend towards significance with the addition of LBNP during -12° HDT, decreasing the

CSF volume to 260 ± 9.3 ml ($p = 0.055$). WM volume was found to have a significant main effect of condition ($F(4,71) = 2.7$, $p = 0.04$), with increased white matter volume during -12° HDT with LBNP compared to -12° HDT alone (579.6 ± 7.9 ml and 571.6 ± 8.6 ml, respectively, $p < 0.001$). GM volume was found to have a significant main effect of time ($F(1,71) = 6.5$, $p = 0.013$). However, both GM and WM volume displayed variations in baseline values (Table 3).

Table 3: MRI-derived cerebrospinal fluid (CSF), white matter and gray matter volumes at supine baseline (BDC) at during various head-down tilt (HDT) conditions

Condition	Time Point	
	BDC	**HDT**
	CSF Volume (ml)	
-6°	261 ± 28	264 ± 29
-12°	259 ± 30	264 ± 31*
-18°	258 ± 29	262 ± 31
-12° HDT + 1% CO_2	258 ± 30	261 ± 28
-12° HDT + LBNP	257 ± 28	260 ± 26
	White Matter Volume (ml)	
-6°	577 ± 20	571 ± 23
-12°	569 ± 24	572 ± 24
-18°	571 ± 19	571 ± 23
-12° HDT + 1% CO_2	575 ± 19	571 ± 22
-12° HDT + LBNP	574 ± 21	580 ± 22
	Gray Matter Volume (ml)	
-6°	718 ± 54	730 ± 52*
-12°	729 ± 50	726 ± 51
-18°	729 ± 47	731 ± 50
-12° HDT + 1% CO_2	724 ± 54	732 ± 52
-12° HDT + LBNP	721 ± 57	729 ± 54

Data presented as mean ± SD, LBNP = lower body negative pressure, * $p < 0.05$

Optic Nerve Sheath Diameter

Optimal transverse slices of the right and left ON were chosen for analyses. ONSD was measured 3, 4 and 5 mm posterior to the eye globe (Table 4).

Table 4: Optic nerve sheath diameter at 3, 4 and 5 mm posterior to the eye globe at baseline (0°) and after 4 h head-down tilt (HDT) in various conditions

	Measurement Point (Distance Behind Eye Globe)		
Condition	**3 mm**	**4 mm**	**5 mm**
0°	5.96 ± 0.62	5.82 ± 0.59	5.5 ± 0.53
-6° HDT	6.26 ± 0.54***	6.20 ± 0.66***	5.87 ± 0.65***
-12° HDT	6.32 ± 0.54***	6.24 ± 0.52***	5.86 ± 0.44***
-18° HDT	6.51 ± 0.57***	6.35 ± 0.62***	5.94 ± 0.6***
-12° HDT + 1% CO_2	6.29 ± 0.54**	6.20 ± 0.59***	5.82 ± 0.53***
-12° HDT + LBNP	6.16 ± 0.63	6.01 ± 0.64*	5.64 ± 0.6

Data presented as mean ± SD, LBNP = lower body negative pressure, * $p < 0.05$, ** $p < 0.01$, *** $p < 0.001$

ONSD measured 3 mm behind the eye globe are additionally presented in Figure 14, as this is the standard measurement distance in literature. ONSD had a significant main effect of time ($F(1,159) = 95$, $p < 0.001$) and condition ($F(4,159) = 2.5$, $p = 0.045$) with a significant time-condition interaction ($F(4,159) = 2.9$, $p = 0.02$) when measured 3 mm behind the globe. However, eye lateralization was not significant ($p = 0.3$). ONSD was found to increase from baseline during -6° ($p < 0.001$), -12° ($p < 0.001$), and -18° HDT ($p < 0.001$, Figure 14), with subsequent increase from -12° to -18° HDT ($p = 0.02$).The addition of a 1% CO_2 atmosphere to -12° HDT, however, had no further effects on ONSD compared to -12° HDT with ambient atmosphere ($p = 0.66$). Interestingly, the addition of -20 mmHg LBNP decreased ONSD compared to -12° HDT alone ($p = 0.03$), however ONSD was still slightly increased (trend towards significance) compared to supine baseline ($p = 0.08$, Figure 14).

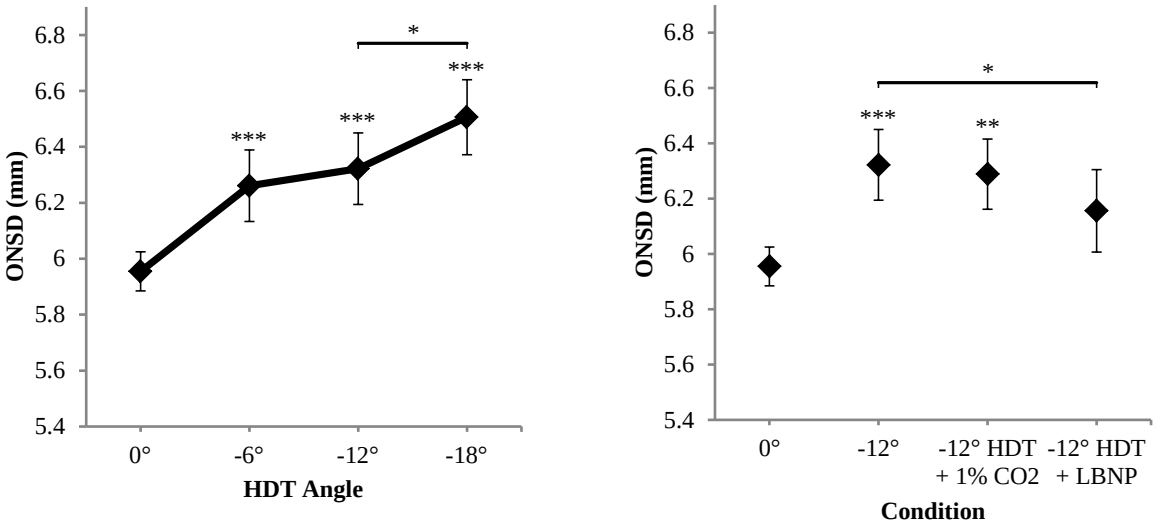

Figure 14: Optic nerve sheath diameter (ONSD) measured 3 mm behind the eye globe at 0° baseline and during various head-down tilt (HDT) conditions, LBNP = lower body negative pressure, * $p < 0.05$, ** $p < 0.01$, *** $p < 0.001$

Cardiovascular and Respiratory Parameters[§]

A significant main effect of time was found for MAP ($p = 0.046$), DBP ($p < 0.001$), SBP ($p < 0.001$) and HR ($p = 0.026$), and a significant main effect of condition was found for MAP ($p < 0.001$), DBP ($p = 0.01$) and HR ($p < 0.001$). Post hoc comparisons to baseline are shown in Table 5. No time-condition interactions were found to be significant for any cardiovascular parameter.

[§] Cardiovascular and respiratory parameters from the enVIIP study have been published (83, 84)

Table 5: Cardiovascular parameters measured at baseline (BDC) and after 1 h, 2 h, 3 h and 4 h head-down tilt (HDT) during various conditions

Condition	Time Point				
	BDC	1 h HDT	2 h HDT	3 h HDT	4 h HDT
	Mean Arterial Pressure (mmHg)				
-6°	73.2 ± 10.8	77.4 ± 12.7	79.6 ± 11.0	82 ± 15.3	87.9 ± 11.2***
-12°	75.3 ± 13.7	79.4 ± 9.2	78.5 ± 13.5	81.8 ± 17	84.7 ± 14.3
-18°	71 ± 7.2	74 ± 7.8	78.5 ± 14.6	84.3 ± 8.4**	82.1 ± 10.8*
-12° + 1% CO_2	76.9 ± 12.1	77.3 ± 10.4	79.9 ± 7.9	81.4 ± 7.7	84 ± 12.2
-12° + LBNP	73.6 ± 6.3	81.1 ± 9.4	83.4 ± 10.4	89.1 ± 12.1***	92.9 ± 10.5***
	Systolic Blood Pressure (mmHg)				
-6°	123.3 ± 17.4	127.7 ± 13.9	129.6 ± 12.9	135.8 ± 19.8	141 ± 14.7**
-12°	125.3 ± 9.9	126.1 ± 14.1	128.1 ± 15.6	135.4 ± 18.7	138.2 ± 15.9
-18°	124.7 ± 11.4	121 ± 16	126.5 ± 16.9	134.1 ± 15.5	131.5 ± 20.3
-12° + 1% CO_2	134.4 ± 14.7	125.4 ± 12.9	128.1 ± 14.1	132.4 ± 11.8	135.9 ± 16
-12° + LBNP	127.3 ± 11.5	127.4 ± 10.5	130.3 ± 14.7	140.8 ± 12.8	140.8 ± 13.6
	Diastolic Blood Pressure (mmHg)				
-6°	56.3 ± 9	60.1 ± 11.6	63.1 ± 9.4	64.1 ± 12.9	68.7 ± 9.7**
-12°	58.8 ± 13.4	63.4 ± 8.1	61.4 ± 12.8	63.6 ± 16.8	66.1 ± 13.2
-18°	53.3 ± 6.8	58.5 ± 7.2	62.2 ± 12.1	67.2 ± 7.9**	65 ± 9.1*
-12° + 1% CO_2	59.3 ± 11.4	61.4 ± 9.6	63.3 ± 6.8	64.2 ± 7.7	66.5 ± 10.5
-12° + LBNP	57.2 ± 6.1	65.6 ± 9.6	66.6 ± 9.5	70.9 ± 12.2**	75.3 ± 10.7***
	Heart Rate (BPM)				
-6°	61.9 ± 9.7	59.5 ± 7.9	60.1 ± 8.9	60 ± 7.7	60.8 ± 8.1
-12°	65.1 ± 8.8	62.4 ± 9.3	59.7 ± 9.4	60.6 ± 10.7	63.3 ± 11.7
-18°	59.8 ± 8.2	57.6 ± 6.7	58 ± 7.4	59 ± 6.3	58 ± 9.3
-12° + 1% CO_2	60.1 ± 9.6	58.4 ± 9.8	58.6 ± 6.5	55.7 ± 9.4	60.4 ± 11.9
-12° + LBNP	61.9 ± 10.7	61.4 ± 9.9	58.7 ± 10.2	59.4 ± 12	62.6 ± 13.1

Data presented as mean ± SD, LBNP= lower body negative pressure, BPM = beats per minute, * $p < 0.05$, ** $p < 0.01$, *** $p < 0.001$

Respiratory parameters are shown in Table 6. End tidal CO_2 had a significant time-condition interaction ($F(4,77) = 4.2$, $p = 0.004$) and post-hoc analysis revealed increased end tidal CO_2 during -12° HDT with 1% CO_2 compared to -12° HDT with ambient air ($p = 0.004$). No significant main effects were found for minute ventilation.

Table 6: Respiratory parameters at supine baseline (BDC) and after 3 h head-down tilt (HDT) during various conditions

Condition	Time Point	
	BDC	HDT
	$ETCO_2$ (%)	
-6°	5.14 ± 0.74	4.52 ± 0.56
-12°	4.98 ± 0.96	4.76 ± 0.87
-18°	4.8 ± 0.97	4.67 ± 0.75
-12° + 1% CO_2	4.8 ± 0.68	5.23 ± 0.75
-12° + LBNP	4.87 ± 0.8	4.8 ± 0.56
	Minute Ventilation (l/min)	
-6°	7.96 ± 3.12	8.17 ± 2.75
-12°	9 ± 3.02	9.51 ± 3.66
-18°	8.52 ± 3.97	8.8 ± 4.2
-12° + 1% CO_2	8.51 ± 3.98	8.17 ± 3.45
-12° + LBNP	8.26 ± 3.31	8.66 ± 3.17

Data presented as mean ± SD, $ETCO_2$ = end tidal CO_2, LBNP = lower body negative pressure

8.2 The SpaceCOT Study: Studying the Physiological and Anatomical Cerebral Effects of CO_2 and Tilt on Intracranial and Intraocular Pressure

8.2.1 Study Design[**]

The SpaceCOT study was an internationally collaborative study between several institutions (a full list of investigators and institutions is provided in the Appendix, Document A 4). The study consisted of a randomized, double-blinded cross-over design with two conditions: 26 h -12° HDT with ambient air and 26 h -12° HDT with 0.5% CO_2 (Figure 15). The two HDT conditions exhibited identical study procedures, with the exception that prior to baseline data collection on day 1 (before the first condition), subjects came in one day early for a familiarization session to be introduced to all experimental techniques and the timeline of the study. Baseline data was collected in the seated, upright position, followed by a random HDT condition the following day. Atmospheric conditioning is possible in the entire bedrest module of the envihab facility (all bedrooms, bathrooms and common spaces) and was monitored by an independent operator, allowing for the condition to be blinded. In addition, after 26 h HDT (and while still in the -12° HDT position), subjects were exposed to a 3% CO_2 atmosphere through a mask and tank system for 3 h to determine the effects of short-term exposure to a high CO_2 concentration, similar to what astronauts may experience in areas with poor ventilation on the ISS.

[**] The SpaceCOT study design and Figure 15 are included in paper #3 from section 11.1 (currently in revision)

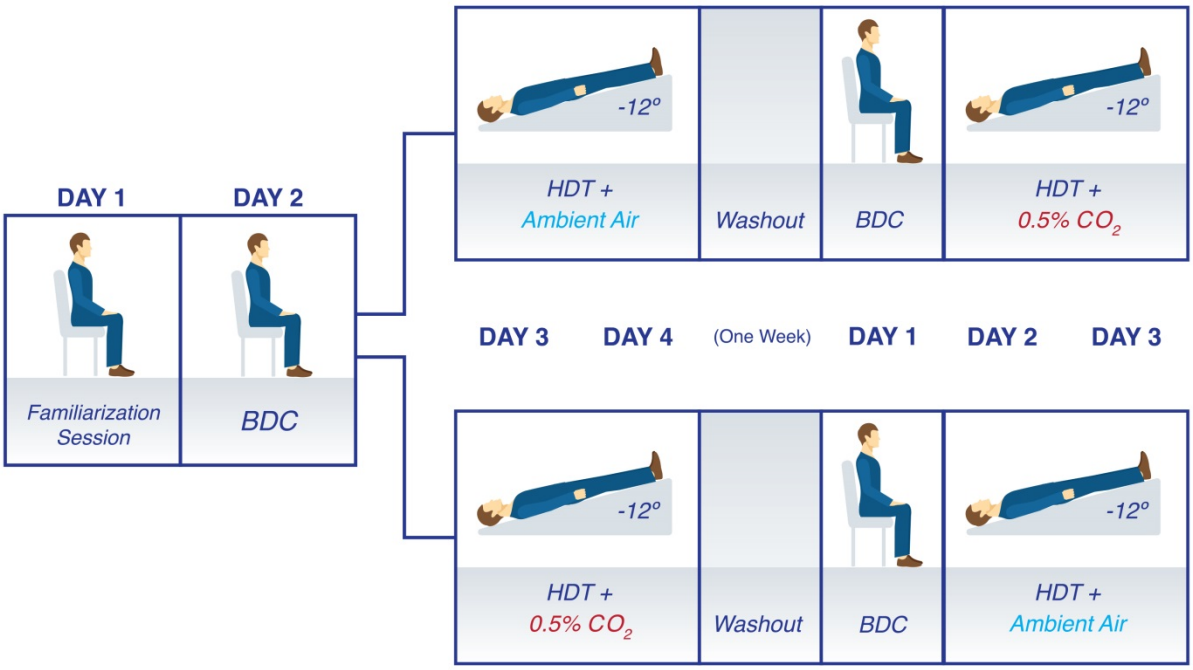

Figure 15: The SpaceCOT study consisted of a randomized, cross-over design with two campaigns: the first campaign included a familiarization session followed by a full day of baseline data collection (BDC) and then 29 h of -12° head-down tilt (HDT) with either ambient air of 0.5% CO_2. After a one week washout period, the subjects returned for the second campaign consisting of a full day of BDC followed by 29 h of -12° HDT with either 0.5% CO_2 or ambient air.

During the full 29 h of bedrest, all subjects strictly adhered to the -12° HDT position (including during all daily activities such as eating, washing and going to the bathroom). Subjects were allowed to lie on their side, however, one shoulder was in contact with the mattress at all times (sitting or standing not permitted). Nutritional intake was controlled and standardized according to well-established formulas issued by the World Health Organization (135). The presented findings from the SpaceCOT study represent a subset of results from the larger collaborative study. A complete timeline of all measurements in the study is provided in Table A 2 of the Appendix.

8.2.2 Subjects

Six healthy, male subjects (mean ± SD age: 41 ± 5 y, height: 177 ± 4 cm and weight: 82 ± 8 kg) were enrolled in the study. Prior to inclusion in the study, all subjects underwent a comprehensive medical examination including psychological questionnaire, oral medical history interview, blood and urine samples, resting and stress electrocardiogram (through

cycle ergometer exercise), an eye examination, a stand test for orthostatic tolerance and thrombosis screening. In addition, subjects were introduced to -12° HDT, to the MRI, and to the Vittamed non-invasive ICP measurement to ensure eligibility and full understanding of the study intervention. Inclusion criteria included male subjects age 30-55 with cardiovascular, exercise capacity and mental health approximately matching the astronaut corps. Exclusion criteria included smoking, drug or alcohol abuse, migraine and existing ophthalmic conditions.

8.2.3 Materials and Methods

Intraocular and Intracranial Pressure Measurements

IOP was measured with an Icare Pro tonometer (Icare, Helsinki, Finland) at baseline in the seated position, and after 1.5 h, 6.5 h and 22.5 h HDT. In addition, IOP was measured during exposure to 3% CO_2 (27 h HDT). IOP was measured 3 times in each eye in a randomized order. ICP was measured with the Vittamed non-invasive ICP meter (Vittamed, Kaunas, Lithuania) at seated baseline and after 3 h, 7 h and 22 h HDT. ICP was measured 1-2 times at each measurement time point.

Statistical Analysis

ANOVA and linear mixed effect models were created with time and atmosphere as main effects, allowing for a time-atmosphere interaction, and subject ID as a random effect. For IOP, side was included as an additional term to determine the effect of lateralization. The level for statistical significance was set to $\alpha = 0.05$ and β was set to 0.2. When main effects were found to be statistically significant, Bonferroni post-hoc analyses were used to for further comparison. Statistical analyses were carried out with IBM SPSS Statistics Version 20 (IBM, Armonk, NY).

8.2.4 Results

Intraocular Pressure

IOP was found to have a significant main effect of time ($F(4,368) = 37.8$, $p < 0.001$), atmosphere ($F(1,368) = 5.03$, $p = 0.026$) and side ($F(1,368) = 10.6$, $p = 0.001$), however, with no significant interactions. In both atmospheric conditions, IOP increased from seated baseline during 3 h, 7 h and 22 h HDT exposure (Figure 16). After 27 h HDT with ambient air, the addition of short exposure to 3% CO_2 decreased IOP back to baseline values ($p = 0.03$).

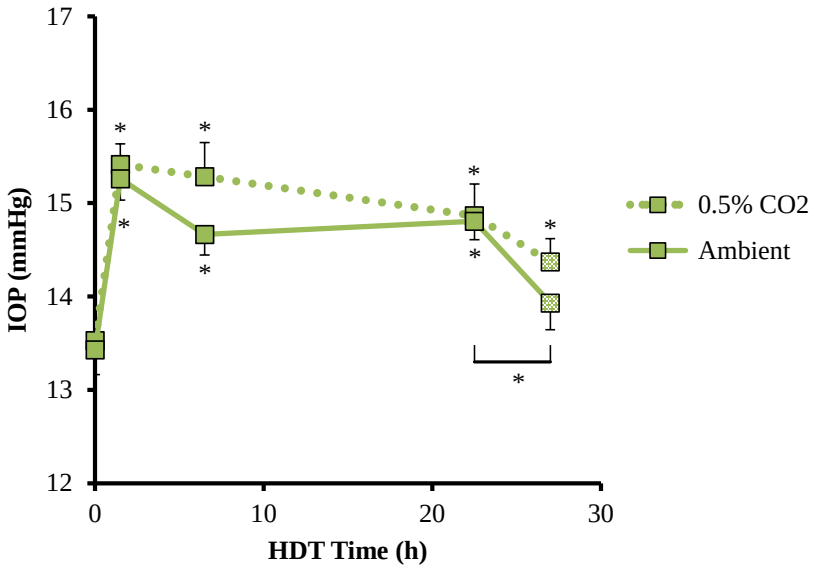

Figure 16: Intraocular pressure (IOP) at seated baseline and at various time points of exposure to -12° head-down tilt (HDT) with ambient air (solid line) or 0.5% CO_2 (dotted line). IOP was also measured after 27 h HDT during 3% CO_2 exposure. * $p < 0.05$

Intracranial Pressure[††]

ICP was found to have a significant main effect of atmosphere ($F(1,69) = 5.2$, $p = 0.025$), but not time ($F(3,69) = 1.3$, $p = 0.29$), with no significant interaction term ($F(3,69) = 0.6$, $p = 0.6$) (Figure 17).

[††] Intracranial pressure results from the SpaceCOT Study have been submitted for publication (paper #6, section 11.1)

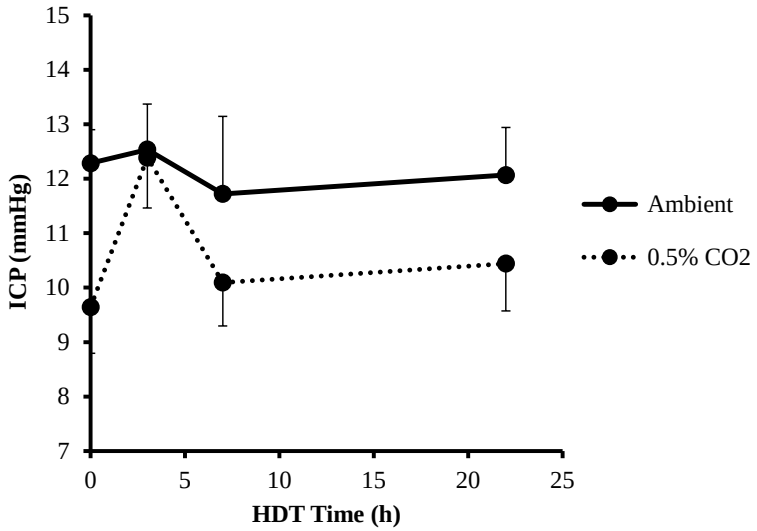

Figure 17: Intracranial pressure (ICP) at seated baseline and after 3 h, 7 h and 22 h head-down tilt (HDT) with ambient air (solid line) or 0.5% CO_2 (dotted line)

8.3 The SETI Study: Studying the Effects of Tilt with Lower Body Negative Pressure on Intraocular Pressure

8.3.1 Study Design

The third study, the SETI study, was designed to further elucidate the effects of a stronger level of LBNP (-40 mmHg) for shorter durations with an extended range of tilt angles on IOP. The experimental protocol (Figure 18) consisted of 12 randomized conditions: +12°, 0°, -6°, -12°, -18°, -24° tilt, and +12°, 0°, -6°, -12°, -18°, -24° tilt with -40 mmHg LBNP. Subjects remained in the 0° position for 30 min prior to the first condition. Then, each randomized tilt angle (with or without LBNP) was maintained for 5 min followed by a 10 min recovery period in the supine position before proceeding to the next condition. After the 6th condition, the subject was removed from the tilt table/LBNP chamber for a urination break and to consume 100 ml of water. The experiment then resumed with the last 6 randomized conditions.

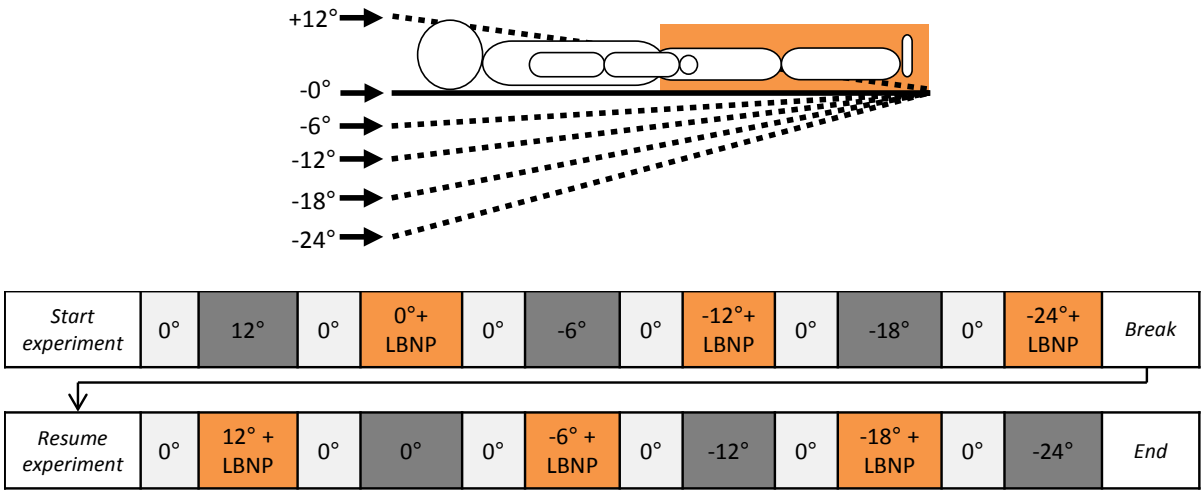

Figure 18: The SETI Study consisted of 6 tilt angles with and without -40 mmHg lower body negative pressure (LBNP) for a total of 12 randomized conditions. Each tilt condition was maintained for 5 min followed by 10 min in the 0° position before proceeding to the next condition.

The experiment was conducted on a custom-built automatic tilt table with an integrated LBNP chamber (shown in the Appendix, Figure A 3). The LBNP chamber was sealed at the iliac crest for each subject and air conditioning was maintained inside the LBNP chamber during all conditions.

8.3.2 Subjects

Sixteen healthy subjects (8 male, 8 female, mean ± SD age: 27 ± 4 y, height: 174 ± 10 cm and weight: 69 ± 13 kg) were enrolled in the SETI study. All subjects underwent a basic medical examination prior to inclusion in the study which included an oral medical history interview, resting electrocardiogram, exercise test for endurance capacity and a standing test for orthostatic intolerance assessment. Inclusion criteria consisted of subjects between the ages of 20-45 yrs, BMI of 20-26 kg/m^2 and a height of 158-190 cm. Subject exclusion criteria included smoking, current prescription medication use, history of cardiovascular diseases and severe orthostatic intolerance.

8.3.3 Materials and Methods

Intraocular Pressure Measurements

IOP was measured with an Icare Pro tonometer (Icare, Helsinki, Finland). Measurements were taken between the 9-10^{th} min at supine baseline between each condition, and between the 4-5^{th} min of tilt. Two-three IOP measurements were taken in each eye at every time point in a randomized order.

Statistical Analysis

All statistical analyses were carried out with R version 3.1.2 64-bit (www.r-project.org) in the R-studio environment (version 0.98.1049). ANOVA and linear mixed effect models were constructed with time (baseline and HDT), condition and side as main effects and subject as a random effect. In addition, the model allowed for a time-condition interaction. Bonferroni post-hoc analyses were implemented for further comparison when main effects were found to be significant. The level for statistical significance was set to $\alpha = 0.05$ and β was set to 0.2.

8.3.4 Results[‡‡]

Intraocular Pressure

IOP had significant main effects of both time ($F(1,767) = 65.5$, $p < 0.001$) and condition ($F(11,767) = 17.9$, $p < 0.001$), with a significant time-condition interaction ($F(11,767) = 21.7$, $p < 0.001$). In addition, there was a trend towards significance for eye lateralization ($F(1,767) = 5.1$, $p = 0.05$). Post-hoc analysis revealed that IOP increased from an average baseline of 14.7 ± 0.1 mmHg to 15.7 ± 0.4 mmHg during -12° HDT ($p = 0.02$), 16.5 ± 0.3 mmHg during -18° HDT ($p < 0.001$) and 18.4 ± 0.4 mmHg during -24° HDT ($p < 0.001$) (Figure 19). The use of -40 mmHg LBNP during HDT successfully counteracted these increases in -12° and -18° HDT, with no significant increase from baseline during these conditions ($p = 0.99$ and $p = 0.73$, respectively). LBNP also lowered the IOP to 16 ± 0.3 mmHg during -24° HDT, however, IOP was still increased from supine baseline ($p < 0.001$).

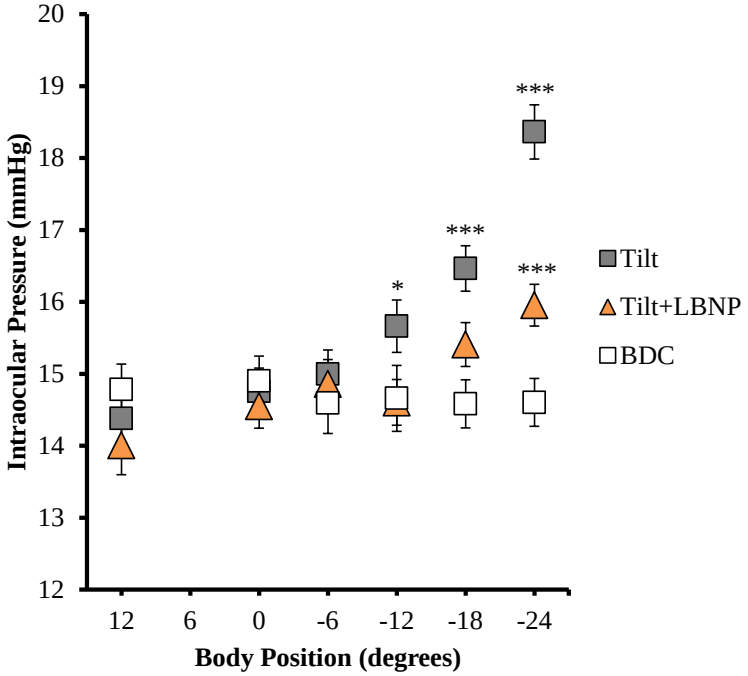

Figure 19: Intraocular Pressure at supine baseline (BDC) and during various degrees of whole body tilt with and without lower body negative pressure (LBNP); * $p < 0.05$, *** $p < 0.001$

[‡‡] Intraocular pressure results from the SETI study have been published (84).

9 Discussion

The recently discovered structural and functional ophthalmic changes that occur during and after long-duration spaceflight represent a maladaptive physiological response to extended microgravity exposure. While the exact etiology of these ocular changes is currently unknown, cephalad fluid shifting due to the loss of physiologic hydrostatic pressure gradients in microgravity is hypothesized to be a major underlying factor. Here, three studies were implemented to further understand the effects of cephalad fluid shifting through HDT on cerebral and ocular anatomy and physiology as well as the additive or attenuating effects of increased ambient CO_2 and LBNP, respectively. Notably, two of the presented studies represent the first experiments to investigate the combined effects of HDT and increased ambient CO_2, hypothesized to be a more realistic analog to the unique ISS environment. Furthermore, the use of LBNP during HDT was tested as a potential countermeasure to cephalad fluid shifting at low and strong levels for short (5 min) and moderate durations (5 h) to test for feasibility of use and efficacy. Overall, the presented experiments and subsequent findings set a foundation for future studies investigating cerebral and ocular anatomy and physiology in a ground-based spaceflight analog to build upon and have determined key factors that may help elucidate the causative mechanisms of ocular changes in astronauts, namely the roles of the translaminar pressure difference, cerebral hemodynamics and cerebral venous congestion.

9.1 Cerebral Hemodynamics

Central to the hypothesized underlying mechanisms of ocular changes in astronauts is a disruption in the cerebral hemodynamic system, likely due to decreased cerebral venous outflow and increased cerebral venous pressure (Figure 3). PC-MRI was utilized to study the effects of cephalad fluid shifting through various degrees of HDT as well as increased ambient CO_2 on the CSA, blood flow velocity and blood volume flow in the major vessels of the neck. The results demonstrated that HDT induced a decrease in arterial and venous blood flow and velocity as well as a large increase in IJV CSA. Notably, breathing 1% CO_2 during HDT increased blood flow on both the arterial and venous side compared to HDT with ambient atmosphere, bringing blood flow closer to supine baseline values.

CBF velocity has been investigated previously in both HDT and microgravity, however, with inconsistent results. Previously, CBF velocity through the middle cerebral

artery (MCA) was found to increase when going from the upright seated position to the supine position, however no further change was detected going from the supine to the -15° HDT position in healthy subjects (10). In another study, during 24 h exposure to -6° HDT, CBF velocity through the MCA was found to increase compared to seated baseline values, peaking at 3 h HDT and remaining increased during the full 24 h (60). During 48 h exposure to -10° HDT, MCA CBF velocity also increased immediately, but slowly decreased over 48 h HDT, back to seated baseline values (38). However, in another study where subjects underwent 21 d exposure to -6° HDT, MCA CBF velocity decreased immediately and remained below baseline values, although baseline posture was not reported (115). During spaceflight, no change in MCA CBF velocity was detected after 10 h or 1-2 weeks of microgravity exposure (12, 54). The discrepancy between the decreased arterial blood flow velocity found in the enVIIP study and the aforementioned HDT and spaceflight studies may be due to differences in methodologies (TCD vs. PC-MRI), comparative baseline posture or vessels measured. Notably, the ICA is known to have a lower blood flow velocity than the MCA (70), and changes in blood flow and velocity induced by environmental factors have been shown to affect vessels differently (130).

Furthermore, both total arterial inflow and jugular venous outflow were found to decrease during HDT in a non-linear manner. Regulation of CBF is vital for brain homeostasis and is controlled by a number of interrelated physiological factors including cerebral autoregulation, cerebral perfusion pressure (CPP; MAP - ICP), metabolic demands, partial pressures of O_2 and CO_2, and the autonomic nervous system (131). Due to impeded intracranial venous outflow during HDT, post-capillary pressure may have been increased, affecting the CPP gradient and thus, resulting in the demonstrated decrease in arterial blood flow. However, between -12° and -18° HDT, blood flow did not decrease further, but rather achieved steady-state or even increased slightly. Potential explanations considered include an accumulation of CBF-regulating metabolites including K^+ and CO_2 or an increased cerebral metabolic rate of oxygen consumption due to anxiety; however, no change in pulse rate was detected. Further, it is possible that shifting of abdominal contents during HDT affected minute ventilation, thus raising the $PaCO_2$ and increasing CBF. However, no changes in minute ventilation were detected during any HDT angle and $ETCO_2$ was unchanged between -12° and -18° HDT. Interestingly, cerebral hemodynamic impairment, hypo-perfusion and altered CBF regulation have been proposed as etiological factors in mild cognitive

impairment (85). In healthy controls, an acute lowering of CBF by 30% is associated with mild symptoms of cerebral hypo-perfusion, and lowering CBF by 50-60% can induce mental confusion (113). Further investigation of CBF and cognitive abilities during longer-duration exposure to HDT are warranted. Currently, astronauts do not appear to have significant cognitive issues during 6-month missions in space as they are still able to perform their tasks nominally. However, when discussing longer exploration missions (2+ years), it is unknown how the cerebral vascular system will be affected and potential cognitive issues thereafter.

Compared to the cerebral arterial system, fewer studies have been devoted to the physiological assessment of the cerebral venous system, which is known to have asymmetric anatomy along with significant individual and hemispheric variations (4, 104). However, the cerebrovascular system is central to the maintenance of cerebral perfusion and ICP. Progressive increases in IJV CSA with HDT found in the enVIIP study are presumably due to increased jugular venous pressure from the newly established hydrostatic pressure gradient and demonstrate the compliance of the venous system. Increased IJV CSA has been previously described during -6° HDT exposure and was found to remain increased after 42 days of HDT (8). Increased IJV CSA has also been found in microgravity, remaining distended even after 5 months of spaceflight (8, 47); however, this could also be due to tissue weight unloading in the neck. In a study by Arbeille et al. (2015), increases in both IJV and portal vein volumes were found after 15 days of microgravity exposure (178% and 36%, respectively) and remained increased after ~5 months in space, indicating blood pooling in the cephalad and, to a lesser extent, pelvic regions during spaceflight (9).

Jugular venous outflow followed a similar pattern as arterial inflow during HDT. Extra-jugular pathways (i.e., the vertebral veins) were not measured in the current study; however, the IJVs are known to be the dominant outflow pathway in the supine and presumably HDT positions (80). The IJVs accounted for ~70% of the arterial inflow at supine baseline and during HDT, in-line with previously reported values (5, 13, 114). Interestingly, the proportion of cerebral venous outflow through the IJVs increased to about 85% during -12° HDT with the addition of 1% CO_2, suggesting a relative reduction in return through the vertebral veins. Notably, increased ambient CO_2 during HDT counteracted the HDT-induced decrease in cerebral arterial inflow and venous outflow, bringing blood volume flow close to supine baseline levels. Hypercapnia and increased $PaCO_2$ is known to have potent vasodilatory effects, increasing CBF. However, the combined effects of HDT and CO_2 have

not been investigated. Paradoxically, a low-level hypercapnic environment appears to be beneficial instead of detrimental to the blood flow rates, tending to return them back to baseline values.

9.2 Intraocular and Intracranial Pressure

The aforementioned disruptions to the cerebral hemodynamic system are hypothesized to be the main underlying factor influencing both IOP and ICP. In the presented experiments, IOP and ICP increased with HDT, although in a divergent way. IOP was found to increase with steeper HDT angles immediately (the SETI study) and remained increased after several hours of HDT (the enVIIP study). However, a slow decrease in IOP was seen over 22 h HDT exposure (the SpaceCOT study). ICP on the other hand was only found to increase significantly with steeper HDT (-18° HDT). Thus, it is important to take both ICP and IOP into consideration when discussing pathologies related to the ONH and subsequent vision changes as disruptions to the homeostatic TLPD can have significant effects on ocular structures and vision.

Previous studies have demonstrated that IOP increases immediately upon exposure to both real (7, 76) and simulated microgravity (75), consistent with the presented results of the SETI and enVIIP study. This immediate increase in IOP is hypothesized to be due to increased cerebral venous pressure and vortex venous pressure resulting in engorgement of the choroid; this would then increase intraocular volume resulting in an immediate spike in IOP. Increased choroid thickness/area during HDT (107) as well as short-duration exposure to microgravity (7) have been previously demonstrated. However, in the enVIIP study, no change in sub-foveal choroid thickness was found during HDT. This may be due to instrument and body position limitations in the enVIIP study: the head had to be placed on a horizontal platform in front of the camera and therefore, the head was not in line with the HDT angle possibly alleviating choroidal congestion. In addition to choroidal engorgement, increased episcleral venous pressure and therefore increased aqueous humor outflow resistance may also play a role in the sustained increases in IOP seen in the first days of HDT (79) and spaceflight (32). Interestingly, within one week of both HDT (24) and microgravity exposure (32, 106), IOP appears to normalize back to baseline values. IOP has also been found to decrease below baseline values post-HDT bed rest (79) as well as post-spaceflight (31). As a compensatory decrease in aqueous humor volume in response to increased

choroidal volume is hypothesized to occur in space, re-introduction to the hydrostatic pressure gradients associated with the upright position on Earth would then decrease choroid volume and result in a drop in IOP below baseline until aqueous humor volume returned to normal.

According to the Davson equation (25; Equation 1-1), ICP is highly dependent on the cerebral venous pressure. As the venous system is a fully communicating fluid system and thus subject to hydrostatic pressure gradients (53), ICP is also hypothesized to increase with HDT. Several studies have demonstrated the postural variations of ICP, increasing about 11-14 mmHg when going from the upright to the supine position (34, 96, 99). During 5 min exposure to -10° and -20° HDT, Petersen et al. (2016) found ICP to increase 4.9 and 9.6 mmHg, respectively, from supine baseline. Eklund et al. (2016) found ICP to increase 4 mmHg after 3 min exposure to -9° HDT (34). Other non-invasive methodologies implemented during HDT including tympanic membrane displacement (91) and cranial ultrasound pulse amplitude techniques (75) suggest increased ICP, however, absolute ICP values cannot currently be derived from these techniques. Increased ICP can also cause cortical bridging veins that transverse through the SAS to collapse. These veins thus act as starling resistors, causing increased cerebral venous outflow resistance when CSF pressure exceeds cerebral venous pressure (17).

In any fully communicating fluid system, the pressure at a specific point can be determined by its distance from the hydrostatic indifference point, the point in a fluid system where pressure is unaffected by body position (86). Thus, ICP changes with body position can be predicted by hydrostatic pressures using the following equation:

$$ICP(\alpha) = ICP(0°) - (p \times g \times L) \times \sin(\alpha) \qquad \text{Equation 3-1}$$

where α is the HDT angle, p = density of the liquid, g = acceleration due to gravity, and L is the distance from the reference point. Based on the findings from invasive measures by Petersen et al. (2016), the distance from the external auditory meatus to the reference point (L), which likely corresponds to the hydrostatic indifference point of the venous system, is about 37 cm (96). Thus, the predicted increase in ICP based on hydrostatic pressure gradients alone with -6°, -12° and -18° HDT is 2.9, 5.8 and 8.7 mmHg, respectively. In healthy subjects, no changes in ICP were detected at -6° or -12° HDT in either the enVIIP

or SpaceCOT studies, however, a ~5 mmHg increase in ICP was found after 3.5 h of -18° HDT in the enVIIP study. This discrepancy may partially be accounted for by the non-invasive technique implemented. The TCD-based non-invasive ICP measurement utilized in the enVIIP and SpaceCOT studies has been previously found to have correlation good with invasive measures with a mean difference of 4.5 mmHg between paired measurements (19). It is therefore possible that ICP was slightly increased during -6° and -12° HDT, however, was not detected by the non-invasive measurements. Interestingly, the calculation of ICP based on Equation 3-1 is only applicable to HDT. In head-up tilt positions, the IJVs collapse at the level of the jugular venous valves - approximately 11 cm below the external auditory meatus (99). This results in the creation of a separate hydrostatic column, preventing very negative ICP values in the upright position. In microgravity, however, all hydrostatic pressure gradients are eliminated, fluids shift headward with notable facial edema (67) and decreased leg volume (89) and the IJVs remain continuously open. In a primate, ICP was measured directly during a 9 d spaceflight on-board a Russian Cosmos-2229 biosatellite; ICP was found to increase 25-30% immediately compared to seated baseline and decrease over the second half of the mission close to baseline values, although still slightly elevated (118). More recently, ICP was measured in parabolic flight, allowing sequences of 20 s of microgravity exposure followed by hyper-gravity; ICP was found to be increased during microgravity exposure compared to seated baseline levels (13 vs 4 mmHg, respectively), although, was decreased from supine baseline (15 mmHg; 58).

Taken together, postural changes on Earth result in a much larger change in ICP than IOP when going from the supine to the upright positions - about 12-13 mmHg (96, 99) vs. 2-3 mmHg (7, 75), respectively. Thus, a large TLPD exists 2/3^{rds} of the day whilst in the upright position with a decreased TLPD for the remaining 1/3rd of the day while in the supine position, although still positive. As there is no upright position in microgravity and ICP is hypothesized to remain slightly elevated, a sustained decreased TLPD is hypothesized to occur 24 h/day, which may be similar to remaining in the HDT position continuously. Changes in the TLPD influence strains on the ONH, notably within the retrolaminar ON, which can initiate cellular responses (16) and tissue remodeling effects in the ONH (30). However, the true translaminar pressure gradient is not just equal to the difference in IOP and ICP but rather biomechanical and material properties of the various ocular tissues must be taken into account. A modeling study by Feola et al. (2016) found that in addition to IOP

and ICP, material properties of the peripapillary sclera, annular ring, lamina cribrosa, ON and pia matter also have strong influences on strains in the ONH (35). Notably, lamina cribrosa stiffness and thickness can affect the translaminar pressure gradient, with a thicker lamina cribrosa spreading the gradient out over a greater distance and reducing shear stress (90). Interestingly, with increasing age, lamina cribrosa thickness increases due to increased collagen (68), however, compliance decreases thereby potentially increasing susceptibility to permanent deformation (2). Thus, anatomical differences may be a factor in the variance in severity of ocular changes observed in astronauts presenting with the VIIP syndrome, as any changes in ICP or IOP will result in an amplified translaminar pressure gradient across a thinner lamina cribrosa.

9.3 Intracranial and Orbital Cerebrospinal Fluid

In addition to the venous system, CSF is also subject to hydrostatic pressure gradients. Therefore, when going from the upright to the supine to the HDT position, a portion of CSF is displaced from the spinal to the intracranial SAS. This increase in intracranial CSF volume was demonstrated in the enVIIP study. In a longer duration study, Roberts et al. (2015) found no change in CSF, WM or GM volumes after 42-60 d of -6° HDT bed rest (102). Interestingly, Alperin et al. (2013) found increased intracranial CSF and GM volume in IIH patients compared to age- and weight-matched controls, potentially due to impaired CSF homeostasis and reduced cerebral drainage through the IJVs (6). Notably, the HDT-induced increase in CSF volume in the enVIIP study was mitigated with the use of LBNP in the -12° HDT position, back to baseline values. This was likely due to LBNP redistributing venous blood volume to the lower limbs during HDT, indirectly impacting intracranial CSF volume.

The intracranial CSF-filled SAS also extends around the ON. This is a unique point in the cephalad CSF circulation as it lies outside of the rigid cranium (Figure 2), and therefore distends when ICP is elevated, particularly in the retrobulbar ONS (21, 48, 66). Geeraerts et al. (2008) found that 3 mm behind the eye globe, mean MRI-derived ONSD was higher in traumatic brain injury patients with an ICP > 20 mmHg (6.31 ± 0.5 mm) compared to traumatic brain injury patients with ICP ≤ 20 mmHg (5.72 ± 0.71 mm) as well as healthy controls (5.08 ± 0.52 mm; 36). Interestingly, Kramer et al. (2012) scanned 27 astronauts (mean age ± SD: 48 ± 4.5 yrs) post-spaceflight and performed repeated imaging of 8

astronauts after an additional spaceflight (69). Mean ONSD was found to be 6.2 ± 1.1 mm, greater than reported values for healthy controls, alluding to increased ICP. However, all data were obtained post-flight, thus no baseline or control data are available for comparison. Although non-invasive measures of ICP in the enVIIP study only found increased ICP during -18° HDT, the progressive increases in ONSD with HDT suggests increased ICP during all HDT angles. However, pressure within the ON SAS may not necessarily reflect global ICP. The ONS SAS is extremely narrow with numerous trabeculae and septae restricting free flow of CSF (64). Thus, the ON SAS may form a separate compartment in some cases. This has been demonstrated in patients with asymmetric papilledema, showing altered CSF biomarkers in ONS vs. spinal CSF (61).

Interestingly, in the enVIIP study, the average ONSD 3 mm behind the eye globe at supine baseline was 5.96 ± 0.07 mm, slightly higher than mean reported values for healthy controls (15, 40). This may be due to the fact that a straight ahead eye gaze was maintained and strictly controlled for during ocular scanning in the present study, which is rarely mentioned in other protocols. This is important as Weigel et al. (2006) demonstrated that ONSD measurements are sensitive to eye gaze positioning, with a straight gaze resulting in a larger ONSD measurement than a 30° abduction gaze in the same individuals (5.7 vs. 5.4 mm, respectively; 110). In addition, a larger range of ONSD values have been found in measurements made with MRI compared to ultrasound in health adults (4.7 – 7.9 mm vs. 4.6 – 6.4 mm, respectively; (15), and comparisons between ultrasound- and MRI-derived ONSD measures warrant caution (41).

9.4 Increased Ambient Carbon Dioxide

As CO_2 is a natural metabolic byproduct expelled through respiration, ambient CO_2 levels will rise within closed environments such as the ISS unless active mechanisms are implemented to scrub the atmosphere. Thus, CO_2 levels are, on average, 10x higher on the ISS compared to terrestrial levels (0.5% vs. 0.04%, respectively), with a spacecraft maximum allowable concentration limit of 0.5% CO_2 for 1000 d exposure (55). As a potent cerebral arterial vasodilator, CO_2 is hypothesized to contribute the existing cephalad fluid shift induced-increase in ICP via further increasing intracranial blood volume (Figure 3; 52). The combination of cephalad fluid shifting and exposure to increased ambient CO_2 is unique to the microgravity environment and therefore important for any ground-based simulation

studies to simulate. It should be noted though that exposure to a CO_2-enriched atmosphere may not directly translate to increased CO_2 uptake or increased end tidal CO_2 due to enhanced ventilatory dissipation of CO_2. For example, in the enVIIP study, exposure to -12° HDT with 1% CO_2 was found to increase end tidal CO_2 by 0.47% compared to -12° HDT with ambient air. In another study, 3% CO_2 exposure was found to increase end tidal CO_2 by 0.6% in the supine position (51). However, on the ISS, end tidal CO_2 has been reported to be increased from preflight baseline (50). Interestingly, while the removal of gravity in space results in more uniform ventilation and perfusion in the lung, gas exchange is unchanged (97). In HDT, the cardiopulmonary effects are similar to that of the supine position (98).

Cerebral CO_2 reactivity was found to remain intact in the enVIIP study as exposure to -12° HDT with 1% CO_2 increased both cerebral arterial inflow and jugular venous outflow compared to -12° HDT with ambient air. Tymko et al. (2015) also found no change in cerebrovascular reactivity with extreme -45° and -90° tilt (122). Interestingly, Zuj et al. (2012) found impaired cerebrovascular CO_2 reactivity and autoregulation in the MCA after long-duration spaceflight, possibly due to chronic exposure to increased ambient CO_2 on the ISS (133). In addition, headache incidence on the ISS has been found to be correlated with CO_2 levels and suggests increased susceptibility at lower ambient CO_2 levels (71). Individual CO_2 sensitivity and retention may play a role in why some astronauts appear to be more affected by CO_2 than others; however, this may also be due to individual exposure to large fluctuations in CO_2. In the presented studies, elevated ambient CO_2 had little or no additive effect on IOP or ICP during short- (the enVIIP study) or moderate-duration (the SpaceCOT study) HDT. Further, no additional changes were detected in intracranial volumes, ONSD, sub-foveal choroidal thickness or cardiovascular parameters with the addition of low level CO_2 during HDT. Thus, increased ambient CO_2 may not play a large role in the development of ocular abnormalities during spaceflight as originally hypothesized. However, further studies are warranted to determine the effects of long-term exposure to elevated ambient CO_2 on cerebral hemodynamics as well as the interplay with additional environmental factors on the ISS.

9.5 Lower Body Negative Pressure

While increased ambient CO_2 was hypothesized to be an exacerbating factor to HDT-induced changes in cerebral and ocular physiology, LBNP was tested as a potential

countermeasure to HDT-induced cephalad fluid shifting and downstream ocular effects. Implementation of -15 to -30 mmHg LBNP in the supine position elicits the same physiological responses as the loss of ~1 L of centrally available blood volume (101), and is frequently used to study the effects of hemorrhage and orthostatic tolerance (43). In addition, LBNP induces a decrease in CBF velocity as well as CVP (56) and an increase in MAP (56, 73, 121).

In the SETI study, exposure to -40 mmHg LBNP during various degrees of HDT was demonstrated to have immediate effects on IOP, attenuating HDT-induced increases in IOP up to -18° HDT. This demonstrates the ability of LBNP to directly affect the eye, likely due to LBNP redistributing venous blood to the lower limbs, reducing CVP and cerebral venous pressure and thus reducing aqueous humor outflow resistance and choroidal blood volume. However, immediately upon cessation of LBNP and HDT, IOP returned to baseline values. Thus, LBNP-induced changes in IOP may not be sustainable. For LBNP to be a feasible countermeasure against microgravity-induced headward fluid shifting and the cascade of cerebral and ocular effects, it will likely need to be applied for longer durations (i.e., overnight) to act as a simulation of normal diurnal posture changes that occur during daily life on Earth, specifically by simulating the upright position. However, implementation of strong LBNP (-40 to -50 mmHg) can result in syncope in some subjects after just 5-10 min exposure (101, 121). Therefore, in order to determine the feasibility of using LBNP over longer durations, low level (-20 mmHg) LBNP was implemented during -12° HDT for a total of 5 h. At this LBNP level, subjects tolerated the countermeasure with reasonable comfort. However, IOP remained increased from the supine baseline after 3.5 h and no change in ICP was detected. Macias et al. (2015) found that 10-min exposure to low-level (-25 mmHg) LBNP during -15° HDT returned IOP to supine baseline levels and reduced transcranial ultrasound pulse amplitude, alluding to decreased ICP although no absolute value is available from the implemented technique (75). Although low-level LBNP during HDT immediately decreased IOP back to supine baseline levels in that study, the changes may not be sustainable over longer durations as evidenced by the results of the enVIIP study.

While low-level LBNP had minimal effects on IOP and ICP over multiple hours, a notable reduction in orbital and intracranial CSF volume was found compared to -12° HDT alone. This novel finding is likely due to an LBNP-induced decrease in CVP and enhanced cerebral drainage. Although CVP was not measured in the present study, exposure to 5 min

LBNP at -15, -30 and -45 mmHg has been shown to decrease CVP by 4.5, 6.3 and 7.7 mmHg, respectively (56). The ability of LBNP, an approach primarily targeting venous blood distribution, to directly influence orbital as well as intracranial CSF volumes indicates great potential in this approach for future countermeasures against increased periorbital CSF-pressure and resulting ocular changes. However, a balance between comfort and effectiveness must be determined for feasibility of implementation over multiple hours.

9.6 Idiopathic Intracranial Hypertension and the VIIP Syndrome

Although there are several similarities between the structural ophthalmic changes seen in both IIH patients and astronauts presenting with the VIIP syndrome, there are also marked differences between the two. IIH primarily affects obese women of child bearing age (125), and is frequently accompanied by pulse synchronous tinnitus and diplopia, not found in astronauts. The VIIP syndrome has been predominantly found in healthy male astronauts with a mesomorphic build, however, this may be due to affect a greater proportion of males in space over the past 15 years than females. Interestingly, only 10% of IIH patients presenting with papilledema also have choroidal folds, the presence of which is normally associated with high ICP (108). In contrast, about 60% of astronauts with papilledema also present with choroidal folds (77) that are strongly unilateral and predominately present in the right eye, perhaps alluding to global or local (periorbital) increased CSF pressure in microgravity. This may, however, be due to the relatively low sample number compared to clinical studies on Earth or due to increased susceptibility to mechanical folding due to choroidal expansion in microgravity (77).

Interestingly, the ocular changes in astronauts appear to affect the right eye more than the left (78). On the contrary, asymmetric papilledema in patients with IIH is fairly uncommon, occurring in less than 4% of patients (20). Bidot et al. (2015) found that in IIH patients with asymmetric papilledema, the eye with the lower grade edema also had a smaller bony optic canal and hypothesized that a smaller bony optic canal is protective by preventing CSF pressure to be fully transmitted along the ON (20). However, this does not explain why the right side is consistently more affected in microgravity as it is highly unlikely that all astronauts display the same anatomical asymmetry. Although this hypothesis warrants further investigation, it would be interesting analyze bony optic canal size in VIIP-affected and non-affected astronauts in the future. Lateral variations were found in several

instances in the presented studies. First, all presented studies showed at least a trend towards significance for an effect of lateralization on IOP. While this may also be due to the relatively small sample sizes, asymmetric IOP could have notable effects on the TLPD, especially when coupled with potential asymmetric bony optic canals and periorbital CSF pressure. Interestingly, the likelihood of developing primary open-angle glaucoma has been found to increase with increasing IOP asymmetry as well (129). In addition, about 75% of subjects in the enVIIP study had a higher flow rate through the right IJV, in-line to previously reported values in healthy subjects (112). The cerebral venous system is known to have inter-individual variations and significant lateralization throughout the system (4, 33, 116). However, the significance and clinical implications of physiological bilateral variations has yet to be determined and warrants future investigation.

Taken together, although several similarities can be drawn between IIH and the ocular changes experienced by astronauts, the etiology of the VIIP syndrome appears to be unique to the microgravity environment. However, it is notable that both syndromes include signs consistent with a lack of ICP reductions normally experienced in the upright position due to either an abnormally increased ICP in the upright position in IIH or a lack of upright position all together in space.

9.7 Limitations

There are several limitations to consider when interpreting the results of the presented studies. First, the studies exhibited relatively small sample sizes which could have prevented some results from reaching statistical significance, and thus, results were interpreted with caution. Second, one of the main limitations of HDT bed rest as an analog is that unlike in microgravity where all gravitational forces are eliminated, the Gx (dorsal-ventral) gravitational gradient is maintained during HDT which may result in a different cardiopulmonary response compared to microgravity. In addition, a small headward gradient is created approximating 0.1 Gz [= sin(-6°)]. While this foot-to-head gradient is meant to induce a headward fluid shift as experienced in microgravity, it is of importance to note that the physiological means of the fluid shift are very different in nature as no hydrostatic pressure gradients exist in space. Third, the HDT with increased ambient CO_2 studies did not use computer controlled systems to continually alter individual $PaCO_2$ to a controlled level. Rather, subjects were exposed to a constantly increased ambient CO_2

breathing mixture as this is more representative of the spaceflight environment. However, it should be noted that individual ventilatory responses to CO_2 can be variable. Thus, some subjects may have had a higher $PaCO_2$ and stronger physiological reactions thereof. It should also be noted that while the presented work focused on the hypothesis that impaired cerebral hemodynamics and cephalad fluid shifting are the main hypothesized contributor to the VIIP syndrome, other contributing factors have been proposed including a high sodium diet, resistive exercise (3), enzymatic polymorphisms in the 1-C metabolism cycle (134) and anatomical shifting in microgravity (128).

10 Conclusion and Future Perspectives

Overall, the presented studies investigated cerebral and ocular physiology during various degrees of HDT with and without increased ambient CO_2 to further understand the effects of cephalad fluid shifting and the possible etiology of ocular changes in astronauts. The overarching hypothesis depicted in Figure 3 was that alterations in cerebral hemodynamics, namely increased cerebral venous pressure, can induce a cascade of cerebral and ocular effects that may ultimately result in the vision and structural ophthalmic changes seen in astronauts. The results indicate that HDT leads to cerebral venous congestion demonstrated by the large increase in IJV CSA and decreased jugular venous outflow flow from PC-MRI derived measures. Furthermore, HDT-induced increases in intracranial CSF volume and ONSD are consistent with decreased CSF absorption due to elevated cerebral venous pressure. In addition, an important downstream consequence of HDT-induced alterations in cerebral hemodynamics is a change in the translaminar pressure gradient (Figure 3). Interestingly, a small, positive intraocular-intracranial pressure difference (IOP > ICP) is maintained during both acute and overnight HDT exposure. This is in contrary to the hypothesized shift to a negative intraocular-intracranial pressure difference that can result in significant structural and functional ophthalmic changes, for example in patients with IIH. However, even though a positive intraocular-intracranial pressure difference is maintained, it is smaller than the nominal pressure difference that occurs in the upright position on Earth due to a very low or even negative intracranial pressure in this position. Thus, there is a constantly elevated pressure on the back of the eye during HDT and possibly also in space. The lack of periorbital pressure alleviation due to disruptions in cerebral hemodynamics may play a role in the ultimate structural and functional ophthalmic changes that develop in association with the VIIP syndrome.

In addition to cephalad fluid shifting due to the loss of hydrostatic pressure gradients in space, exposure to increased ambient CO_2 on the ISS was hypothesized to be an exacerbating factor to an existing microgravity-induces increase in ICP (Figure 3). However, in the presented studies, increased ambient CO_2 in combination with HDT had little additive effect on ICP or IOP during short- (3 h) or moderate-duration (29 h) exposure. Further, no additional effects were seen on ONSD or intracranial CSF volume during HDT with increased ambient CO_2. However, exposure to elevated ambient CO_2 was found to have notable

effects on cerebral hemodynamics including increasing cerebral arterial blood flow and venous outflow compared to HDT alone. The long-term implications for the CO_2-induced changes in cerebral hemodynamics in combination with real or simulated microgravity are unknown and warrant further investigation to determine potential implications for the VIIP syndrome.

Finding a way to mitigate vision changes in space is vital to ensure long-duration exploration class mission feasibility and success. Therefore, LBNP was implemented in the HDT position to test its ability to redistribute venous blood volume to the lower limbs as a potential countermeasure to cephalad fluid shifting. This approach directly targets the primary hypothesized causative mechanism underlying the VIIP syndrome, increased cerebral venous pressure. Notably, 5 h exposure to low-level LBNP (-20 mmHg) during -12° HDT was able to successfully attenuate the HDT-induced increase in periorbital CSF (ONSD) as well as intracranial CSF volume. Although -20 mmHg LBNP had additional no effect on ICP or IOP during HDT, exposure to -40 mmHg LBNP for short durations was able to reduce HDT-induced increases in IOP during a range of tilt angles. Thus, LBNP is a promising technique to counteract cephalad fluid shifting by redistributing venous volume to the lower limbs and attenuate HDT-induced elevations in intracranial as well as periorbital CSF volume.

Overall, the presented studies represent novel investigations into the cerebral and ocular effects of various degrees of cephalad fluid shifting through a range of HDT angles as well as the unique combination of HDT and increased ambient CO_2 as a more realistic analog of the ISS. LBNP was also established as a promising countermeasure to headward fluid shifting and demonstrated direct effects on intracranial and orbital CSF. These studies contributed to the understanding of potential mechanisms involved in the development of ocular changes in astronauts, notably the central role of cerebral hemodynamics and cerebral venous congestion as well as the intraocular-intracranial pressure difference.

11 Appendix

11.1 Publications and Presentations

First Author Publications:

1. **Marshall-Goebel K**, Mulder E, Bershad E, Laing C, Eklund A, Malm J, Stern C, Rittweger J. Intracranial and intraocular pressure during various degrees of head-down tilt. *Aerosp Med Hum Perform* 88(1): 10-16, 2017.
2. **Marshall-Goebel K**, Ambarki K, Eklund A, Malm J, Mulder E, Gerlach D, Bershad E, Rittweger J. Effects of short-term exposure to head-down tilt on cerebral hemodynamics: a prospective evaluation of a spaceflight analog using phase-contrast MRI. *J Appl Physiol* 120: 1466-1473, 2016.
3. **Marshall-Goebel K**, Mulder E, Donoviel D, Strangman G, Suarez J, Venkatasubba Rao C, Frings-Meuthen P, Limper U, Rittweger J, Bershad E. An international collaboration studying the physiological and anatomical cerebral effects of carbon dioxide during head-down tilt bed rest: the SPACECOT study. *J Appl Physiol* (In Press) 2017.
4. **Marshall-Goebel K**, Terlevic R, Gerlach D, Simone Kuehn, Mulder E Rittweger J. Lower body negative pressure reduces optic nerve sheath diameter during head-down tilt. (In preparation) 2017.

Co-Author Publications:

5. Gerlach DA, **Marshall-Goebel K**, Hasan KM, Kramer L, Alperin N, Rittweger J. MRI-derived diffusion parameters in the human optic nerve and its surrounding sheath during head down tilt. *Microgravity* (In revision) 2017.
6. Strangman G, Zhang Q, **Marshall-Goebel K**, Mulder E, Stevens B, Clark J, Bershad E. Increased cerebral blood volume pulsatility during head-down tilt with elevated carbon dioxide: the SPACECOT study. *J Appl Physiol* (In revision) 2017.
7. Kramer LA, Hasan KM, Sargsyan AE, **Marshall-Goebel K**, Rittweger J, Donoviel D, Higashi S, Mwangi B, Gerlach D, Bershad E. Quantitative MRI volumetry, diffusivity, cerebrovascular flow and cranial hydrodynamics following head-down tilt and hypercapnia: the SPACECOT study. *J Appl Physiol* (In Press) 2017.

8. Michael AP, **Marshall-Bowman K**. Spaceflight-induced intracranial hypertension. *Aerosp Med Hum Perform* 86(6): 557–562, 2015.

Conference Presentations:

1. **Marshall-Goebel K**, Rittweger J, Suarez JI, Rao CV, Donoviel D, Mulder E, Bershad E. Effects of head-down tilt with and without 0.5% carbon dioxide on intracranial and intraocular pressure. Aerospace Medical Association Conference, Oral Presentation, Atlantic City, NJ, USA, Apr 2016.
2. **Marshall-Goebel K**, Rittweger J, Suarez JI, Rao CV, Limper U, Mulder E, Donoviel D, Bershad E. Effects of head-down tilt with or without 0.5% CO_2 on intracranial and intraocular pressure: results from the Space-COT study. NASA Human Research Program Investigators Workshop, Poster Presentation, Galveston, TX, USA, Feb 2016.
3. **Marshall-Bowman K**, Ambarki K, Eklund A, Malm J, Mulder E, Gerlach D, Bershad E, Rittweger J. Implementation of various degrees of head down tilt to study the etiology of the VIIP Syndrome. International Astronautical Congress, Oral Presentation, Jerusalem, Israel, Oct 2015.
4. **Marshall-Bowman K**, Mulder E, Rittweger J. Effects of head-down tilt, carbon dioxide and lower body negative pressure in humans: results from the enVIIP study. International Astronautical Congress, Oral Panel Presentation, Jerusalem, Israel, Oct 2015.
5. **Marshall-Bowman K**, Rittweger J. Cerebral and ocular fluid balance as a function of space-related environmental factors: insights into the visual impairment and intracranial pressure syndrome. NASA Human Research Program Investigators Workshop, Oral Presentation (invited speaker), Galveston, TX, USA, Jan 2015.
6. **Marshall-Bowman K**, Mulder E, Rittweger J. Utilizing the envihab for visual impairment intracranial pressure (VIIP) research. 19th IAA Humans in Space Symposium, Oral Presentation, Cologne, Germany, July 2013.

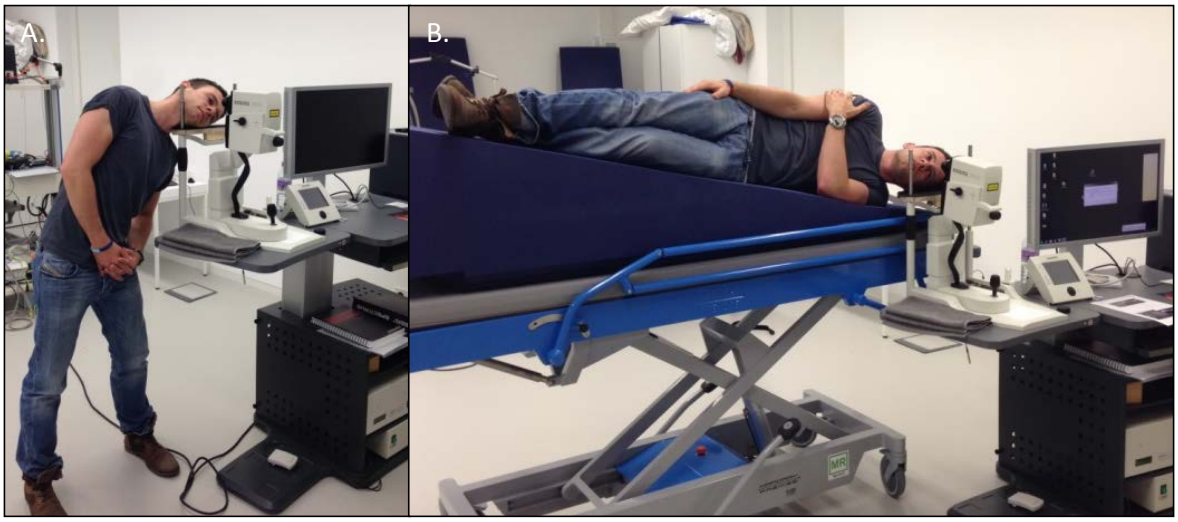

Figure A 1: Spectral domain optical coherence tomography imaging performed in the A) upright and B) head-down tilt positions

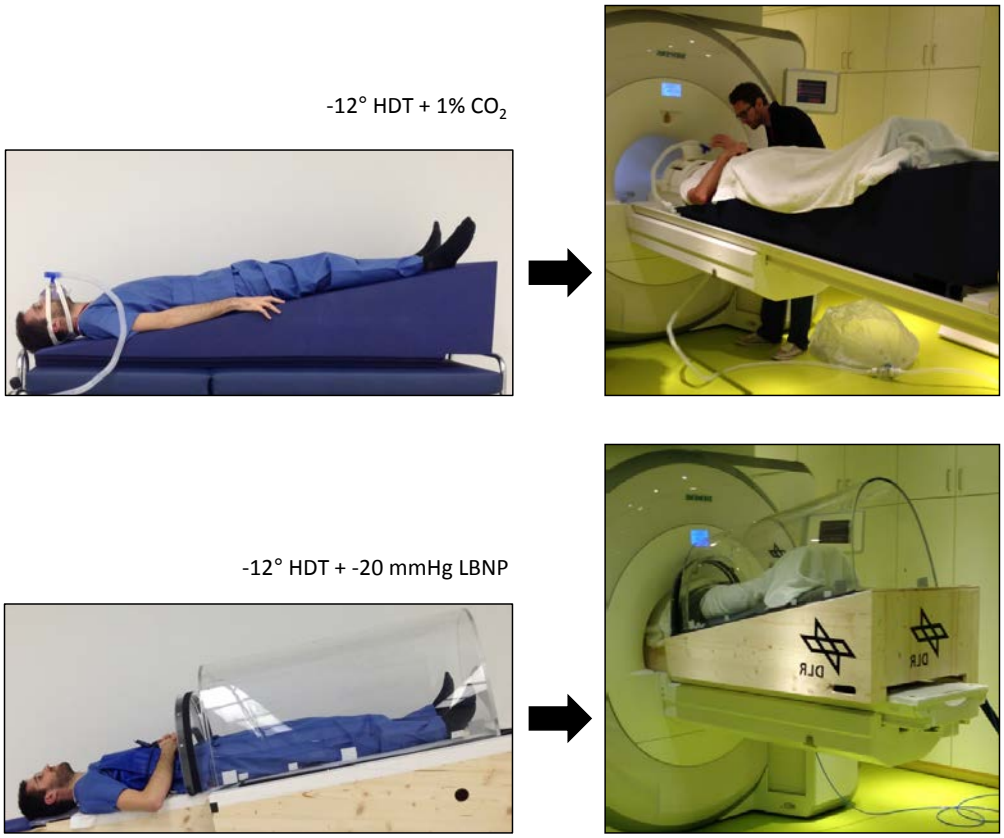

Figure A 2: Custom-built MRI-compatible systems for administration of 1% CO_2 and -20 mmHg lower body negative pressure (LBNP) during -12° head-down tilt (HDT).

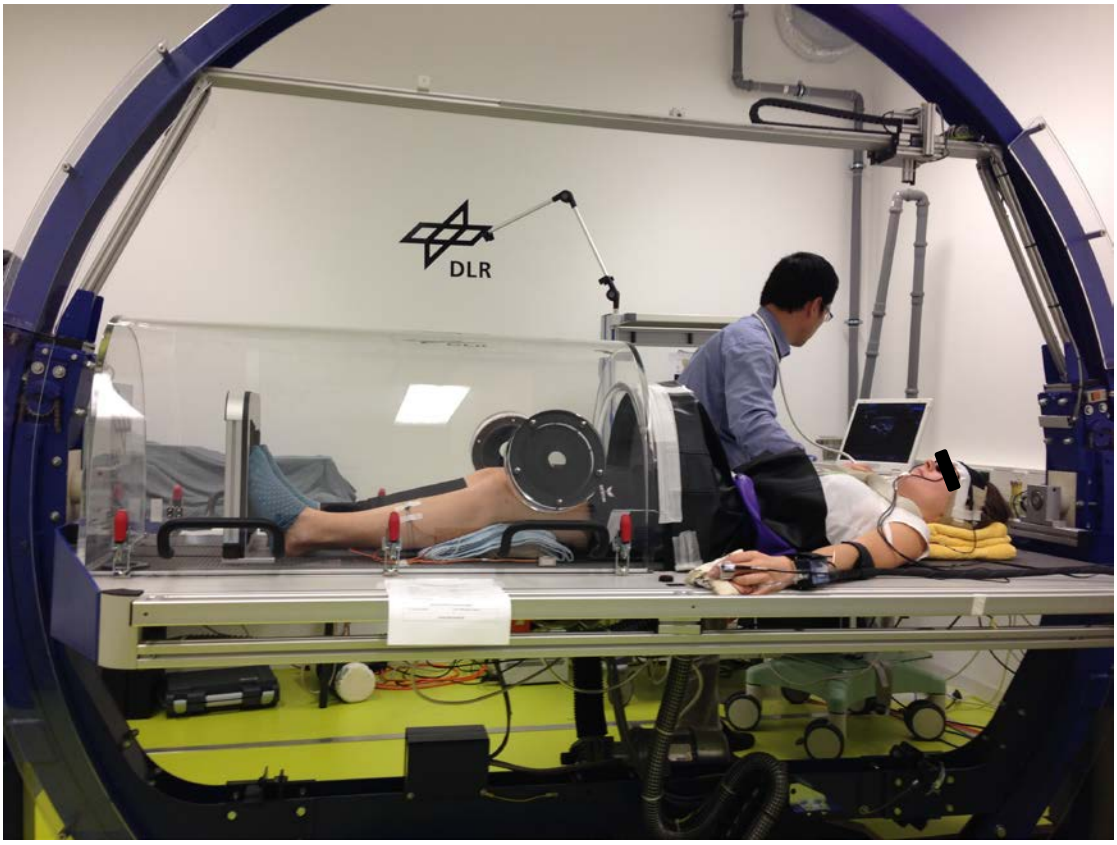

Figure A 3: SETI study setup with the automatic tilt table and integrated lower body negative pressure chamber

Table A 1: Example daily schedule for one condition of the enVIIP study

Time	Subject 1	Subject 2
7:00	***BDC***	
7:30	OCT BS	
8:00	*Breakfast*	
8:30	ICP	***BDC***
9:00	Cardio Innocor	OCT BS
9:30	MRI	*Breakfast*
10:00		ICP
10:30	IOP/OCT BS/US	Cardio Innocor
11:00	*Snack*	MRI
11:30	***Start HDT***	
12:00		IOP/OCT BS/US
12:30	Cardio	*Snack*
13:00	OCT	***Start HDT***
13:30	Cardio	
14:00	*Snack*	Cardio
14:30	Cardio Innocor	OCT
15:00	OCT IOP ICP	Cardio
15:30	Cardio	*Snack*
16:00	MRI	Cardio Innocor
16:30		OCT IOP ICP
17:00	BS US	Cardio
17:30		MRI
18:00		
18:30		BS US
19:00		

BDC = baseline data collection, OCT = optical coherence tomography, BS = blood sample, ICP = Vittamed non-invasive intracranial pressure measurement, cardio = cardiovascular measures, Innocor = respiratory measures, MRI = magnetic resonance imaging, IOP = intraocular pressure, US = urine sample, HDT = head down tilt.

Table A 2: Example schedule for one campaign of the SpaceCOT Study

Study Day: BDC				
Condition	ambient atmosphere	ambient atmosphere	ambient atmosphere	**Condition**
Subject	**A**	**B**	**C**	**Subject**
6:30	**Temp, BP, HR**	**Temp, BP, HR**	**Temp, BP, HR**	6:30
6:45	**Urine 1, BW**	**Urine 1, BW**	**Urine 1, BW**	6:45
7:00	**BD; CO-Hb**	**BD; CO-Hb**	**BD; CO-Hb**	7:00
7:15				7:15
7:30	**Breakfast/Drink**	**Breakfast/Drink**	**Breakfast/Drink**	7:30
7:45				7:45
8:00	**Cognition** fam supine			8:00
8:15				8:15
8:30	**Plasma volume**			8:30
8:45				8:45
9:00	**CO-Hb**	**Cognition** fam supine		9:00
9:15	**Flow-mediated dilation**			9:15
9:30		**Plasma volume**	**Cognition** fam supine	9:30
9:45	**Puffy face**			9:45
10:00	**internal jugular vein + tilt**	**CO-Hb**		10:00
10:15		**Flow-mediated dilation**		10:15
10:30			**Plasma volume**	10:30
10:45		**Puffy face**		10:45
11:00	**Cognition / NIRS**	**internal jugular vein + tilt**	**CO-Hb**	11:00
11:15			**Flow-mediated dilation**	11:15
11:30	**TCD / Finometer**			11:30
11:45			**Puffy face**	11:45
12:00	**Cflow / Fino / BGA**	**Cognition / NIRS**	**internal jugular vein + tilt**	12:00
12:15				12:15
12:30	**IOP and OCT**	**TCD / Finometer**		12:30
12:45				12:45
13:00	**Lunch/Drink**	**Cflow / Fino / BGA**	**Lunch/Drink**	13:00
13:15				13:15
13:30	**Vittamed**	**IOP and OCT**	**Cognition / NIRS**	13:30
13:45				13:45
14:00		**Lunch/Drink**	**TCD / Finometer**	14:00
14:15	**Sniffin' Sticks**			14:15
14:30	**supine spiro/CO/ETCO2 Phono / BGA**	**Vittamed**	**Cflow / Fino / BGA**	14:30
14:45				14:45
15:00	**Cerebrotech / Fino**		**IOP and OCT**	15:00
15:15	**MRI**	**Sniffin' Sticks**		15:15
15:30		**supine spiro/CO/ETCO2 Phono / BGA**	**Vittamed**	15:30
15:45				15:45
16:00		**Cerebrotech / Fino**		16:00
16:15		**MRI**	**Sniffin' Sticks**	16:15
16:30	**Tilt Table + Echocardiography**		**supine spiro/CO/ETCO2 Phono / BGA**	16:30
16:45				16:45
17:00			**Cerebrotech / Fino**	17:00
17:15			**MRI**	17:15
17:30		**Tilt Table + Echocardiography**		17:30
17:45				17:45
18:00				18:00
18:15				18:15
18:30			**Tilt Table + Echocardiography**	18:30
18:45				18:45
19:00	**Dinner**	**Dinner**		19:00
19:15				19:15
19:30			**Dinner**	19:30
19:45				19:45
20:00	**PANAS + GHQ-28 Headache questionnaire**	**PANAS + GHQ-28 Headache questionnaire**	**PANAS + GHQ-28 Headache questionnaire**	20:00
20:15				20:15
20:30				20:30

20:45				20:45
21:00				21:00
21:15				21:15
21:30	Drink	Drink	Drink	21:30
21:45	LOG	LOG	LOG	21:45
22:00	Bedtime	Bedtime	Bedtime	22:00
22:15				22:15
22:30				22:30
22:45				22:45

Study Day: HDT

Condition	ambient atmosphere (start CO_2 at 11:00)	ambient atmosphere (start CO_2 at 11:00)	ambient atmosphere (start CO_2 at 11:00)	Condition
Subject	A	B	C	Subject
6:30	Temp, BP, HR	Temp, BP, HR	Temp, BP, HR	6:30
6:45	Urine 2, BW	Urine 2, BW	Urine 2, BW	6:45
7:00	BD	BD	BD	7:00
7:15				7:15
7:30	Breakfast/Drink			7:30
7:45				7:45
8:00	seated spiro/CO/ETCO2 Phono / BGA	Breakfast/Drink	Breakfast/Drink	8:00
8:15				8:15
8:30	supine spiro/CO/ETCO2 Phono / BGA			8:30
8:45				8:45
9:00	Puffy face	seated spiro/CO/ETCO2 Phono / BGA	Cognition / NIRS seated	9:00
9:15				9:15
9:30	Cognition / NIRS seated	supine spiro/CO/ETCO2 Phono / BGA		9:30
9:45				9:45
10:00		Puffy face	seated spiro/CO/ETCO2 Phono / BGA	10:00
10:15	Urine 3	Cognition / NIRS seated		10:15
10:30	START 0.5% CO_2 and -12° HDT		supine spiro/CO/ETCO2 Phono / BGA	10:30
10:45				10:45
11:00	Cognition / NIRS		Puffy face	11:00
11:15		Urine 3		11:15
11:30	TCD / Finometer	START 0.5% CO_2 and -12° HDT		11:30
11:45				11:45
12:00	Cflow / Fino / BGA	Cognition / NIRS		12:00
12:15	Cerebrotech / Fino / BGA		Urine 3	12:15
12:30	IOP and OCT	TCD / Finometer	START 0.5% CO_2 and -12° HDT	12:30
12:45				12:45
13:00	Lunch/Drink	Cflow / Fino / BGA	Cognition / NIRS	13:00
13:15		Cerebrotech / Fino / BGA		13:15
13:30	Vittamed	IOP and OCT	TCD / Finometer	13:30
13:45				13:45
14:00		Lunch/Drink	Cflow / Fino / BGA	14:00
14:15	Sniffin' Sticks		Cerebrotech / Fino / BGA	14:15
14:30	spirometry/CO/ETCO2 Phono / BGA	Vittamed	IOP and OCT	14:30
14:45				14:45
15:00			Lunch/Drink	15:00
15:15		Sniffin' Sticks		15:15
15:30	URINE 4 + BD	spirometry/CO/ETCO2 Phono / BGA	Vittamed	15:30
15:45	Puffy face			15:45
16:00	Cognition / NIRS			16:00
16:15			Sniffin' Sticks	16:15
16:30	TCD / Finometer	URINE 4 + BD	spirometry/CO/ETCO2 Phono / BGA	16:30
16:45		Puffy face		16:45
17:00	Cflow / Fino / BGA	Cognition / NIRS		17:00
17:15	Cerebrotech / Fino / BGA			17:15
17:30	IOP and OCT	TCD / Finometer	URINE 4 + BD	17:30
17:45			Puffy face	17:45
18:00	Vittamed	Cflow / Fino / BGA	Cognition / NIRS	18:00
18:15		Cerebrotech / Fino / BGA		18:15
18:30		IOP and OCT	TCD / Finometer	18:30

18:45	Sniffin' Sticks			18:45
19:00	Dinner	Vittamed	Cflow / Fino / BGA	19:00
19:15			Cerebrotech / Fino / BGA	19:15
19:30			IOP and OCT	19:30
19:45		Sniffin' Sticks		19:45
20:00	spirometry/CO/ETCO2 Phono / BGA	Dinner	Vittamed	20:00
20:15				20:15
20:30		spirometry/CO/ETCO2 Phono / BGA		20:30
20:45	Headache questionnaire		Sniffin' Sticks	20:45
21:00			Dinner	21:00
21:15		Headache questionnaire		21:15
21:30	Drink	Drink	spirometry/CO/ETCO2 Phono / BGA	21:30
21:45	LOG	LOG		21:45
22:00	Bedtime	Bedtime	Headache questionnaire	22:00
22:15			LOG	22:15
22:30			Drink	22:30
22:45			Bedtime	22:45

Study Day: HDT2

Condition	0.5% CO_2	0.5% CO_2	0.5% CO_2	Condition
Subject	A	B	C	Subject
6:30	Temp, BP, HR	Temp, BP, HR	Temp, BP, HR	6:30
6:45	Urine 4, BW	Urine 4, BW	Urine 4, BW	6:45
7:00	Breakfast/Drink			7:00
7:15		Breakfast/Drink	Breakfast/Drink	7:15
7:30	spirometry/CO/ETCO2 Phono / BGA			7:30
7:45				7:45
8:00	Cognition / NIRS			8:00
8:15				8:15
8:30	Vittamed	spirometry/CO/ETCO2 Phono / BGA		8:30
8:45				8:45
9:00		Cognition / NIRS		9:00
9:15	Sniffin' Sticks			9:15
9:30	IOP and OCT	Vittamed	spirometry/CO/ETCO2 Phono / BGA	9:30
9:45				9:45
10:00	TCD / Finometer		Cognition / NIRS	10:00
10:15		Sniffin' Sticks		10:15
10:30	Cflow / Fino / BGA	IOP and OCT	Vittamed	10:30
10:45	Cerebrotech / Fino / BGA			10:45
11:00	URINE 4 + BD	TCD / Finometer		11:00
11:15	MRI		Sniffin' Sticks	11:15
11:30		Cflow / Fino / BGA	IOP and OCT	11:30
11:45		Cerebrotech / Fino / BGA		11:45
12:00		URINE 4 + BD	TCD / Finometer	12:00
12:15		MRI		12:15
12:30	FMD, puffy face		Cflow / Fino / BGA	12:30
12:45			Cerebrotech / Fino / BGA	12:45
13:00	Lunch/Drink		URINE 4 + BD	13:00
13:15	Urine 5		MRI	13:15
13:30	START of 3% CO_2	FMD, puffy face		13:30
13:45	TCD / Cflow / Finometer			13:45
14:00		Lunch/Drink		14:00
14:15	IOP / ETCO2 / BGA	Urine 5		14:15
14:30		START of 3% CO_2	FMD, puffy face	14:30
14:45	Cerebrotech / Finometer	TCD / Cflow / Finometer		14:45
15:00	MRI		Lunch/Drink	15:00
15:15		IOP / ETCO2 / BGA	Urine 5	15:15
15:30			START of 3% CO_2	15:30
15:45	BD	Cerebrotech / Finometer	TCD / Cflow / Finometer	15:45
16:00	FMD, puffy face END of 3%	MRI		16:00
16:15	END of 3% CO_2		IOP / ETCO2 / BGA	16:15
16:30	Tilt Table +			16:30

16:45	Echocardiography	BD	Cerebrotech / Finometer	16:45
17:00		FMD, puffy face END of 3%	MRI	17:00
17:15		END of 3% CO_2		17:15
17:30	Urine 6, BW	Tilt Table + Echocardiography		17:30
17:45	spirometry/CO/ETCO2 Phono / BGA		BD	17:45
18:00			FMD, puffy face END of 3%	18:00
18:15			END of 3% CO_2	18:15
18:30	PANAS/GHQ-28/ Headache SCOT survey	Urine 6, BW	Tilt Table + Echocardiography	18:30
18:45		spirometry/CO/ETCO2 Phono / BGA		18:45
19:00	Dinner			19:00
19:15				19:15
19:30	LOG	PANAS/GHQ-28/ Headache SCOT survey	Urine 6, BW	19:30
19:45	Departure DLR		spirometry/CO/ETCO2 Phono / BGA	19:45
20:00		Dinner		20:00
20:15				20:15
20:30		LOG	PANAS/GHQ-28/ Headache SCOT survey	20:30
20:45		Departure DLR		20:45
21:00			Dinner	21:00
21:15				21:15
21:30			LOG	21:30
21:45			Departure DLR	21:45
22:00				22:00
22:15				22:15
22:30				22:30
22:45				22:45

Temp = body temperature, BP = blood pressure, HR = heart rate, BW = body weight, BD = blood draw, CO-Hb = plasma volume via carbon monoxide rebreathing technique, fam = familiarization session, Puffy face = forehead tissue ultrasound, NIRS = Near-infrared spectroscopy, TCD = transcranial Doppler ultrasound, Cflow = cortical microvasculature cerebral blood flow measurement, Fino = finometer cardiovascular parameters measurement, BGA = blood gas analysis, IOP = intraocular pressure, OCT = optical coherence tomography, Vittamed = non-invasive ICP measurement, Sniffin' Sticks = olfactory threshold test, Spiro = spirometry derived respiratory parameters measurement, ETCO2 = end tidal CO_2, Phono = phonocardiography, Cerebrotech = volumetric integral phase-shift spectroscopy measurement, MRI = magnetic resonance imaging, PANAS = positive and negative affect schedule questionnaire, GHQ = general health questionnaire, LOG = subject anecdotal daily incidence log, FMD = brachial artery flow mediated dilation measurement, SCOT survey = end of study survey.

Document A 1: Ethical approval letter from the Ärztekammer Nordrhein for the enVIIP study

ÄRZTEKAMMER NORDRHEIN
Körperschaft des öffentlichen Rechts

ETHIKKOMMISSION

Deutsches Zentrum für
Luft- und Raumfahrt e.V.
Herrn Prof. Dr. med. Rupert Gerzer
Linder Höhe
51147 Köln

15.04.2014 Dr. Dr. Pl./Se

Berufsrechtliche Beratung vor der Durchführung biomedizinischer Forschung am Menschen nach § 15 Berufsordnung
Cerebral and ocular fluid balance as a function of hydrostatic pressure gradients and environmental factors: Insights into the VIIP syndrome (enVIIP)

Unser Zeichen: 2013477
Laufende Nummer der nachträglichen Änderung: 2/2014/87881
hier: Ihr Telefax vom 11. April 2014 mit Probandeninformation in deutscher Sprache, Version vom 10.04.2014, Probandeninformation in englischer Sprache, Version vom 10.04.2014, Einverständniserklärung zur Untersuchung des Blutes auf HIV und Hepatitis

Sehr geehrter Herr Professor Gerzer,

die Ethikkommission der Ärztekammer Nordrhein hat Ihr oben genanntes Telefax mit der Probandeninformation in deutscher Sprache, Version vom 10.04.2014, der Probandeninformation in englischer Sprache, Version vom 10.04.2014 sowie der Einverständniserklärung zur Untersuchung des Blutes auf HIV und Hepatitis zur Kenntnis genommen. Damit konnten Sie alle Punkte unseres Schreibens vom 07.04.2014 zufrieden stellend umsetzen, so dass keine berufsethischen und berufsrechtlichen Bedenken mehr gegen die Durchführung der Studie bestehen.

Vorsorglich weist die Ethikkommission darauf hin, dass die ärztliche und juristische Verantwortung für die Durchführung des Projektes uneingeschränkt bei Ihnen und Ihren Mitarbeitern verbleibt.

Ärztekammer Nordrhein
Tersteegenstraße 9 · 40474 Düsseldorf
Telefon 0211/4302-2272 · Telefax 0211/4302-2279
E-Mail ethik@aekno.de
Internet: www.aekno.de

Bankverbindung
Deutsche Apotheker- und Ärztebank eG,
Düsseldorf (BLZ 300 606 01) DOC 1145 290
IBAN DE89 3006 0601 0001 1452 90
BIC DAAEDEDD

Kernarbeitszeit: Montag bis Donnerstag 9 Uhr bis 16 Uhr, Freitag 9 Uhr bis 14 Uhr

ÄRZTEKAMMER NORDRHEIN
Körperschaft des öffentlichen Rechts

ETHIKKOMMISSION

Seite 2 **lfd. Nummer 2013477**

Wir machen darauf aufmerksam, dass sich das oben genannte Votum nur auf die bisher eingereichten Unterlagen bezieht. Nachträgliche Änderungen in Organisation und Ablauf der klinischen Prüfung, die nach Ihrer Auffassung vom Votum der Ethikkommission umfasst sein sollten, sollten umgehend zur Beratung mitgeteilt und die geänderten Passagen deutlich kenntlich gemacht werden. Änderungen, zu denen Sie keine Stellungnahme der Ethikkommission wünschen, sind demgegenüber nicht vorzulegen.

Wir gehen davon aus, dass durch Sie die Prüfärzte in unserem Kammerbezirk über die Änderungen informiert werden.

Mit freundlichen Grüßen

Prof. Dr. med. K. Racké
Vorsitzender der Ethikkommission

Ärztekammer Nordrhein
Tersteegenstraße 9 · 40474 Düsseldorf
Telefon 0211/4302-2272 Telefax 0211/4302-22 79
E-Mail: ethik@aekno.de
Internet: www.aekno.de

Bankverbindung
Deutsche Apotheker- und Ärztebank eG,
Düsseldorf (BLZ 300606 01) 0001 145 290
IBAN: DE89 3006 0601 0001 1452 90
BIC: DAAEDEDD

Kernarbeitszeit: Montag bis Donnerstag 9 Uhr bis 16 Uhr, Freitag 9 Uhr bis 14 Uhr

Document A 2: Ethical approval letter from the Ärztekammer Nordrhein for the SpaceCOT study

ÄRZTEKAMMER NORDRHEIN
Körperschaft des öffentlichen Rechts

ETHIKKOMMISSION

Herrn
Prof. Dr. med. Jörn Rittweger
Deutsches Zentrum für
Luft- und Raumfahrt e.V.
Linder Höhe
51147 Köln

per Telefax: 02203 - 61159

06.05.2015 Prof. Pfo./Ieh
lfd. Nummer 2015135

Berufsrechtliche Beratung vor der Durchführung biomedizinischer Forschung am Menschen nach § 15 Berufsordnung

Studying the Physiological and Anatomical Cerebral Effects of CO_2 and Tilt
Space-COT study

hier: Ihr Telefax vom 05.05.2015

Sehr geehrter Herr Professor Rittweger,

die Ethikkommission der Ärztekammer Nordrhein hat Ihr oben genanntes Schreiben mit der Versicherungsbestätigung vom 04.05.2015 und der Probandenaufklärung Version 2 vom 04.05.2015 zur Kenntnis genommen.

Damit konnten Sie alle Punkte unseres Votums vom 30.04.2015 zufriedenstellend umsetzen, so dass keine berufsethischen und berufsrechtlichen Bedenken mehr gegen die Durchführung der Studie bestehen.

Vorsorglich weist die Ethikkommission darauf hin, dass die ärztliche und juristische Verantwortung für die Durchführung der Studie uneingeschränkt bei Ihnen und Ihren Mitarbeitern verbleibt.

Wir machen darauf aufmerksam, dass sich das oben genannte Votum nur auf die bisher eingereichten Unterlagen bezieht. Nachträgliche Änderungen in Organisation und Ablauf der klinischen Prüfung, die nach Ihrer Auffassung vom Votum der Ethikkommission umfasst sein sollen, sollten umgehend zur Beratung mitgeteilt und die geänderten Passagen deutlich kenntlich gemacht werden.

Informationen und Änderungen, zu denen Sie kein Votum der Ethikkommission mit einem entsprechenden Antrag erbitten möchten, sind demgegenüber nicht zuzusenden.

Ärztekammer Nordrhein
Tersteegenstraße 9 · 40474 Düsseldorf
Telefon 0211/4302-2272 · Telefax 0211/4302-2279
E-Mail: ethik@aekno.de
Internet: www.aekno.de

Bankverbindung
Deutsche Apotheker- und Ärztebank eG,
Düsseldorf (BLZ 30060601) 3001145390
IBAN DE89300606013001145390
BIC DAAEDEDD

Kernsprechzeit: Montag bis Donnerstag 8 Uhr bis 16 Uhr, Freitag 8 Uhr bis 14 Uhr

ÄRZTEKAMMER NORDRHEIN
Körperschaft des öffentlichen Rechts

ETHIKKOMMISSION

Seite 2 **lfd. Nummer: 2015135**

Wir gehen davon aus, dass durch Sie die Prüfärzte in unserem Kammerbezirk über die Änderungen informiert werden.

Mit freundlichen Grüßen
gez.

Ausgefertigt:
i. A.

Prof. Dr. med. Martin Pfohl
Stellvertr. Vorsitzender
der Ethikkommission

David Friedländer, LL.M.
Referent der Ethikkommission

Ärztekammer Nordrhein
Tersteegenstraße 9 · 40474 Düsseldorf
Telefon 02 11/4302-2272 · Telefax 02 11/4302-2279
E-Mail: ethik@aekno.de
Internet: www.aekno.de

Bankverbindung
Deutsche Apotheker- und Ärztebank eG
Düsseldorf (BLZ 300 606 01) 0001 146 290
IBAN DE69 3006 0601 0001 1462 90
BIC DAAEDEDD

Kernarbeitszeit: Montag bis Donnerstag 9 Uhr bis 16 Uhr, Freitag 9 Uhr bis 14 Uhr

Document A 3: Ethical approval letter from the Ärztekammer Nordrhein for the SETI study

Ärztekammer Nordrhein
Körperschaft des
öffentlichen Rechts

Ärztekammer Nordrhein, Tersteegenstraße 9, 40474 Düsseldorf

Frau
Christine Becker
Deutsches Zentrum für
Luft- und Raumfahrt e.V.
Linder Höhe
51147 Köln

ETHIKKOMMISSION

Ansprechpartnerin:
Sandra Helmke
ethik@aekno.de
Tel 0211 4302 – 2274
Fax 0211 4302 – 2279

Ihr Schreiben vom:	Ihr Zeichen:	Unsere lfd. Nummer:	Datum:
23.11.2015		2015361	23.11.2015

Berufsrechtliche Beratung nach § 15 Berufsordnung vor der Durchführung biomedizinischer Forschung am Menschen

Studying the Effect of Tilting with LBNP on head-ward arterial, venous and intraocular pressure increases (SETI)

Eingereichte Unterlagen: *Ihre E-Mail vom 23.11.2015 inkl. Versicherungsbestätigung zur Probandenversicherung vom 20.11.2015*

Sehr geehrte Frau Becker,

die Ethikkommission der Ärztekammer Nordrhein hat Ihre oben genannte E-Mail vom 23.11.2015 mit Versicherungsbestätigung zur Probandenversicherung vom 20.11.2015 zur Kenntnis genommen.

Damit konnten Sie alle Punkte unseres Votums vom 18.11.2015 zufrieden stellend umsetzen, so dass keine berufsethischen und berufsrechtlichen Bedenken mehr gegen die Durchführung der Studie bestehen.

Vorsorglich weist die Ethikkommission darauf hin, dass die ärztliche und juristische Verantwortung für die Durchführung der Studie uneingeschränkt bei Ihnen und Ihren Mitarbeitern verbleibt.

Wir machen darauf aufmerksam, dass sich das oben genannte Votum nur auf die bisher eingereichten Unterlagen bezieht. Nachträgliche Änderungen in Organisation und Ablauf der klinischen Prüfung, die nach Ihrer Auffassung vom Votum der Ethikkommission umfasst sein sollen, sollten umgehend zur Beratung mitgeteilt und die geänderten Passagen deutlich kenntlich gemacht werden.

Informationen und Änderungen, zu denen Sie kein Votum der Ethikkommission mit einem entsprechenden Antrag erbitten möchten, sind demgegenüber nicht zuzusenden.

Tersteegenstraße 9
40474 Düsseldorf
Postfach 30 07 62
40401 Düsseldorf
Telefon 0211 4302-0
Fax 0211 4302-1200
Mail aerztekammer@aekno.de
Web www.aekno.de

Sprechzeiten:
Mo bis Do 9 Uhr bis 15 Uhr
Freitag 9 Uhr bis 14 Uhr

Bankverbindung:
Deutsche Apotheker- und Ärztebank eG Düsseldorf
IBAN DE43 3006 0601 0005 0029 02
BIC/SWIFT-Code DAAEDEDD

Ärztekammer Nordrhein

Wir gehen davon aus, dass die Prüfer in unserem Kammerbezirk (Prof. Dr. med. habil. Jörn Rittweger und Dr. rer. nat. Klaus Müller) durch Sie über dieses Votum informiert werden.

Mit freundlichen Grüßen
gez.

Prof. Dr. med. Winfried Siffert
Stellvertr. Vorsitzender
der Ethikkommission

Document A 4: SpaceCOT study co-investigators list

Institute of Aerospace Medicine, German Aerospace Center [*Cologne, Germany*]

Karina Marshall-Bowman, MS
Jörn Rittweger, MD
Edwin Mulder, PhD
Ulrich Limper, MD
Petra Frings-Meuthen, PhD
Darius Gerlach, MS
Claudia Stern, MD
Bernd Johannes, PhD

Department of Neurology, University of Cologne [*Cologne, Germany*]

Henning Stetefeld, PhD, MD
Christian Dohmen, PhD, MD

Space Medicine Office, European Space Agency [*Cologne, Germany*]

Tobias Weber, PhD

Center for Space Medicine, Baylor College of Medicine [*Houston, TX, USA*]

Eric M. Bershad, MD
Jose I. Suarez, MD
Chethan P. Venkatasubba Rao, MD
Jonathan Clark, MD, MPH
Dorit Donoviel, PhD
Haleh Sangi, PhD
Rahul Damani, MD

Harvard Medical School [*Boston, MA, USA*]

Gary Strangman, PhD

Department of Psychiatry, University of Pennsylvania [*Philadelphia, PA, USA*]

Mathias Basner, MD, PhD

University of Texas – Houston [*Houston, TX, USA*]

Larry Kramer, MD
Khader Hasan, PhD

The SpaceCOT study was supported by the National Space Biomedical Research Institute (NSBRI) through NASA NCC 9-58, Baylor College of Medicine Center for Space Medicine and the German Aerospace Center (DLR) Institute of Aerospace Medicine.

12 References

1. **Ainslie PN**, **Duffin J**. Integration of cerebrovascular CO2 reactivity and chemoreflex control of breathing: mechanisms of regulation, measurement, and interpretation. *Am J Physiol - Regul Integr Comp Physiol* 296: R1473–R1495, 2009.

2. **Albon J**, **Purslow PP**, **Karwatowski WSS**, **Easty DL**. Age related compliance of the lamina cribrosa in human eyes. *Br J Ophthalmol* 84: 318–323, 2000.

3. **Alexander DJ**, **Gibson CR**, **Hamilton DR**, **Lee SMC**, **Mader TH**, **Otto C**, **Oubre CM**, **Pass AF**, **Platts SH**, **Scott JM**, **Smith SM**, **Stenger MB**, **Westby CM**, **Zanello SB**. Evidence Report: Risk of Spaceflight-Induced Intracranial Hypertension and Vision Alterations [Online]. National Aeronautics and Space Administration, Lyndon B. Johnson Space Center. http://humanresearchroadmap.nasa.gov/Evidence/reports/VIIP.pdf.

4. **Alper F**, **Kantarci M**, **Dane S**, **Gumustekin K**, **Onbas O**, **Durur I**. Importance of anatomical asymmetries of transverse sinuses: an MR venographic study. *Cerebrovasc Dis* 18: 236–239, 2004.

5. **Alperin N**, **Lee SH**, **Sivaramakrishnan A**, **Hushek SG**. Quantifying the effect of posture on intracranial physiology in humans by MRI flow studies. *J Magn Reson Imaging* 22: 591–596, 2005.

6. **Alperin N**, **Ranganathan S**, **Bagci AM**, **Adams DJ**, **Ertl-Wagner B**, **Saraf-Lavi E**, **Sklar EM**, **Lam BL**. MRI evidence of impaired CSF homeostasis in obesity-associated idiopathic intracranial hypertension. *Am J Neuroradiol* 34: 29–34, 2013.

7. **Anderson AP**, **Swan JG**, **Phillips SD**, **Knaus DA**, **Kattamis NT**, **Toutain-Kidd CM**, **Zegans ME**, **Fellows AM**, **Buckey JC**. Acute effects of changes to the gravitational vector on the eye. *J Appl Physiol* 120: 939–946, 2016.

8. **Arbeille P**, **Fomina G**, **Roumy J**, **Alferova I**, **Tobal N**, **Herault S**. Adaptation of the left heart, cerebral and femoral arteries, and jugular and femoral veins during short- and long-term head-down tilt and spaceflights. *Eur J Appl Physiol* 86: 157–168, 2001.

9. **Arbeille P**, **Provost R**, **Zuj K**, **Vincent N**. Measurements of jugular, portal, femoral, and calf vein cross-sectional area for the assessment of venous blood redistribution with long duration spaceflight (vessel imaging experiment). *Eur J Appl Physiol* 115: 2099–2106, 2015.

10. **Aries MJ**, **Elting JW**, **Stewart R**, **Keyser JD**, **Kremer B**, **Vroomen P**. Cerebral blood flow velocity changes during upright positioning in bed after acute stroke: an observational study. *BMJ Open* 3: e002960, 2013.

11. **Avezaat CJ**, **van Eijndhoven JH**, **Wyper DJ**. Cerebrospinal fluid pulse pressure and intracranial volume-pressure relationships. *J Neurol Neurosurg Psychiatry* 42: 687–700, 1979.

12. **Bagian JP**, **Hackett P**. Cerebral blood flow: comparison of ground-based and spaceflight data and correlation with space adaptation syndrome. *J Clin Pharmacol* 31: 1036–1040, 1991.

13. **Balédent O**, **Henry-Feugeas MC**, **Idy-Peretti I**. Cerebrospinal fluid dynamics and relation with blood flow: a magnetic resonance study with semiautomated cerebrospinal fluid segmentation. *Invest Radiol* 36: 368–377, 2001.

14. **Barratt MR**, **Pool SL**. *Principles of Clinical Medicine for Space Flight*. Springer, 2008.

15. **Bäuerle J**, **Schuchardt F**, **Schroeder L**, **Egger K**, **Weigel M**, **Harloff A**. Reproducibility and accuracy of optic nerve sheath diameter assessment using ultrasound compared to magnetic resonance imaging. *BMC Neurol* 13: 187, 2013.

16. **Beckel JM**, **Argall AJ**, **Lim JC**, **Xia J**, **Lu W**, **Coffey EE**, **Macarak EJ**, **Shahidullah M**, **Delamere NA**, **Zode GS**, **Sheffield VC**, **Shestopalov VI**, **Laties AM**, **Mitchell CH**. Mechanosensitive release of adenosine 5'-triphosphate through pannexin channels and mechanosensitive upregulation of pannexin channels in optic nerve head astrocytes: A mechanism for purinergic involvement in chronic strain. *Glia* 62: 1486–1501, 2014.

17. **Beggs CB**. Venous hemodynamics in neurological disorders: an analytical review with hydrodynamic analysis. *BMC Med* 11: 142, 2013.

18. **Berdahl JP**, **Fautsch MP**, **Stinnett SS**, **Allingham RR**. Intracranial pressure in primary open angle glaucoma, normal tension glaucoma, and ocular hypertension: a case–control study. *Invest Ophthalmol Vis Sci* 49: 5412–5418, 2008.

19. **Bershad EM**, **Anand A**, **DeSantis SM**, **Yang M**, **Tang RA**, **Calvillo E**, **Malkin-Gosdin L**, **Foroozan R**, **Damani R**, **Maldonado N**, **Gupta P**, **Tan B**, **Rao CPV**, **Suarez JI**, **Clark JB**, **Sutton JP**, **Donoviel DB**. Clinical validation of a transcranial Doppler-based noninvasive intracranial pressure meter: a prospective cross-sectional study. *World Neurosurg* 89: 647–653.e1, 2016.

20. **Bidot S**, **Bruce BB**, **Saindane AM**, **Newman NJ**, **Biousse V**. Asymmetric papilledema in idiopathic intracranial hypertension. *J Neuroophthalmol* 35: 31–36, 2015.

21. **Bidot S**, **Saindane AM**, **Peragallo JH**, **Bruce BB**, **Newman NJ**, **Biousse V**. Brain imaging in idiopathic intracranial hypertension. *J Neuroophthalmol* 35: 400–411, 2015.

22. **Binder DK**, **Horton JC**, **Lawton MT**, **McDermott MW**. Idiopathic intracranial hypertension. *Neurosurgery* 54: 538–552, 2004.

23. **Brinker T**, **Stopa E**, **Morrison J**, **Klinge P**. A new look at cerebrospinal fluid circulation. *Fluids Barriers CNS* 11: 10, 2014.

24. **Chiquet C**, **Custaud M-A**, **Le Traon AP**, **Millet C**, **Gharib C**, **Denis P**. Changes in intraocular pressure during prolonged (7-day) head-down tilt bedrest. *J Glaucoma* 12: 204–208, 2003.

25. **Cipolla MJ**. *The Cerebral Circulation*. 2nd ed. Morgan and Claypool Life Sciences, 2016.

26. **Cooke WH**, **Ryan KL**, **Convertino VA**. Lower body negative pressure as a model to study progression to acute hemorrhagic shock in humans. *J Appl Physiol* 96: 1249–1261, 2004.

27. **Czosnyka M**, **Pickard JD**. Monitoring and interpretation of intracranial pressure. *J Neurol Neurosurg Psychiatry* 75: 813–821, 2004.

28. **Davson H**, **Hollingsworth G**, **Segal MB**. The mechanism of drainage of the cerebrospinal fluid. *Brain* 93: 665–678, 1970.

29. **Donnelly J**, **Budohoski KP**, **Smielewski P**, **Czosnyka M**. Regulation of the cerebral circulation: bedside assessment and clinical implications. *Crit Care* 20: 129, 2016.

30. **Downs JC**, **Roberts MD**, **Burgoyne CF**. The mechanical environment of the optic nerve head in glaucoma. *Optom Vis Sci* 85: 425–435, 2008.

31. **Draeger J**, **Schwartz R**, **Groenhoff S**, **Stern C**. Self-tonometry under microgravity conditions. *Clin Investig* 71: 700–703, 1993.

32. **Draeger J**, **Schwartz R**, **Groenhoff S**, **Stern C**. [Self tonometry during the German 1993 Spacelab D2 mission]. *Ophthalmologe* 91: 697–699, 1994.

33. **Durgun B**, **Ilglt ET**, **Cizmeli MO**, **Atasever A**. Evaluation by angiography of the lateral dominance of the drainage of the dural venous sinuses. *Surg Radiol Anat* 15: 125–130, 1993.

34. **Eklund A**, **Jóhannesson G**, **Johansson E**, **Holmlund P**, **Qvarlander S**, **Ambarki K**, **Wåhlin A**, **Koskinen L-OD**, **Malm J**. The pressure difference between eye and brain changes with posture. *Ann Neurol* 80: 269–276, 2016.

35. **Feola AJ**, **Myers JG**, **Raykin J**, **Mulugeta L**, **Nelson ES**, **Samuels BC**, **Ethier CR**. Finite Element Modeling of Factors Influencing Optic Nerve Head Deformation Due to Intracranial Pressure. *Invest Ophthalmol Vis Sci* 57: 1901, 2016.

36. **Fortney SM**, **Schneider VS**, **Greenleaf JE**. The Physiology of Bed Rest. In: *Handbook of Physiology: Environmental Physiology*. New York: Oxford University Press, 1996, p. 889–939.

37. **Fortune JB**, **Feustel PJ**, **deLuna C**, **Graca L**, **Hasselbarth J**, **Kupinski AM**. Cerebral blood flow and blood volume in response to O2 and CO2 changes in normal humans. *J Trauma* 39: 463–471, 1995.

38. **Frey MA**, **Mader TH**, **Bagian JP**, **Charles JB**, **Meehan RT**. Cerebral blood velocity and other cardiovascular responses to 2 days of head-down tilt. *J Appl Physiol* 74: 319–325, 1993.

39. **Frisén L**. Swelling of the optic nerve head: a staging scheme. *J Neurol Neurosurg Psychiatry* 45: 13–18, 1982.

40. **Geeraerts T**, **Newcombe VF**, **Coles JP**, **Abate MG**, **Perkes IE**, **Hutchinson PJ**, **Outtrim JG**, **Chatfield DA**, **Menon DK**. Use of T2-weighted magnetic resonance imaging of the optic nerve sheath to detect raised intracranial pressure. *Crit Care* 12: R114, 2008.

41. **Giger-Tobler C**, **Eisenack J**, **Holzmann D**, **Pangalu A**, **Sturm V**, **Killer HE**, **Landau K**, **Jaggi GP**. Measurement of optic nerve sheath diameter: differences between methods? A pilot study. *Klin Monbl Augenheilkd* 232: 467–470, 2015.

42. **Goel M**, **Picciani RG**, **Lee RK**, **Bhattacharya SK**. Aqueous humor dynamics: a review. *Open Ophthalmol J* 4: 52–59, 2010.

43. **Goswami N**, **Loeppky JA**, **Hinghofer-Szalkay H**. LBNP: past protocols and technical considerations for experimental design. *Aviat Space Environ Med* 79: 459–471, 2008.

44. **Grubb RL**, **Raichle ME**, **Eichling JO**, **Ter-Pogossian MM**. The effects of changes in PaCO2 cerebral blood volume, blood flow, and vascular mean transit time. *Stroke* 5: 630–639, 1974.

45. **Hargens AR**, **Richardson S**. Cardiovascular adaptations, fluid shifts, and countermeasures related to space flight. *Respir Physiol Neurobiol* 169 Suppl 1: S30–33, 2009.

46. **Heiberg E**, **Sjögren J**, **Ugander M**, **Carlsson M**, **Engblom H**, **Arheden H**. Design and validation of Segment--freely available software for cardiovascular image analysis. *BMC Med Imaging* 10: 1, 2010.

47. **Herault S**, **Fomina G**, **Alferova I**, **Kotovskaya A**, **Poliakov V**, **Arbeille P**. Cardiac, arterial and venous adaptation to weightlessness during 6-month MIR spaceflights with and without thigh cuffs (bracelets). *Eur J Appl Physiol* 81: 384–390, 2000.

48. **Hoffmann J**, **Schmidt C**, **Kunte H**, **Klingebiel R**, **Harms L**, **Huppertz H-J**, **Lüdemann L**, **Wiener E**. Volumetric assessment of optic nerve sheath and hypophysis in idiopathic intracranial hypertension. *Am J Neuroradiol* 35: 513–518, 2014.

49. **Hoiland RL**, **Tymko MM**, **Bain AR**, **Wildfong KW**, **Monteleone B**, **Ainslie PN**. Carbon dioxide-mediated vasomotion of extra-cranial cerebral arteries in humans: a role for prostaglandins? *J Physiol* 594: 3463–3481, 2016.

50. **Hughson RL**, **Yee NJ**, **Greaves DK**. Elevated end-tidal PCO2 during long-duration spaceflight. *Aerosp Med Hum Perform* 87: 894–897, 2016.

51. **Imray CHE**, **Walsh S**, **Clarke T**, **Tiivas C**, **Hoar H**, **Harvey TC**, **Chan CWM**, **Forster PJG**, **Bradwell AR**, **Wright AD**, **Birmingham Medical Research Expeditionary Society**. Effects of breathing air containing 3% carbon dioxide, 35% oxygen or a mixture of 3% carbon dioxide/35% oxygen on cerebral and peripheral oxygenation at 150 m and 3459 m. *Clin Sci* 104: 203–210, 2003.

52. **Ito H**, **Kanno I**, **Ibaraki M**, **Hatazawa J**, **Miura S**. Changes in human cerebral blood flow and cerebral blood volume during hypercapnia and hypocapnia measured by positron emission tomography. *J Cereb Blood Flow Metab* 23: 665–670, 2003.

53. **Iwabuchi T**, **Sobata E**, **Suzuki M**, **Suzuki S**, **Yamashita M**. Dural sinus pressure as related to neurosurgical positions. *Neurosurgery* 12: 203–207, 1983.

54. **Iwasaki K**, **Levine BD**, **Zhang R**, **Zuckerman JH**, **Pawelczyk JA**, **Diedrich A**, **Ertl AC**, **Cox JF**, **Cooke WH**, **Giller CA**, **Ray CA**, **Lane LD**, **Buckey JC**, **Baisch FJ**, **Eckberg DL**, **Robertson D**, **Biaggioni I**, **Blomqvist CG**. Human cerebral autoregulation before, during and after spaceflight. *J Physiol* 579: 799–810, 2007.

55. **James J**. Carbon Dioxide [Online]. In: *Spacecraft Maximum Allowable Concentrations for Selected Airborne Contaminants: Volume 5*. National Academies Press, p. 112–124. http://www.nap.edu/catalog/12529.

56. **Johnson BD**, **van Helmond N**, **Curry TB**, **van Buskirk CM**, **Convertino VA**, **Joyner MJ**. Reductions in central venous pressure by lower body negative pressure or blood loss elicit similar hemodynamic responses. *J Appl Physiol* 117: 131–141, 2014.

57. **Johnston RS**, **Dietlein LF**. *Biomedical Results from Skylab*. Washington, D.C.: National Aeronautics and Space Administration, 1977.

58. **Kakurin LI**, **Lobachik VI**, **Mikhailov VM**, **Senkevich YA**. Antiorthostatic hypokinesia as a method of weightlessness simulation. *Aviat Space Environ Med* 47: 1083–1086, 1976.

59. **Katkovskiĭ BS**, **Georgievskiĭ VS**, **Machinskiĭ GV**, **Mikhaĭlov VM**, **Pometov ID**. [Some physiological effects caused by 30 days of bed rest in different body positions]. *Kosm Biol Aviakosm Med* 14: 55–58, 1980.

60. **Kawai Y**, **Murthy G**, **Watenpaugh DE**, **Breit GA**, **Deroshia CW**, **Hargens AR**. Cerebral blood flow velocity in humans exposed to 24 h of head-down tilt. *J Appl Physiol* 74: 3046–3051, 1993.

61. **Killer HE**, **Jaggi GP**, **Flammer J**, **Miller NR**, **Huber AR**. The optic nerve: a new window into cerebrospinal fluid composition? *Brain* 129: 1027–1030, 2006.

62. **Killer HE**, **Jaggi GP**, **Flammer J**, **Miller NR**, **Huber AR**, **Mironov A**. Cerebrospinal fluid dynamics between the intracranial and the subarachnoid space of the optic nerve. Is it always bidirectional? *Brain* 130: 514–520, 2007.

63. **Killer HE**, **Jaggi GP**, **Miller NR**. Papilledema revisited: is its pathophysiology really understood? *Clin Exp Ophthalmol* 37: 444–447, 2009.

64. **Killer HE**, **Laeng HR**, **Flammer J**, **Groscurth P**. Architecture of arachnoid trabeculae, pillars, and septa in the subarachnoid space of the human optic nerve: anatomy and clinical considerations. *Br J Ophthalmol* 87: 777–781, 2003.

65. **Killer HE**, **Laeng HR**, **Groscurth P**. Lymphatic capillaries in the meninges of the human optic nerve. *J Neuroophthalmol* 19: 222–228, 1999.

66. **Kimberly HH**, **Shah S**, **Marill K**, **Noble V**. Correlation of optic nerve sheath diameter with direct measurement of intracranial pressure. *Acad Emerg Med* 15: 201–204, 2008.

67. **Kirsch KA**, **Baartz FJ**, **Gunga HC**, **Röcker L**. Fluid shifts into and out of superficial tissues under microgravity and terrestrial conditions. *Clin Investig* 71: 687–689, 1993.

68. **Kotecha A**, **Izadi S**, **Jeffery G**. Age-related changes in the thickness of the human lamina cribrosa. *Br J Ophthalmol* 90: 1531–1534, 2006.

69. **Kramer LA**, **Sargsyan AE**, **Hasan KM**, **Polk JD**, **Hamilton DR**. Orbital and intracranial effects of microgravity: findings at 3-T MR imaging. *Radiology* 263: 819–827, 2012.

70. **Krejza J**, **Szydlik P**, **Liebeskind DS**, **Kochanowicz J**, **Bronov O**, **Mariak Z**, **Melhem ER**. Age and sex variability and normal reference values for the VMCA/VICA index. *Am J Neuroradiol* 26: 730–735, 2005.

71. **Law J**, **Van Baalen M**, **Foy M**, **Mason SS**, **Mendez C**, **Wear ML**, **Meyers VE**, **Alexander D**. Relationship between carbon dioxide levels and reported headaches on the International Space Station. *J Occup Environ Med* 56: 477–483, 2014.

72. **Lawley J**, **Williams M**, **Petersen L**, **Zhang R**, **Whitworth T**, **Levine B**. ICP during daily life in healthy adults: what does microgravity add to the mix? *FASEB J* 29: 990.10, 2015.

73. **Lewis NCS**, **Smith KJ**, **Bain AR**, **Wildfong KW**, **Numan T**, **Ainslie PN**. Impact of transient hypotension on regional cerebral blood flow in humans. *Clin Sci* 129: 169–178, 2015.

74. **Lotz J**, **Meier C**, **Leppert A**, **Galanski M**. Cardiovascular flow measurement with phase-contrast MR imaging: basic facts and implementation. *Radiographics* 22: 651–671, 2002.

75. **Macias BR**, **Liu JHK**, **Grande-Gutierrez N**, **Hargens AR**. Intraocular and intracranial pressures during head-down tilt with lower body negative pressure. *Aerosp Med Hum Perform* 86: 3–7, 2015.

76. **Mader TH**, **Gibson CR**, **Caputo M**, **Hunter N**, **Taylor G**, **Charles J**, **Meehan RT**. Intraocular pressure and retinal vascular changes during transient exposure to microgravity. *Am J Ophthalmol* 115: 347–350, 1993.

77. **Mader TH**, **Gibson CR**, **Lee AG**. Choroidal folds in astronauts. *Invest Ophthalmol Vis Sci* 57: 592, 2016.

78. **Mader TH**, **Gibson CR**, **Pass AF**, **Kramer LA**, **Lee AG**, **Fogarty J**, **Tarver WJ**, **Dervay JP**, **Hamilton DR**, **Sargsyan A**, **Phillips JL**, **Tran D**, **Lipsky W**, **Choi J**, **Stern C**, **Kuyumjian R**, **Polk JD**. Optic disc edema, globe flattening, choroidal folds, and hyperopic shifts observed in astronauts after long-duration space flight. *Ophthalmology* 118: 2058–2069, 2011.

79. **Mader TH**, **Taylor GR**, **Hunter N**, **Caputo M**, **Meehan RT**. Intraocular pressure, retinal vascular, and visual acuity changes during 48 hours of 10 degrees head-down tilt. *Aviat Space Environ Med* 61: 810–813, 1990.

80. **Manuel Valdueza J**, **von Münster T**, **Hoffman O**, **Schreiber S**, **Max Einhäupl K**. Postural dependency of the cerebral venous outflow. *The Lancet* 355: 200–201, 2000.

81. **Manzey D**, **Lorenz B**. Joint NASA-ESA-DARA study part three: effects of chronically elevated CO2 on mental performance during 26 days of confinement. *Aviat Space Environ Med* 69: 506–514, 1998.

82. **Marshall-Bowman K**, **Barratt MR**, **Gibson CR**. Ophthalmic changes and increased intracranial pressure associated with long duration spaceflight: An emerging understanding. *Acta Astronaut* 87: 77–87, 2013.

83. **Marshall-Goebel K**, **Ambarki K**, **Eklund A**, **Malm J**, **Mulder E**, **Gerlach D**, **Bershad E**, **Rittweger J**. Effects of short-term exposure to head-down tilt on cerebral hemodynamics: a prospective evaluation of a spaceflight analog using phase-contrast MRI. *J Appl Physiol* 120: 1466–1473, 2016.

84. **Marshall-Goebel K**, **Mulder E**, **Bershad E**, **Laing C**, **Eklund A**, **Malm J**, **Stern C**, **Rittweger J**. Intracranial and intraocular pressure during various degrees of head-down tilt. *Aerosp Med Hum Perform* 88: 10–16, 2017.

85. **Marshall RS**, **Lazar RM**. Pumps, aqueducts, and drought management vascular physiology in vascular cognitive impairment. *Stroke* 42: 221–226, 2011.

86. **Martin-Du Pan RC**, **Benoit R**, **Girardier L**. The role of body position and gravity in the symptoms and treatment of various medical diseases. *Swiss Med Wkly* 134: 543–551, 2004.

87. **McComb JG**. Recent research into the nature of cerebrospinal fluid formation and absorption. *J Neurosurg* 59: 369–383, 1983.

88. **Mokri B**. The Monro-Kellie hypothesis: applications in CSF volume depletion. *Neurology* 56: 1746–1748, 2001.

89. **Moore TP**, **Thornton WE**. Space shuttle inflight and postflight fluid shifts measured by leg volume changes. *Aviat Space Environ Med* 58: A91–96, 1987.

90. **Morgan WH**, **Balaratnasingam C**, **Lind CRP**, **Colley S**, **Kang MH**, **House PH**, **Yu D-Y**. Cerebrospinal fluid pressure and the eye. *Br J Ophthalmol* 100: 71–77, 2016.

91. **Murthy G**, **Marchbanks RJ**, **Watenpaugh DE**, **Meyer JU**, **Eliashberg N**, **Hargens AR**. Increased intracranial pressure in humans during simulated microgravity. *Physiologist* 35: S184–185, 1992.

92. **Myasnikov VI**, **Stepanova SI**. Features of cerebral hemodynamics in cosmonauts before and after flight on the MIR orbital station. In: *Orbital Station MIR, Space Biology*

and Medicine. Moscow: Institute of Biomedical Problems of the Russian Academy of Sciences, 2008, p. 300–305.

93. **Norsk P**, **Asmar A**, **Damgaard M**, **Christensen NJ**. Fluid shifts, vasodilatation and ambulatory blood pressure reduction during long duration spaceflight. *J Physiol* 593: 573–584, 2015.

94. **Norsk P**, **Bonde-Petersen F**, **Warberg J**. Influence of central venous pressure change on plasma vasopressin in humans. *J Appl Physiol* 61: 1352–1357, 1986.

95. **Orešković D**, **Klarica M**. The formation of cerebrospinal fluid: Nearly a hundred years of interpretations and misinterpretations. *Brain Res Rev* 64: 241–262, 2010.

96. **Petersen LG**, **Petersen JCG**, **Andresen M**, **Secher NH**, **Juhler M**. Postural influence on intracranial and cerebral perfusion pressure in ambulatory neurosurgical patients. *Am J Physiol - Regul Integr Comp Physiol* 310: R100–R104, 2016.

97. **Prisk GK**. Microgravity and the respiratory system. *Eur Respir J* 43: 1459–1471, 2014.

98. **Prisk GK**, **Fine JM**, **Elliott AR**, **West JB**. Effect of 6 degrees head-down tilt on cardiopulmonary function: comparison with microgravity. *Aviat Space Environ Med* 73: 8–16, 2002.

99. **Qvarlander S**, **Sundström N**, **Malm J**, **Eklund A**. Postural effects on intracranial pressure: modeling and clinical evaluation. *J Appl Physiol* 115: 1474–1480, 2013.

100. **Ragauskas A**, **Bartusis L**, **Piper I**, **Zakelis R**, **Matijosaitis V**, **Petrikonis K**, **Rastenyte D**. Improved diagnostic value of a TCD-based non-invasive ICP measurement method compared with the sonographic ONSD method for detecting elevated intracranial pressure. *Neurol Res* 36: 607–614, 2014.

101. **Rickards CA**, **Johnson BD**, **Harvey RE**, **Convertino VA**, **Joyner MJ**, **Barnes JN**. Cerebral blood velocity regulation during progressive blood loss compared with lower body negative pressure in humans. *J Appl Physiol* 119: 677–685, 2015.

102. **Roberts DR**, **Zhu X**, **Tabesh A**, **Duffy EW**, **Ramsey DA**, **Brown TR**. Structural brain changes following long-term 6° head-down tilt bed rest as an analog for spaceflight. *Am J Neuroradiol* 36: 2048–2054, 2015.

103. **Saeedi O**, **Pillar A**, **Jefferys J**, **Arora K**, **Friedman D**, **Quigley H**. Change in choroidal thickness and axial length with change in intraocular pressure after trabeculectomy. *Br J Ophthalmol* 98: 976–979, 2014.

104. **Schaller B**. Physiology of cerebral venous blood flow: from experimental data in animals to normal function in humans. *Brain Res Rev* 46: 243–260, 2004.

105. **Schmidt D**. The mystery of cotton-wool spots - a review of recent and historical descriptions. *Eur J Med Res* 13: 231–266, 2008.

106. **Schwartz R**, **Draeger J**, **Groenhoff S**, **Flade KD**. [Results of self-tonometry during the 1st German-Russian MIR mission 1992]. *Ophthalmologe* 90: 640–642, 1993.

107. **Shinojima A**, **Iwasaki K-I**, **Aoki K**, **Ogawa Y**, **Yanagida R**, **Yuzawa M**. Subfoveal choroidal thickness and foveal retinal thickness during head-down tilt. *Aviat Space Environ Med* 83: 388–393, 2012.

108. **Sibony PA**, **Kupersmith MJ**, **Feldon SE**, **Wang J-K**, **Garvin M**. Retinal and choroidal folds in papilledema. *Invest Ophthalmol Vis Sci* 56: 5670–5680, 2015.

109. **Sliwka U**, **Krasney JA**, **Simon SG**, **Schmidt P**, **Noth J**. Effects of sustained low-level elevations of carbon dioxide on cerebral blood flow and autoregulation of the intracerebral arteries in humans. *Aviat Space Environ Med* 69: 299–306, 1998.

110. **Son CH**, **Zapata JL**, **Lin C**. Investigation of airflow and accumulation of carbon dioxide in the service module crew quarters. *SAE Tech Pap* 2002-01-2341, 2002.

111. **Srichai MB**, **Lim RP**, **Wong S**, **Lee VS**. Cardiovascular applications of phase-contrast MRI. *Am J Roentgenol* 192: 662–675, 2009.

112. **Stoquart-ElSankari S**, **Lehmann P**, **Villette A**, **Czosnyka M**, **Meyer M-E**, **Deramond H**, **Balédent O**. A phase-contrast MRI study of physiologic cerebral venous flow. *J Cereb Blood Flow Metab* 29: 1208–1215, 2009.

113. **Strandgaard S**. Autoregulation of cerebral blood flow in hypertensive patients. The modifying influence of prolonged antihypertensive treatment on the tolerance to acute, drug-induced hypotension. *Circulation* 53: 720–727, 1976.

114. **Sundström P**, **Wåhlin A**, **Ambarki K**, **Birgander R**, **Eklund A**, **Malm J**. Venous and cerebrospinal fluid flow in multiple sclerosis: A case-control study. *Ann Neurol* 68: 255–259, 2010.

115. **Sun X-Q**, **Yao Y-J**, **Yang C-B**, **Jiang S-Z**, **Jiang C-L**, **Liang W-B**. Effect of lower-body negative pressure on cerebral blood flow velocity during 21 days head-down tilt bed rest. *Med Sci Monit* 11: CR1–5, 2005.

116. **Suzuki Y**, **Ikeda H**, **Shimadu M**, **Ikeda Y**, **Matsumoto K**. Variations of the basal vein: identification using three-dimensional CT angiography. *Am J Neuroradiol* 22: 670–676, 2001.

117. **Taibbi G**, **Cromwell RL**, **Kapoor KG**, **Godley BF**, **Vizzeri G**. The effect of microgravity on ocular structures and visual function: a review. *Surv Ophthalmol* 58: 155–163, 2013.

118. **Trambovetskiĭ EV**, **Krotov VP**, **Korol'kov VI**. [Intracranial pressure in monkeys during the flight of Cosmos-2229]. *Aviakosm Ekol Med* 29: 37–41, 1995.

119. **Traon AP-L**, **Heer M**, **Narici MV**, **Rittweger J**, **Vernikos J**. From space to Earth: advances in human physiology from 20 years of bed rest studies (1986–2006). *Eur J Appl Physiol* 101: 143–194, 2007.

120. **Tso M.**, **Hayreh S.** Optic disc edema in raised intracranial pressure: IV Axoplasmic transport in experimental papilledema. *Arch Ophthalmol* 95: 1458–1462, 1977.

121. **Tymko MM**, **Rickards CA**, **Skow RJ**, **Ingram-Cotton NC**, **Howatt MK**, **Day TA**. The effects of superimposed tilt and lower body negative pressure on anterior and posterior cerebral circulations. *Physiol Rep* 4: e12957, 2016.

122. **Tymko MM**, **Skow RJ**, **MacKay CM**, **Day TA**. Steady-state tilt has no effect on cerebrovascular CO2 reactivity in anterior and posterior cerebral circulations. *Exp Physiol* 100: 839–851, 2015.

123. **Ursino M**, **Lodi CA**. A simple mathematical model of the interaction between intracranial pressure and cerebral hemodynamics. *J Appl Physiol* 82: 1256–1269, 1997.

124. **Wagshul ME**, **Eide PK**, **Madsen JR**. The pulsating brain: A review of experimental and clinical studies of intracranial pulsatility. *Fluids Barriers CNS* 8: 5, 2011.

125. **Wall M**. Idiopathic intracranial hypertension. *Neurol Clin* 28: 593–617, 2010.

126. **Watenpaugh DE**. Analogs of microgravity: head-down tilt and water immersion. *J Appl Physiol* 120: 904–914, 2016.

127. **Weigel M**, **Lagrèze WA**, **Lazzaro A**, **Hennig J**, **Bley TA**. Fast and quantitative high-resolution magnetic resonance imaging of the optic nerve at 3.0 tesla. *Invest Radiol* 41: 83–86, 2006.

128. **Wiener TC**. Space obstructive syndrome: intracranial hypertension, intraocular pressure, and papilledema in space. *Aviat Space Environ Med* 83: 64–66, 2012.

129. **Williams AL**, **Gatla S**, **Leiby BE**, **Fahmy I**, **Biswas A**, **de Barros DM**, **Ramakrishnan R**, **Bhardwaj S**, **Wright C**, **Dubey S**, **Lynch JF**, **Bayer A**, **Khandelwal R**, **Ichhpujani P**, **Gheith M**, **Siam G**, **Feldman RM**, **Henderer JD**, **Spaeth GL**. The value of intraocular pressure asymmetry in diagnosing glaucoma. *J Glaucoma* 22: 215–218, 2013.

130. **Willie CK**, **Macleod DB**, **Shaw AD**, **Smith KJ**, **Tzeng YC**, **Eves ND**, **Ikeda K**, **Graham J**, **Lewis NC**, **Day TA**, **Ainslie PN**. Regional brain blood flow in man during acute changes in arterial blood gases. *J Physiol* 590: 3261–3275, 2012.

131. **Willie CK**, **Tzeng Y-C**, **Fisher JA**, **Ainslie PN**. Integrative regulation of human brain blood flow. *J Physiol* 592: 841–859, 2014.

132. **Wilson MH**. Monro-Kellie 2.0: The dynamic vascular and venous pathophysiological components of intracranial pressure. *J Cereb Blood Flow Metab* 36: 1338–1350, 2016.

133. **Zuj KA**, **Arbeille P**, **Shoemaker JK**, **Blaber AP**, **Greaves DK**, **Xu D**, **Hughson RL**. Impaired cerebrovascular autoregulation and reduced CO2 reactivity after long duration spaceflight. *Am J Physiol Heart Circ Physiol* 302: H2592–H2598, 2012.

134. **Zwart SR**, **Gibson CR**, **Mader TH**, **Ericson K**, **Ploutz-Snyder R**, **Heer M**, **Smith SM**. Vision changes after spaceflight are related to alterations in folate- and vitamin B-12-dependent one-carbon metabolism. *J Nutr* 142: 427–431, 2012.

135. Human Energy Requirements: Report of a Joint FAO/WHO/UNU Expert Consultation [Online]. World Health Organization, Food and Agriculture Organization of the United Nations. http://www.who.int/nutrition/publications/nutrientrequirements/9251052123/en/.

13 Acknowledgements

I would like to express my sincere gratitude to my supervisor, Prof. Rittweger, for his continued support and guidance throughout my PhD journey and for pushing me to strive for excellence. I would also like to sincerely thank my tutors, Prof. Cursiefen and Prof. Hoehn, for their insightful feedback and encouragement throughout the thesis process. In addition, I would like to express my heartfelt gratitude to Dr. Krassimira Ivanova for always going above and beyond to support me over the years and teaching me the true intricacies of being a scientist.

I also would like to thank Dr. Edwin Mulder for taking the time to guide me through the difficulties of conducting bed rest studies and always being there for me. In addition, I would like to thank Christine Becker for her immense help in daily matters. I was frequently overwhelmed by the amount of work that had to be done in the German language and I absolutely could not have succeeded without her selfless help.

I would also like to extend my gratitude to the team of people from the Institute of Aerospace Medicine and Department of Space Physiology at DLR including (but not limited to) Dr. Bernd Johannes, Peter Gauger, Wolfram Sies, Ben Niederberger, Darius Gerlach, Annette von Waechter, Dr. Klaus Mueller, Dr. Ulrich Limper, Charles Laing, and Elfriede Huth. The studies we conducted together were a great team effort that I was honored to be a part of – I thank you for your enthusiasm and assistance over the years!

I would also like to thank Dr. Anders Eklund, Dr. Jan Malm, Dr. Peter Norsk and Dr. Christian Otto for their support, intellectual contributions and most of all, for being so open and sharing their expertise with me over the course of my PhD work.

I would also like to recognize two Masters students, Robert Terlević and Stepan Pazekha, as well as Dr. Nimesh Patel and Dr. Khalid Ambarki, for their contributions and assistance with various image analysis techniques. Furthermore, I would like to thank the entire SpaceCOT investigators group for the vast team effort it took to successfully conduct the SpaceCOT

study and in particular, Dr. Eric Bershad and Dr. Dorit Donoviel for their great leadership and perseverance. I would also like to thank my dear friend Christie Grabelle for her graphic design support and expertise.

I would also like also thank the subjects in the enVIIP, SpaceCOT and SETI studies for dedicating themselves and their time to the advancement of science and helping enable future human exploration of space. I would also like to acknowledge the Helmholtz Space Life Sciences Research School (SpaceLife) PhD scholarship program, funded in equal parts by the Helmholtz Association (grant no.: VH-KO-300) and the German Aerospace Center (DLR), for making this thesis work possible.

In the end, I would like to give a special thanks to my mother, Christine, and my father, David, who always encouraged me to reach for the stars (which I proceeded to take quite literally). I would never have made it this far without their lifelong support especially when times were rough.

And to my husband, for without his endless patience, words of encouragement and unwavering love, this journey would never have been possible.

14 Erklärung

Ich versichere, dass ich die von mir vorgelegte Dissertation selbstständig angefertigt, die benutzten Quellen und Hilfsmittel vollständig angegeben und die Stellen der Arbeit - einschließlich Tabellen, Karten und Abbildungen -, die anderen Werken im Wortlaut oder dem Sinn nach entnommen sind, in jedem Einzelfall als Entlehnung kenntlich gemacht habe; dass diese Dissertation noch keiner anderen Fakultät oder Universität zur Prüfung vorgelegen hat; dass sie - abgesehen von unten angegebenen Teilpublikationen - noch nicht veröffentlicht worden ist sowie, dass ich eine solche Veröffentlichung vor Abschluss des Promotionsverfahrens nicht ohne Genehmigung der Dekanin / dem Dekan vornehmen werde. Die Bestimmungen dieser Ordnung sind mir bekannt. Die von mir vorgelegte Dissertation ist von Prof. Dr. med. Jörn Rittweger betreut worden.

Teilpublikationen im Rahmen des Dissertationsverfahrens

Erst-Autorenschaft:

1. Marshall-Goebel K, Mulder E, Bershad E, Laing C, Eklund A, Malm J, Stern C, Rittweger J. Intracranial and intraocular pressure during various degrees of head-down tilt. *Aerosp Med Hum Perform* 88(1): 10-16, 2017.
2. Marshall-Goebel K, Ambarki K, Eklund A, Malm J, Mulder E, Gerlach D, Bershad E, Rittweger J. Effects of short-term exposure to head-down tilt on cerebral hemodynamics: a prospective evaluation of a spaceflight analog using phase-contrast MRI. *J Appl Physiol* 120: 1466-1473, 2016.

Co-Authorenschaft:

3. Strangman G, Zhang Q, Marshall-Goebel K, Mulder E, Stevens B, Clark J, Bershad E. Increased cerebral blood volume pulsatility during head-down tilt with elevated carbon dioxide: the SPACECOT study. *J Appl Physiol* (In Revision) 2017.
4. Michael AP, Marshall-Bowman K. Spaceflight-induced intracranial hypertension. *Aerosp Med Hum Perform* 86(6): 557–562, 2015.

Kongress-Beiträge:

1. **Marshall-Goebel K**, Rittweger J, Suarez JI, Rao CV, Donoviel D, Mulder E, Bershad E. Effects of head-down tilt with and without 0.5% carbon dioxide on intracranial and intraocular pressure. Aerospace Medical Association Conference, Oral Presentation, Atlantic City, NJ, USA, Apr 2016.
2. **Marshall-Goebel K**, Rittweger J, Suarez JI, Rao CV, Limper U, Mulder E, Donoviel D, Bershad E. Effects of head-down tilt with or without 0.5% CO_2 on intracranial and intraocular pressure: results from the Space-COT study. NASA Human Research Program Investigators Workshop, Poster Presentation, Galveston, TX, USA, Feb 2016.
3. **Marshall-Bowman K**, Ambarki K, Eklund A, Malm J, Mulder E, Gerlach D, Bershad E, Rittweger J. Implementation of various degrees of head down tilt to study the etiology of the VIIP Syndrome. International Astronautical Congress, Oral Presentation, Jerusalem, Israel, Oct 2015.
4. **Marshall-Bowman K**, Mulder E, Rittweger J. Effects of head-down tilt, carbon dioxide and lower body negative pressure in humans: results from the enVIIP study. International Astronautical Congress, Oral Panel Presentation, Jerusalem, Israel, Oct 2015.
5. **Marshall-Bowman K**, Rittweger J. Cerebral and ocular fluid balance as a function of space-related environmental factors: insights into the visual impairment and intracranial pressure syndrome. NASA Human Research Program Investigators Workshop, Oral Presentation (invited speaker), Galveston, TX, USA, Jan 2015.

7.11.2016

Datum

Unterschrift